IJSBAR
International Journal of Sciences: Basic and Applied Research

International Journal of Sciences: Basic and Applied Research

SHEAR STRENGTHENING OF REINFORCED CONCRETE BEAMS WITH NEAR SURFACE MOUNTED FRP REINFORCEMENT

By Ammar Adil Shamil Al-Ali

Volume 8, 2014
ISSN (Print & Online): 2307-4531

www.gssrr.org

Published by:
GSSRR
Global Society of Scientific Research and Researchers

Visit: www.gssrr.org

ISSN 2307-4531 (Print & Online)

IJSBAR proceedings are currently indexed by:

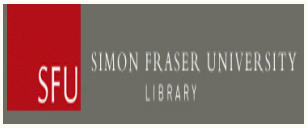

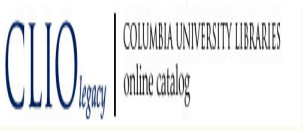


SHEAR STRENGTHENING OF REINFORCED CONCRETE BEAMS WITH NEAR SURFACE MOUNTED FRP REINFORCEMENT

ISSN(online & Print) 2307-4531

The IJSBAR is published and hosted by the Global Society of Scientific Research and Researchers (GSSRR). Address: Khlda - Wasfi Al Tall Street, P.O.Box : 2245 Amman 11953, info@gssrr.org, Amman, Hashemite Kingdom of Jordan

University of Nottingham

Department of Civil Engineering

SHEAR STRENGTHENING OF REINFORCED CONCRETE BEAMS WITH NEAR SURFACE MOUNTED FRP REINFORCEMENT

BY

Ammar Adil Shamil Al Ali

4154140

Supervisor: Dr. Dionysios Bournas

A dissertation submitted in accordance with the requirements of the University of Nottingham for the degree of Master of Science in Civil Engineering

August 2013

DECLARATION

I declare that what is presented in this dissertation is my own work and it has not been submitted for any other degree. All sources which have been used in this dissertation are acknowledged by means of references.

ABSTRACT

During the last two decades, increasing the shear capacity of the existing reinforced concrete (RC) elements, such as RC beams has become an important issue around the world. The use of Near Surface Mounted (NSM) strengthening technique has contributed significantly in achieving that. However, the theoretical shear contribution of this technique in RC beams is still not yet fully achieved, and there is not a final design guidance to estimate this contribution accurately. Therefore, this dissertation aims first to study the effects of different parameters on the effectiveness of this technique in shear strengthening of RC beams, evaluating the current theoretical models. Finally, this dissertation aims to propose a modified analytical model to compute the theoretical shear contribution of NSM technique in RC beams accurately.

The study of the impacts of various parameters, such as the type and material of the NSM reinforcement, angle of orientation, spacing, and percentage of existing steel stirrups, percentage of composite materials, concrete strength and the anchorage of the FRP reinforcement, on the effectiveness of such strengthening technique is first considered in this dissertation. From examining these influences using the findings of the previous experimental tests, it was discovered that these factors play an important role in the effectiveness of this technique. In fact, it was found that, they can contribute significantly in increasing the efficiency of NSM technique by means of shear strengthening technique in RC beams.

Furthermore, experimental database was generated in this project using all the available technical papers in the field of NSM shear strengthening of RC beams. This was then used to evaluate the current theoretical models. Only three of the current theoretical models, which are the ones that proposed by A.K.M Anwarul Islam, (Dias and Barros) and T.C. Triantafillou, were selected and evaluated in this dissertation because of the complexity of some models and data availability. The evaluation of these three models are not only in terms of the accurate estimation of the analytical values of the shear contribution of NSM technique in RC beams, but also in terms of the considered parameters in the development of them, and their degree of sophistication. The evaluation results of the models showed that the first evaluated model is not that reliable to be used and modified. These results also demonstrated that Dias and Barross' model is more reliable compared to the first evaluated model. Finally, the evaluations of the three models illustrated that the model of T.C. Triantafillou is the best one among the others.

Based on the final evaluation results of the three models, T.C. Triantafillou's model is modified in this dissertation using the generated database. By modifying and introducing new safety factors to this model, 94% of the considered beams of the database are in the safe side. However, since this model was originally designed for RC beam strengthened in shear using externally bonded FRP laminates, the predictive performance of this modified model is assessed. This is achieved by comparing the obtained results from the modified T.C. Triantafillou's model with the results, which were obtained from using the three original models before carrying out any modification processes. In addition to this, Dias and Barross' model is modified in this project, and the obtained results of the two modified models are compared. The assessment results proved that the modified T.C. Triantafillou's model is a sufficient model, which can predict the theoretical shear contribution of NSM technique in RC beams accurately with sufficient agreement with the experimental results. Thus, this model has been adopted to be used as a design-oriented equation in RC beams strengthened in shear using NSM technique. A maximum limit to the effective FRP strain for each type of FRP reinforcement is also defined in this dissertation to maintain the aggregate interlock, and control the shear cracks in the NSM shear strengthened beams.

ACKNOWLEDGEMENTS

The author would like to thank everybody who has supported him to complete this dissertation. First thank should go to my God who usually support me in my work. Special thank for my supervisor, Dr. Dionysios Bournas, for his guidance, support and dedicated supervision of this project.

I would like also to express my gratitude to the establishers of the HCED program in the Iraqi Government in particular the office of Iraqi prime minster for the great financial support they have offered for me during my study in the University of Nottingham.

NOTATIONS

Unless otherwise defined in the text the following notations apply

A_f: Area of FRP reinforcement in shear

A_i: The nominal cross-sectional area of the FRP rods

A_{sw}: The cross sectional area of the arms of a steel stirrup

A_{sl}: The cross sectional area of the longitudinal tensile steel reinforcement

a_f x b_f: The dimensions of the FRP laminates

a/d: The shear span ratio in the NSM shear strengthened beams

b_w: Beam web width

CFRP: Carbon Fiber Reinforced polymer

$Cfi\,(L_{fi;}\ \alpha_{fi})$: The semi-conical surface associated to the i-th strip

d: The distance from the external compression fiber to centroid of the longitudinal tension reinforcement

Dia.: The diameter of the FRP bar/rod

EBR: Externally Bonded Reinforcement

EFRP: Externally Bonded Fiber Reinforced Polymer

E_f: The tension modulus of elasticity of FRP reinforcement

E_{sw}: The modulus of elasticity of steel stirrups

f_c: The compressive strength of concrete

f_{cm}: The tensile strengthen of concrete

f_{ck}: Characteristic compressive cylinder strength of concrete at 28 days

f_{cd}: The design value of the cylinder compressive strength of concrete

f_{fe}: The effective stress in the FRP reinforcements

f_{fu}: The ultimate tensile strength of FRP reinforcement

f_{yf}: The tensile yield strength of FRP bars

f_i: The tensile stress in the rod at the crack location

f_{ywd}: The design yield strength of steel stirrups

FRP: Fiber Reinforced Polymer

F_{max}: The maximum load carrying capacity of the NSM shear strengthened beams

F_f: The force resulting from the tensile stress in the FRP reinforcements crossing the shear failure crack

GFRP: Class Fiber Reinforced polymer

h_w: The height of the beam web

K: The ratio between the experimental and theoretical shear contribution of NSM technique in RC beams

$K_{ave.}$: The average value of the ratio K

L_{tot}: The sum of the effective lengths of all the FRP reinforcements crossed by the crack

n_f: The number of FRP reinforcements crossed by the shear failure crack

NSM technique: Near Surface Mounted technique

RC: Reinforced Concrete

S_f: The spacing of the FRP reinforcement

S_w: The spacing of the steel stirrups in RC beams

V_n: Shear capacity of reinforced concrete beams

V_c: Shear strength provided by concrete

V_s: Shear strength provided by steel stirrups

V_f: The shear contribution of Near Surface Mounted technique in reinforced concrete beams

V_f^{exp}: The experimental value of the shear contribution of NSM technique in RC beams

V_f^{ana}: The theoretical value of the shear contribution of NSM technique in RC beams

$\varepsilon_{fK,e}$: The characteristic value of the FRP reinforcement strain

ε_{fu}: The ultimate strain of the FRP reinforcement

ε^{ana}: The analytical value of the FRP reinforcement strain

ε^{exp}: The experimental value of the FRP reinforcement strain

ε_{max}: The maximum value of the FRP reinforcement strain

τ_{Rd}: The basic design shear strength

τ_b: The average bond strength of the FRP reinforcements

ρ_f: The percentage of the composite material (FRP reinforcement) in the strengthened beams

ρ_{sw}: The percentage of the steel stirrup in the strengthened beams

ρ_{sl}: The percentage of the longitudinal tensile reinforcement

θ_f: The inclination of the FRP reinforcement measured with respect to the horizontal axis of the beam

α: The orientation of the shear failure crack in RC beams

α_{fi}: The angle between the generatrices and the axis of the semi-con attributed to the i-th strip

γ_c: Partial safety factor for concrete

γ_s: The partial safety factor

TABLE OF CONTENTS

DECLARATION i

ABSTRACT ii

ACKNOWLEDGEMENTS iv

NOTATIONS v

TABLE OF CONTENTS viii

LIST OF FIGURES x

LIST OF TABLES xi

1 INTRODUCTION 1

1.1 Background 1

1.2 Problem Statement 2

1.3 Aims and Objectives 2

1.4 Layout of the Dissertation 3

2 LITERATURE REVIEW 4

2.1 Introduction 4

2.2 Using Various Shear Strengthening Techniques in RC Beams 7

2.3 The Impacts of Various Factors on the Effectiveness of NSM Technique in Shear Strengthening 8

2.3.1 Angle of Inclination and Spacing of NSM Reinforcements 8

2.3.2 The Percentage of existing Steel Stirrups 9

2.3.3 Types and Materials of NSM FRP Reinforcements 10

2.3.4 Percentage of Composite Material 11

2.3.4 Concrete Strength 12

2.3.5 The Anchorage of the NSM FRP Reinforcements 14

2.4 Shear Failure Modes 16

2.5 The Existing Theoretical Models for the Calculation of Shear Contribution of Near Surface Mounted Reinforcement 18

2.5.1 De Lorenzis and Nannis' Model 19

2.5.2 Anwarul Islam's Formula 21

2.5.3 Dias and Barross' Model 22

2.5.4 Barros, Bianco and Montis' Model 24

2.6 Summery 26

3 EVALUATIONS OF THE CURRENT THEORETICAL MODELS 28

3.1 Shear Design of Reinforced Concrete Beams 28

3.2 The Selection of the Current Theoretical Models 30

3.3 The Generation of the Experimental Database 31

3.4 The Evaluation of A.K.M Anwarul Islam's Model 32

3.5 The Evaluation of Dias and Barross' Model 34

3.6 The Evaluation of Thanasis C. Triantafillou's Model 43

3.7 Discussion of the Results of Evaluation 49

4 THE CALIBRATION OF MODELS 52

4.1 The Modification of Thanasis C. Triantafillou's Model 53

4.1.1 Strategy for the Modification of the Analytical Model 53

4.1.2 Development of the Analytical Formulation 55

4.2 Validation of the Modified Thanasis C. Triantafillou's Model and Discussion of the Results 58

4.3 The Modification of Dias and Barross' Model 65

4.4 The Results of the Comparison between the Modified Thanasis C. Triantafillou's and Dias and Barross' Models 69

5 CONCLUSIONS 74

5.1 Summery 74

5.2 Recommendation for Future Researches 77

LIST OF REFERENCES 78

APPENDIX (A): THE CREATED EXPERIMENTAL DATABASE 81

APPENDIX (B): THE CALCULATIONS OF CALIBRATION OF THANASI C. TRIANTAFILLOU'S MODEL 92

APPENDIX (C): THE CALCULATIONS OF CALIBRATION OF DIAS AND BARROSS' MODEL 97

LIST OF FIGURES

Figure (1): Instillation processes of NSM technique 5

Figure (2): The effects of the percentage of existing steel stirrups in the NSM shear strengthen beams 10

Figure (3): The effects of the percentage of composite material on the effectiveness of NSM technique 11

Figure (4): The influence of concrete strength on the effectiveness of NSM technique 13

Figure (5): Production process of manually made carbon rods 15

Figure (6): Strengthening procedures using manually made carbon rods 15

Figure (7): Shear failure modes of NSM shear strengthened beams 17

Figure (8): Representation of NSM shear strengthened beam 18

Figure (9): The relationship between (V_f) experimentally and (V_f) analytically calculated using A.K.M Anwarul Islam's model 33

Figure (10): Data for the theoretical definition of the effective strain of the FRP reinforcement in a T-beam 35

Figure (11): The relationship between (V_f) experimentally and (V_f) analytically calculated using Dias and Barross' model 38

Figure (12): (a) Schematic representation of FRP stress bearing mechanism
(b) Simplified normal stress along diagonal crack 44

Figure (13): Effective strain of FRP reinforcement *versus* $[(E_f \rho_f) / (f_{cm}^{2/3})]$ 56

Figure (14): Effective strain of FRP reinforcement *versus* $[(E_{sw} \rho_{sw} + E_f \rho_f) / (f_{cm}^{2/3})]$ 68

LIST OF TABLES

Table (1): Characteristics of using different angle of inclinations of FRP reinforcements 9

Table (2): Comparison between the theoretical and experimental results of De Lorenzis's and Nanni's experiment 20

Table (3): Comparison between the experimental and the theoretical outcomes of Dias's and Barros's model 23

Table (4): Comparison between the experimental and analytical values of both Anwarul Islam's model and Dias and Barross' model 39

Table (5): Comparison between the experimental and theoretical results of Triantafillou's model 48

Table (6): Comparison between the experimental and analytical results using the modified Thanasis C. Triantafillou's model 61

Table (7): Comparison between the experimental and analytical results using the modified Dias and Barross' model 70

Table (A): The created experimental database on shear strengthening of RC beams with NSM FRP reinforcements 81

Table B1: The Calculations of Figure 13A 92

Table B2: The Calculations of Figure 13B 94

Table B3: The Calculations of Figure 13C 95

Table C1: The Calculations of Figure 14A 97

Table C2: The Calculations of Figure 14B 99

Table C3: The Calculations of Figure 14C 100

1 INTRODUCTION

1.1 Background

In reinforced concrete (RC) structure, shear failure is a common issue that might be faced. Earthquakes, hurricanes and other examples of natural disasters can all cause shear failure in the existing reinforced concrete structures before full flexural capacity is reached. The existing reinforced concrete structures, such as bridges and buildings might exhibit shear cracks due to the regular, unpredicted and unconsidered loads in the inferior material behaviour, earlier designs and the loss of the concrete strength because of aging. The shear failure mode of any reinforced concrete referred to by (RC) element should be avoided. This is due to the fact that this type of failure is very brittle and unpredictable. In fact, this kind of failure can lead to serious damages in the RC structures and sometimes cause collapse. Therefore, the need for efficient and cost-effective shear strengthening techniques in RC elements became significant in order to overtake the shear deficiency causes, and their consequences in the existing RC structures (Islam 2008).

The use of fiber reinforced polymer (FRP) based strengthening systems for shear and flexural strengthening of reinforced concrete (RC) structures has been spread widely around the world especially during the last two decades. The reasons behind this can be related to the outstanding properties of the composite materials (FRP reinforcement), which can be summarised to, ease of handling, fast completion of work, availability, high stiffness, high strength to weight ratio, high durability and many others. Near Surface Mounted strengthening technique, which will be referred to in this dissertation by (**NSM)** technique, is a relatively new-FRP based strengthening technique. This technique has been now used widely for shear strengthening of reinforced concrete beams referred to by (**RC beams**). This technique involves the installation of FRP reinforcement into thin grooves open on the concrete cover of the lateral faces of the RC beams. The FRP reinforcements in this technique are positioned orthogonally to the beams axis, or as orthogonal as possible to the shear failure cracks in the case of existing RC beams (Dias and Barros 2012).

The high effectiveness of NSM technique by means of shear strengthening technique in RC beams compared to that of the externally bonded reinforcing (**EFRP)** technique, contributed significantly in being it used for such purpose widely (Dias and Barros 2012). It is important to mention that the EFRP technique is a relatively old FRP based strengthening technique. In fact, it is reported by many this technique has

numerous experimental data regarding the shear strengthening of RC beams, and its analytical shear contribution in the EFRP shear strengthened beams is well known and established. In contrast, it is believed that the theoretical shear contribution of NSM technique in RC beams is not yet fully achieved, and more work need to be carried out in this field (Islam 2008).

1.2 Problem Statement

It is believed that, the determination of the analytical contribution of Near Surface Mounted (NSM) FRP reinforcement in the NSM shear strengthened beams is quite unclear. Despite the fact that there are few theoretical models, which were proposed to compute this contribution, all of them based on experimental tests. In fact, very small experimental data was used to develop these models. In addition, all of the proposed models differ in their evaluation of the shear contribution of NSM FRP reinforcement in RC beams. According to that, it has been reported by many that, there is not a final design guidance to predict the analytical shear contribution of this technique in RC beams accurately. A question therefore can be asked as a problem statement. This question should be also kept in mind throughout this dissertation, as this project was carried out to answer it beside the other objectives. The question is: " Is it possible to have one equation that calculate the theoretical shear contribution of NSM technique in RC beams accurately, and showing sufficient agreement with the experimental results?" This will be answered in this dissertation.

1.3 Aims and Objectives

The main goal of this project is to propose a modified theoretical model to calculate the analytical shear contribution ($\boldsymbol{V_f}$) of NSM technique in reinforced concrete beams, and evaluated it such that it can be used as a design-oriented equation in RC beams.

In addition to the main goal, there are two other objectives, which are very significant to achieve the main aim of this research. The first one is studying the effects of various parameters on the effectiveness of NSM technique by means of shear strengthening technique in RC beams. This will in fact help to assess the effectiveness of this technique in shear strengthening of RC beams. The first objective is base on the experimental findings of previous experiments, which were carried out in this field. This

is examined in chapter two. The other objective is evaluating the current theatrical models in terms of their accuracy in estimating the term (V_f), the considered parameters in the development of them, and their degree of sophistication. This will help in selecting the best model, and then modify it in order to achieve the main aim of the dissertation. The evaluation and the modification processes in this project are based on experimental database, which was created using all the available technical papers in this area. It is important to mention that, Microsoft excel program was used to produce the diagrams, calculations, tables, and modifying the equations in both chapters three and four.

1.4 Layout of the Dissertation

This dissertation consists of five chapters. The first chapter is an introduction to the project, which includes brief overviews regarding the shear failure mode in reinforced concrete structures and the use of Near Surface Mounted (NSM) technique in shear strengthening of RC beams, the problem statement, and the aims and objectives. In chapter two, a literature review of the project is presented, which shows the previous works of some researchers in the field of using this technique in shear strengthening of RC beams. A brief comparison between using different techniques in shear strengthening of reinforced concrete beams is also illustrated in this chapter. A detailed study of the impacts of various factors, which were examined previously in different experiential programs, on the effectiveness of this technique in shear is also considered in chapter two. A brief examination of the current theoretical models, and the shear failure models of the NSM shear strengthened beams are also presented in the literature review.

Chapter three covers a brief overview of the shear design in RC beams, the generated database, the selection of the current theoretical models, the detailed evaluations of A.K.M Anwarul Islam's, (Dias and Barross') and T.C. Triantafillou's models and the discussion of the results of evaluation of the three models. The modifications of T.C. Triantafillou's and (Dias and Barross') models, the discussion of the obtained results of the modified T.C. Triantafillou's model, and comparison between the results of the two modified models are presented in chapter four. Finally, the last chapter, chapter five, presents the summary of the works and the final findings of the project, besides recommendations for further research work.

2 LITERATURE REVIEW

2.1 Introduction

According to Fib (2001), during the last two decades, the enhancement of the civil engineering infrastructures has become one of the most significant issues around the world. This is mainly because of the fact that many of the existing concrete structures nowadays are suffering from many deterioration problems. The shortage of maintenance, increasing the loads on the structures or facing unpredictable loads, like earthquake are some of the factors that play a role in the deterioration issues of concrete structures. Another important factor is that relates to errors that occurred during the design stages of the existing reinforced concrete (RC) structures, such as those due to calculations and design assumptions. Furthermore, it is stated that the requirements of design are always being developed in order to increase the safety issues of the concrete structures (Triantafillou 1998). Therefore, in order to make these existing structures meet such requirements, it is important to use strengthening techniques. Using such techniques can basically contribute significantly in improving the performance of the existing concrete structures. This can be achieved, for example by strengthening the existing reinforced concrete (RC) elements of structures in flexural and shear (Fib 2001).

One of these techniques is that of using Externally-Bonded Fiber reinforced polymer (FRP) laminates referred to by (EFRP) (Fib 2001). In fact, using such technique to strengthen the reinforced concrete elements, such as beams, slabs and columns has been accepted widely. This is quite apparent in the growth of using it in the civil engineering practices especially during the last few years (Cameron 2012, and Ehsani 2005). The popularity of using the FRP based strengthening techniques in the strengthening of RC elements can be in fact because of the outstanding properties of the composite materials that are used in such techniques. These unique properties as mentioned before can be summarised to those of low weight, high tensile strength easy application in the field of work, high stiffness, and good ability to resist corrosion. These materials also have an efficient deformation capacity. Furthermore, fibre reinforced polymer (FRP) reinforcement is available in different sizes, dimensions and shapes. Nevertheless, using externally bonded laminates has been found to be more expensive compared to that of using steel bars for the same purposes. Also, EFRP technique needs more preparation for the surface of RC elements before bonding the FRP laminates. This is basically in order to achieve good bonding behaviour between the RC elements and FRP composites materials (Fib 2001, and Transportation research Board 2011). It is important to emphasise that numerous numbers of researches and experimental

programs have been carried out regarding using externally FRPs technique to strengthen RC elements since the beginning of the 1990's. Additionally, it is mentioned that most of these studies and researches were to some extend able to clarify the contribution of external FRP bonded laminates in the enhancement of both the shear and the flexural behaviour of RC elements (Teng et al. 2002, and Cameron 2012).

The other FRP based strengthening technique which is used to strengthen the RC elements of the existing RC structures is that of using Near Surface Mounted (NSM) technique. This strengthening technique is a relatively new one. Basically, the strengthening goal in this technique is achieved by opening groves in the external faces of RC elements, and filling them slightly by epoxy paste. Then, the NSM reinforcements are placed in these groves, and finally levelling the surfaces by adding extra epoxy. This is well illustrated in figure (1). In order to obtain excellent bonding condition between the FRP reinforcement and surrounding concrete, it was reported by many that the grove size should be between (1.5 to 2) times the diameters of NSM reinforcement bars (De Lorenzis and Nanni 2001).

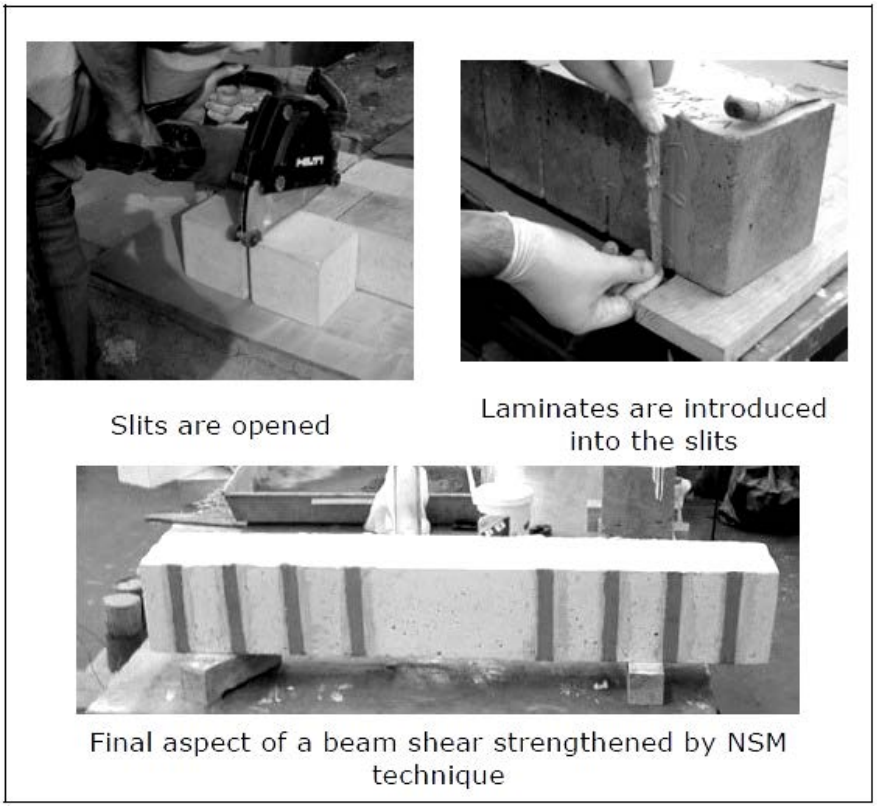

Figure (1): Instillation processes of NSM technique (Dias and Barros 2005)

NSM technique has been found by many to be more efficient and convenient than external bonded FRP technique. This can be for many reasons. Firstly, such strengthening technique does not require any extra surface preparations apart from that

of groves. Furthermore, NSM technique needs less time in term of installation processes. Moreover, the FRP reinforcements in such technique can be anchorage better, so early debonding failure of the NSM reinforcement is prevented leading to increase the efficiency of this technique in RC beams. Finally, additional protections for the FRP reinforcement form environmental effects, such as corrosion are not required, since the FRP reinforcements are embedded in groves (Tanarslan 2010).

NSM technique in fact has many times of applications regarding strengthening the existing reinforced concrete (RC) elements. One of them is shear strengthening of RC beams. In other word, NSM technique is used widely to increase the shear capacity of the existing RC beams (Dias and Barros 2011). However, it is important to emphasise this technique has a limited experimental data for shear strengthening of RC beams. This could be because it is still a relatively new technique (Islam 2008). In fact, many other researchers also agreed that the theoretical calculation of NSM shear contribution in RC beams is not yet fully achieved as well as it is not quite clear. Also, it is believed that there is not a final design guidance that can be used to calculate the theoretical shear contribution of this technique in the NSM shear strengthened beams accurately. Thus, more researches are recommended to be carried out in order to first understand the influences of different variables on such strengthening technique, and propose an efficient theoretical model to calculate the shear contribution of NSM technique taking into account the effects of the various parameters that could affect the effectiveness of this technique by means of shear strengthening technique in RC beams (De Lorenzis and Nanni 2001).

Therefore, it is aimed in this literature review to illustrate and examine the previous experimental works and researches that have been carried out in this field. This includes studying the effects of various parameters on the effectiveness of NSM technique, shear failure modes and shear capacity of the strengthened beams. An examination of the current theoretical models that were proposed to calculate the shear contribution of NSM technique is also considered in the last section.

2.2 Using Various Shear Strengthening Techniques in RC Beams

Many experimental programs have been carried out in order to evaluate the efficacy of using steel stirrups, externally bonded FRP laminates, and Near Surface Mounted techniques in shear strengthening of RC beams. Dias, Barros and Lima (2006), for example, aimed to find the difference of using these techniques in term of their shear efficiency in RC beams. This was achieved by testing four series of RC beams, which were strengthened in shear by using the three different strengthening mechanisms. From the obtained results, it was found that once the shear cracks formed, a sudden loss in the load carrying capacity was recorded in the beams strengthened using steel stirrups. This was accounted to the rapture of steel stirrups that crossed the shear cracks in the tested beams. It was also observed that after the formation of shear cracks, beams strengthened with externally U-jacket FRP failed generally in rapture of the externally laminates. This time this was considered as a consequence of the high tensile stress that generated in FRP laminates after the formation of shear cracks (Dias, Barros and Lima 2006). In addition, it was generally noticed that the shear failure in the NSM shear strengthened beams was not brittle compared to the EFRP shear strengthened beams. Furthermore, by comparing the results of the beams strengthened using NSM technique with that strengthened using Externally FRP technique, it was found that better performance in terms of increasing shear capacity of RC beams, deflection and preventing early debonding failure of the FRP reinforcement were recorded for beams strengthened in shear using NSM technique (Raj and Surumi2012, and Dias, Barros and Lima 2006). In fact, many others agree that an increase of about 55% and 85% in shear capacity of RC beams can be observed if EFRP and NSM technique are used in shear strengthening of RC beams, respectively. Similarly, an increment in the deflection behaviour of the beams of about 77% for EFRP and 307% for NSM technique could be obtained (Dias and Barros 2006). Moreover, it is reported that using NSM technique can raise the maximum tensile stain of the FRP reinforcements to a level, which is greater than that can be obtained by using EFRP technique (Dias and Barros 2009, and Dias and Barros 2011).

Regarding the efficiency of steel stirrups and NSM technique in shear strengthening, it was discovered that using both NSM technique and steel stirrups for shear strengthening of RC beams, seems to have no noticeable differences in term of increasing the load carrying capacity, and the shear capacity of the RC beams. However, when many beams with steel stirrups and NSM reinforcements were tested for the compression purposes, NSM shear strengthened beams showed better deflection performance (Dias and Barros 2006).

2.3 The Impacts of Various Parameters on the Effectiveness of NSM Technique in Shear Strengthening

This section deals mainly with studying the effects of different parameters on the effectiveness of Near Surface Mounted technique by means of shear strengthening technique in reinforced concrete beams. It is worth to mention that all the information presented in this section, is based on previous experimental studies, which have been carried out to find the influences of different parameters on the effectiveness of NSM technique in shear strengthening. These parameters are the types and material of NSM reinforcements, angle of inclination, spacing, percentage of existing steel stirrups, percentage of composite materials, concrete strength and the anchorage of the FRP reinforcements.

2.3.1 Angle of Inclination and Spacing of NSM Reinforcements

Regarding these two parameters, it is reported that increasing the spacing between the Near Surface Mounted FRP reinforcement, and/or increasing the angle of inclination of FRP reinforcement seem to have noticeable effects on the effectiveness of this technique in shear strengthening. This is due to the fact by doing so the distance, that strengthens the interaction between bound stress around the NSM reinforcements, and the surrounding concrete can decrease. Furthermore, doing that could lead to accelerate the formation of shear failure pattern in the strengthened beams (Raj and surumi 2012).

Moreover, many have approved that using inclined FRP reinforcement especially at an angle equal to 45^{o} from the horizontal axis of the beams with close spacing is very effective in terms of increasing the shear contribution of this technique in the NSM shear strengthened beams, increasing the level of mobilization of the FRP reinforcement at the failure, the stiffness, the maximum load carrying capacity and the deformation of the NSM shear strengthened beams at the shear failure stage. In fact, it is mentioned that an increase in the shear resistance of the beams of about 44% can obtained in this case. This increase was found to be higher than that of using vertical NSM reinforcement with close spacing. It important to point out that the main reason behind making the 45^{o} arrangement the most efficient configuration in the strengthened beams, can be the fact that the shear cracks in the beams at failure tend to incline by 45^{o}. Therefore, the shear cracks at failure will be orthogonal in this case to the inclined FRP reinforcement leading to increase the effectiveness of these reinforcements (Dias and Barros 2010, Dias and

Barros 2009, and De Lorenzis and Nanni 2001). Table (1) indicates the differences of using different angle of inclinations in such strengthening technique.

Table (1): Characteristics of using different angle of inclinations of FRP reinforcements

(Teng et al. 2002)

Angle (θ_f)	Description
90^o	It is easy to apply in the RC beams. In general, it is less effective than 60 and 45 degree in term of increasing the effectiveness of this technique in shear. However, if reversed loads such as earthquake are expected, this configuration could be more effective than the inclined one.
60^o and 45^o	They are more effective than 90 degree because they have good ability to control shear cracks in the RC beams especially 45^o.

2.3.2 The Percentage of Existing Steel Stirrups

Another important factor which is also considered in many experimental studies is that of the percentage of the existing steel stirrups in the strengthened beams. In fact, the reason behind examining the importance of this parameter is the fact that NSM technique is used to strengthen existing RC beams that already have certain amount of steel stirrups in them. It is important to mention that the main functions of steel stirrups in RC beams are; they first help to take a portion from the shear force in the beams, and play an important role in decreasing the propagating of shear cracks. Moreover, it is stated that steel stirrups can raise the capacity of dowel action in RC beams, and hold the flexural reinforcements rods together (De Lorenzis and Nanni 2001). Nevertheless, when T-beams were tested considering the effects of the existing steel stirrups on the effectiveness of NSM technique, it was discovered that the effectiveness of NSM technique was higher in RC beams with lower percentage of existing steel stirrups regardless the strength of concrete. In addition, it was stated that the level of influence of this parameter seems to be as larger as smaller the concrete strength of the RC beams is (Dias and Barros 2012). This was also confirmed by many others experimental studies. For instance, in another experimental study, the results of examining the effects of this factor on the effectiveness of this technique are well presented in figure (2).

Basically, this diagram shows the lower this percentage in the tested beams, the higher shear contribution of this technique is (Dias and Barros 2011).

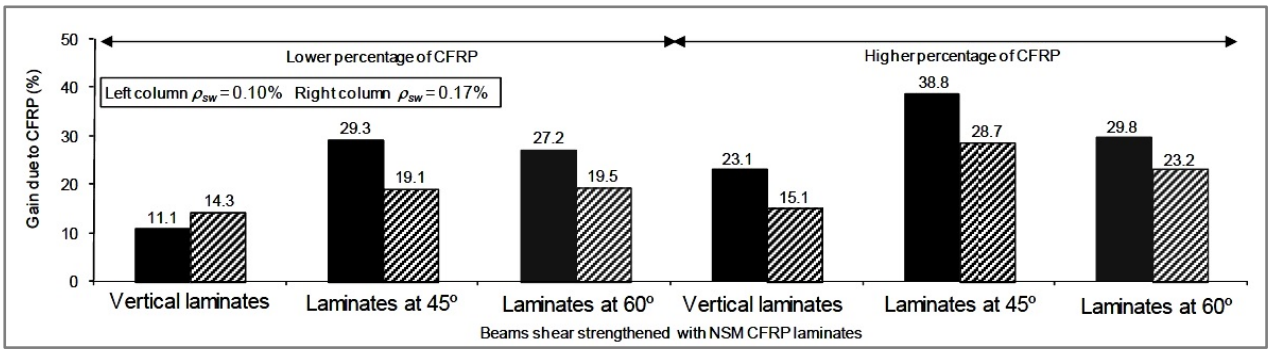

Figure (2): The effects of the percentage of existing steel stirrups in the NSM shear strengthen beams (Dias and Barros 2011).

Interestingly, NSM technique was also discovered by some to be still very adequate in the absence of steel stirrups. In fact, it is stated that an improvement of 35% in the shear capacity of the beams can be obtained in this case (De Lorenzis and Nanni 2001). Another impact of this parameter is that the effective strain of the FRP reinforcement was noticed in many experimental tests to be decreased as the percentage of the existing steel stirrups increase in the NSM shear strengthened beams (Dias and Barros 2012).

2.3.3 Type and Material of NSM FRP Reinforcements

The outstanding physical properties of the composite materials of Near Surface Mounted FRP reinforcement contribute dramatically in the success of being this technique used widely. Fundamentally, these materials can play an important role in increasing the shear capacity of RC beams. However, this increase can be varied, since these materials have various strain capacity, strength and stiffness modules. Basically, many experimental tests approve that using different material and types of NSM reinforcement materials can affect the effectiveness of this technique as a shear strengthening technique in RC beams. For example, it was discovered that using NSM Glass strips is more effective than using NSM Glass rod in term of increasing the ultimate load carrying capacity of the NSM shear strengthened beams. Similarly, by comparing circular carbon NSM rods with rectangular carbon strips, the second types appeared to be more effective in term of increase the shear contribution of NSM technique (Raj and Surumi 2012).

Another example regarding materials type of FRP reinforcements, Rahal and Rumaith (2010) confirmed that using steel and carbon bars in NSM shear strengthening technique seems to have no differences in terms of increase the shear contribution of NSM technique, but conditions such as cost, durability and material availability could be reasons for selecting them.

2.3.4 Percentage of Composite Material

As far as the percentage of NSM composite material is concerned, it is agreed that this variable has important impacts on the effectiveness of NSM technique, and the shear failure modes in the strengthened beams. Dias and Barros (2009), for example, approved this by examining the effects of such parameter in an experiment. Basically, T-beams strengthening by different percentage (amounts) of NSM carbon laminates were used in the experimental study. It was found in this test that the beams that had a minimum percentage of carbon laminate (fewer amounts) failed generally in debonding of the FRP reinforcements. On the other hand, the work of Dias and Barros (2012) indicates that by increasing the amount of composite material to level that can be called (intermediate and high percentage); the shear failure mode can change from debonding of the NSM reinforcements to be by splitting the concrete cover along the flexural reinforcement bars. Despite this, the effectiveness of NSM technique was noticed to be improved by increasing the amount of composite materials in RC beams. In other word, generally the strengthening efficiency of the NSM technique was noticed to be increased in the beams that had higher percentage of composite material (Dias and Barros 2012). This is well shown in figure (3)

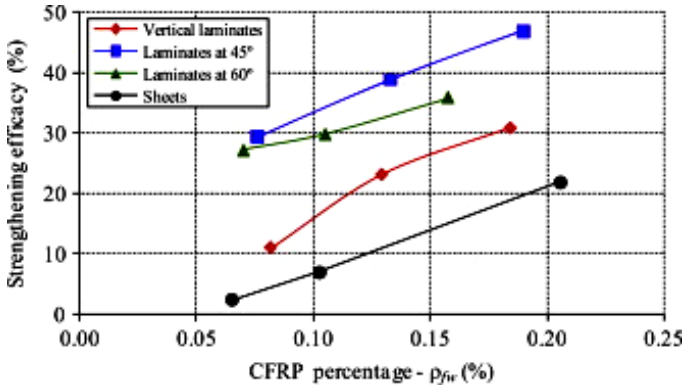

Figure (3): The effects of the percentage of composite material on the effectiveness of NSM technique (Dias and Barros 2012)

2.3.4 Concrete Strength

The influences of using different compressive strengths of concrete on the efficiency, and shear failure modes of the NSM technique in the NSM shear strengthened beams are presented here.

It is believed that the concrete strength has remarkable influence on the effectiveness of the NSM technique. Dias and Barros (2009), for example, stated after testing numbers of T-beams with low compressive strength concrete that, the strength of concrete can play a role in increasing the shear contribution, and the adequacy of NSM technique by means of shear strengthening technique in RC beams. This was based on the fact that using concrete with low strength about (18.6 MPa) in the test resulted in reducing the effective bound length of Near Surface Mounted FRP reinforcements. This was due to the crash failure in the concrete that surrounded the NSM reinforcement bars. The low strength of concrete was in fact the main reason behind this failure. By also comparing the shear capacity of the beams in this test with the results of previous experimental tests, in which high compressive concrete were used, it was concluded that using high strength concrete can lead to high improvements in the shear capacity of the strengthened beams.

Dias and Barros (2012) have also expressed a similar view after taking another experimental study considering this time the impacts of using different compressive strength of concrete. Basically, they noticed that using concrete with high (59.4 MPa) and intermediate (average value of 39.7 MPa) strengths raised the shear contribution of such technique, and enhanced the deflection behaviour of the beams. In fact, average values of the shear contributions of NSM technique in RC beams of about (54.2 KN), (35.4 KN) and (97 KN) were obtained in this test for beams with low, intermediate and high concrete strengths, respectively. This is well illustrated in figure (4). Furthermore, increasing the strength of concrete in the experiment was found to contribute significantly in increasing the effective strain of the NSM reinforcements to reach about 3.6%, 5.6% and 9.6% in beams with low, average and high concrete strengths, respectively. It was also noticed that using concrete with high strength helped in preventing the crush of concrete failure from taking place in the strengthened beams. However, two kinds of shear failures in this case were observed. The first type was the debonding of the NSM reinforcements that crossed the shear cracks at failure in the beams. The second kind was the rupture of the NSM reinforcements.

Finally, it was concluded that using NSM technique for shear strengthening in RC beams with low concrete strength can still be effective, but not as efficient as that of using concrete with higher compressive strengths (Dias and Barros 2012).

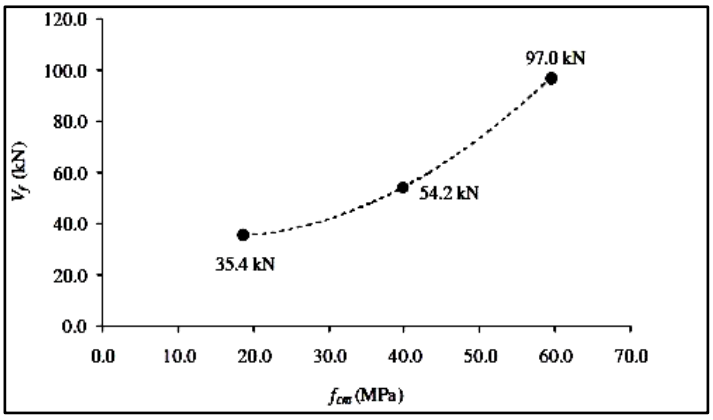

Figure (4): The influnce of concrete strength on the effectivness of NSM technique (Dias and Barros 2012)

2.3.5 The Anchorage of the NSM FRP Reinforcements

According to De Lorenzis and Nanni 2001, anchorage the Near Surface Mounted FRP reinforcement can significantly improve the shear behaviour of the strengthened beams, and raise the shear contribution of such strengthening technique. In fact, anchorage the NSM bars was approved to be able to increase the shear capacity of the RC beams noticeably up to 46% or even more. Additionally, it was discovered that anchorage the NSM reinforcements can be a suitable solution to prevent debonding of the NSM reinforcement, and allowing the strengthened beams to carry more loads. Nevertheless, it is stated that splitting the concrete cover along the flexural reinforcement bars can be obtained in this case. It was also notice that by anchorage the NSM reinforcement bars, the tensile strain of the FRP reinforcements was found to be increased. For example, a maximum strain of 2300 Micro-strain was obtained in the anchored FRP bars in De Lorenzis and Nannis' 2001 experiment.

Similarly, a study by Rahal and Rumaith (2010) confirm that anchorage the carbon bars is more efficient than using vertical bars without anchorage ends. This study also approved that providing more anchorage to the NSM reinforcement rods is very helpful to increase the load carrying capacity of the strengthened areas in the RC beams. Moreover, splitting of the concrete cover along the interface between the flange and web of T-beams was noticed to be prevented by using such system with NSM technique (Rahal and Rumaith 2010).

Jalali, Sharbatar, Chen and Alaee (2012) have also drawn attention to the effects of anchorage NSM reinforcements to beams that have a certain amount of steel stirrups by carring out an experimental program. It should be metioned that in this test, new manners to enhannce the shear performance of NSM reinforcments bars and ancoraging them were proposed and used. This was achieved by warrping dry carbon laminates on wooden bars. Doing so basically leads to use low percentace of composite materials. Figure (5) and figure (6) indicate these new strategies.

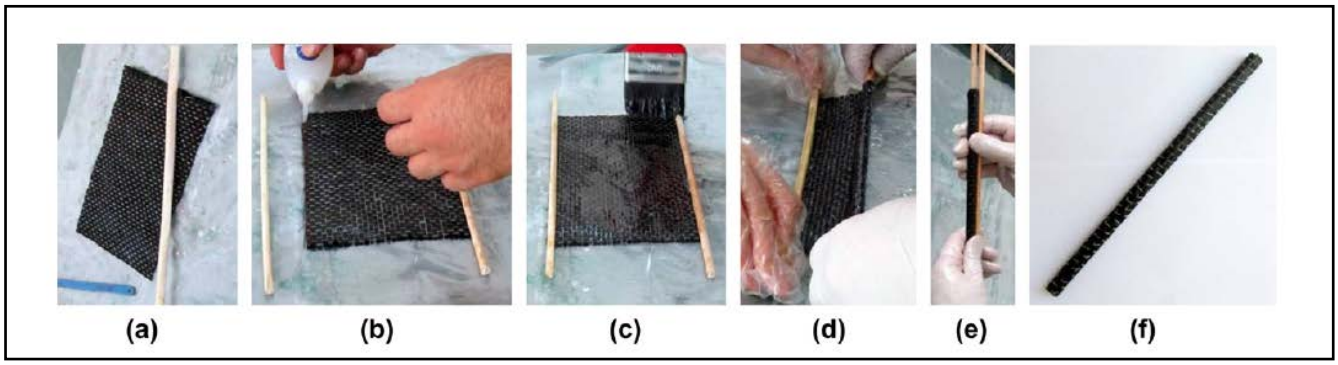

Figure (5): Production process of manually made carbon rods (Jalali, Sharbatar,Chen ,and Alaee 2012)

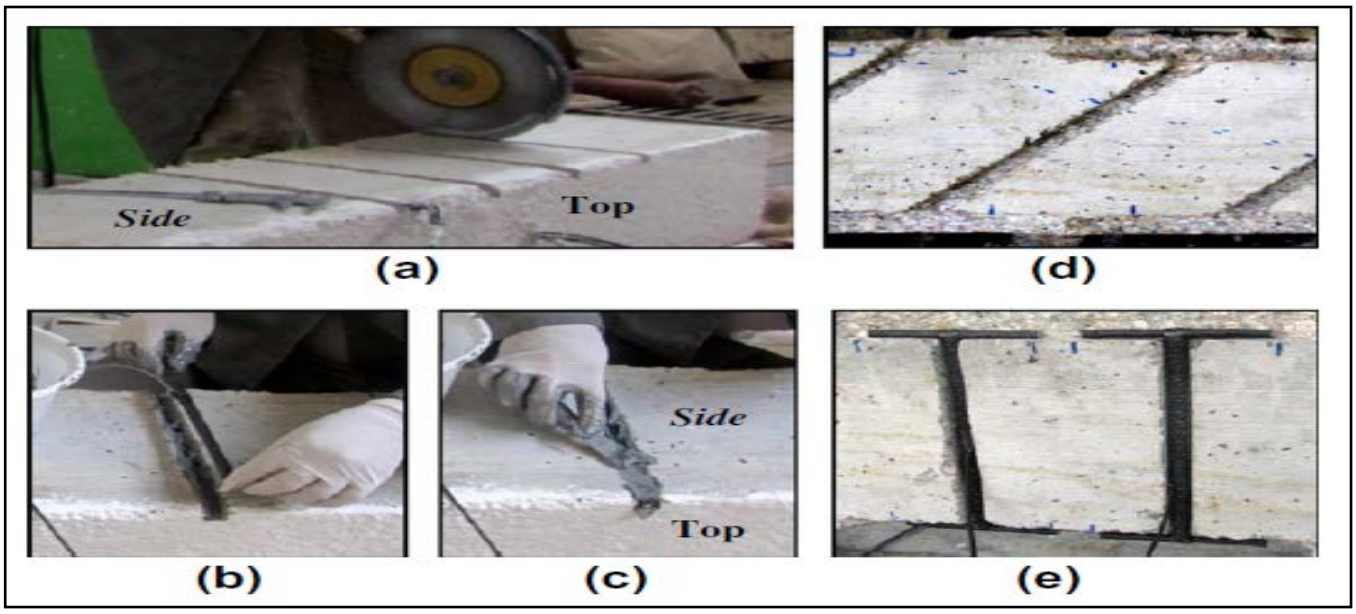

Figure (6): Strengthening procedures using manually made carbon rods: (a) cutting grooves; (b) placing MMFRP rods into grooves; (c) finishing with adhesive, (d) grooves for inclines MMFRP rods with anchors; (e) typical vertical MMFRP with anchors in grooves (Jalali, Sharbatar, Chen ,and Alaee 2012)

The experimental results of this test fundamentally indicated that anchorage the carbon bars can increase the shear contribution of them by about 60%, and this is obviously support the view of De Lorenzis and Nanni. Furthermore, at the ultimate state, the deflection in the tested beams was monitored to be increased between the range (40-75) percent compared to that of beams with unanchored bars.

2.4 Shear Failure Modes

This section demonstrates briefly the shear failure modes that are more likely to occur in the NSM shear strengthened beams, and they are important to be considered in the future in the development and modification of any theoretical model to calculate the shear contribution of such technique. This due to the fact these failure modes affect the efficiency of NSM technique in shear strengthening. Most of the experimental results that are available to the literature including those examined in the previous sections; confirm that the NSM shear strengthened beams might fail generally in shear in one of three types of failures.

De Lorenzis and Nanni (2001) basically are the first who explained the mechanisms of these failures, and then they were approved by others. The first type of failure is that of the debonding of the NSM FRP reinforcements. It is stated this could happen as a consequence of splitting the epoxy cover that intersects by the formed shear cracks in the beams at the shear failure stage. In fact, it is reported that, this failure depends on the type, and the properties of the strengthening materials that are used in this technique. Moreover, it was discovered that the debonding failure can be prevented by either anchorage the NSM reinforcements into the beams (the flange in the case of using T-beam), or by decreasing the spacing between the NSM reinforcements with using the 45^{o} arrangement in relation to beam axis. The reason behind this is the fact that by doing so an increase in the bound strength between Near Surface Mounted FRP reinforcement and surrounding concrete can be achieved. Nevertheless, it is believed that once this failure is prevented, the second type; concrete fracture; is more likely to occur. This sort of failure starts by splitting the concrete cover that is parallel to the longitudinal flexural bars. Factors such as steel stirrups, their spacing, the tensile strength of concrete and the amount of flexural bars can be all played an important role in preventing this failure. This is based on the concept that these factors could help to decrease the tensile stress in the surrounding concrete. It should be also mentioned that, it has been noticed in some experiments that there is another mode of failure which is “tensile rupture of FRP reinforcements.” In fact, Jalali, Sharbatar, Chen and Alaee (2012) stated that this failure may happen due to the high generated tensile strian in the Near Surface Mounted FRP reinforecemnts, that interset by major shear cracks at the failure stage. The last type of failure depends heavily on the type and material of FRP reinforcements. This is because each type of FRP reinofrcement has differnet tensile proprties depending on the FRP materials. These modes of failures are shown in figure (7).

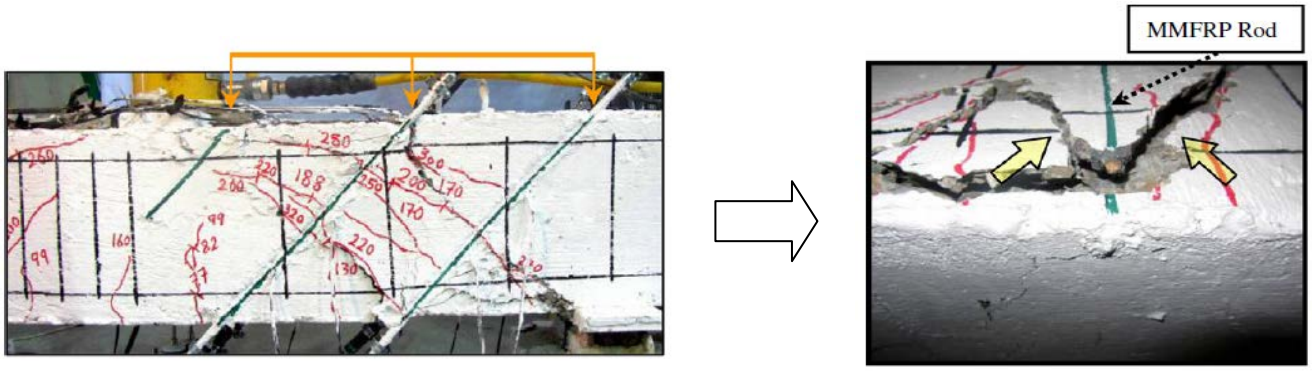

(a) Debonding failure

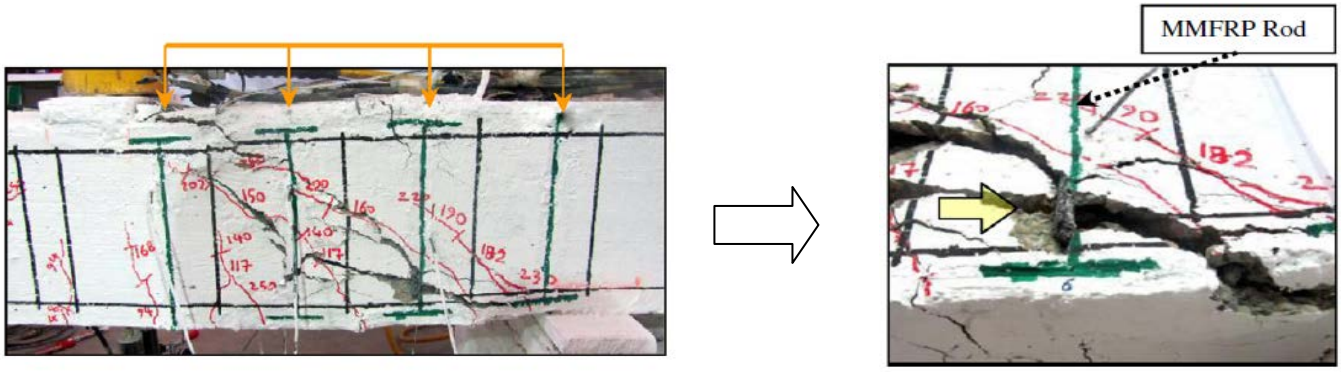

(b) Rapture of FRP Reinforcements

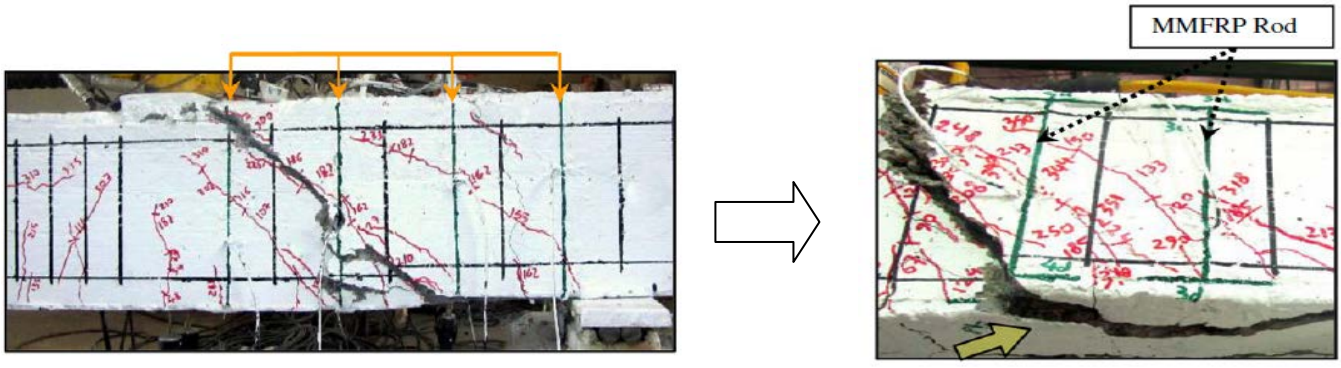

(c) Splitting the concrete cover

Figure (7): Shear failure modes of NSM shear strengthened beams (Jalali, Sharbatar, Chen, and Alaee 2012)

2.5 The Existing Theoretical Models for the Calculation of Shear Contribution of Near Surface Mounted Reinforcement

The shear capacity of any RC beams is equal to the summation of the shear strength provided by concrete and that provided by steel stirrups. However, when NSM reinforcement is used to strengthen the RC beams in shear as shown in figure (8), a third term has been added to the shear capacity equation of the RC beams. This term represents the shear contribution of this technique in RC beams, and it is referred to by (V_f). Based on this, the shear capacity of NSM shear strengthened beams can be calculated simply based on the same concept of equation (2.1).

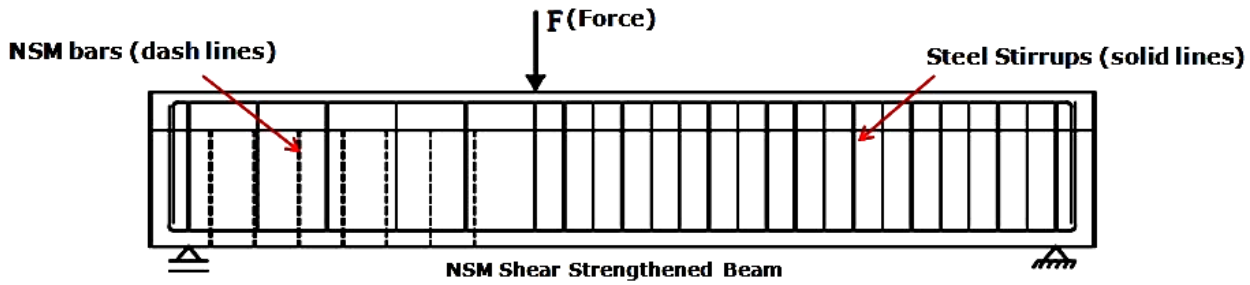

Figure (8): Representation of NSM shear strengthened beam

$$V_n = V_c + V_s + V_f \quad (2.1)$$

Where:

V_n: The shear capacity of the NSM shear strengthened beams

V_c: The shear strength provided by concrete strength.

V_s: The shear strength provided by steel stirrups.

V_f: The shear contribution of NSM technique in RC beams

The terms V_c and V_s can be calculated using the equations that have been already driven and used in many design cods, such as those in the American code (ACI), European code and other specifications. In contrast, this is not the case for the

calculation of shear contribution of NSM technique in RC. In fact, it is agreed that the shear contribution of such technique in RC beams is not yet fully achieved. Although there are few theoretical models to calculate the term $(\boldsymbol{V_f})$, they are based on experimental tests with small data. Furthermore these theoretical equations evaluate the shear contribution of NSM technique based on assumptions that were made corresponding to the obtained experimental results. This basically results in making the determination of the term $(\boldsymbol{V_f})$, in the equation above to be controversial and uncertain (Islam 2008). Therefore, the aim of this section is to examine the current theoretical models briefly as an evaluation method. Since it is believed that when more experimental data is available, these models could be improved more by modifying them. This would help to establish an efficient theoretical model to calculate the term $(\boldsymbol{V_f})$, accurately in the NSM shear strengthened beams.

2.5.1 De Lorenzis and Nannis' Model

According to De Lorenzis and Nanni (2001), a theoretical model was proposed based on an experimental test, which was carried out on eight T beams considering parameters, such as strengthening configuration, anchorage and spacing of NSM reinforcement bars as well as percentage of existing steel stirrups. In this model, the shear contribution of NSM technique can be calculated as a minimum value from two different equations. Basically, the first equation (V_{1F}) computes the shear contribution of such technique assuming that debonding of NSM bars is the govern mode of failure in the strengthened beams. The other kinds of failure modes that are examined in section (2.4) are ignored. In fact, this equation was built up based on three main assumptions. Firstly, the shear cracks have a constant angle of inclination equal to 45 degree. Secondly, at ultimate, there is an even distribution of bound stress over the effective length of the strengthening bars. The third assumption is that in all the NSM reinforcement bars that intersect by shear cracks, the bound stress is ultimate stress. This equation is shown as following.

$$V_{1F} = 2.\sum A_i f_i = 2.\pi.d_b.\tau_b.L_{tot} \qquad (2.2)$$

Where: A_i is the nominal cross-sectional area of the FRP rods, f_i is the tensile stress in the FRP rod at the crack location, and summation is extended to all the rods intersected

by a 45 degree crack. τ_b is the average bond strength of the FRP reinforcements. L_{tot} is the sum of the effective lengths of all the FRP reinforcements crossed by the crack. L_{tot} has to be calculated in the most unfavourable crack position, that is, the position in which it is minimum. Therefore V_{1F} can be written as following;

$$V_{1F} = 2.\pi.d_b.\tau_b.\ L_{tot\ min} \qquad (2.3)$$

Similarly, the second equation (V_{2F}) also bases on the first and the second assumptions above. However, it is stated that this equation can be used when the maximum strain in the NSM FRP bars reaches 4000 Micro-strain. Although the results that obtained using this model showed a quite close agreement when it was compared to the experimental results (table 2), the assumptions of this model might produce some errors. This is due to the fact that the bond behaviour of NSM reinforcement bars and the depth of beams play a significant role in making the second and third assumption above work. Moreover, it is mentioned that the first assumption is not always right, but it does not produce a great error. It is also important to mention that the type of NSM bars can also inspire the bound stress in the strengthened beams. Thus, by changing the FRP reinforcement type, the probability of obtaining a constant bound stress may not be achieved (De Lorenzis and Nanni 2001).

Table (2): Comparison between the theoretical and experimental results of De Lorenzis's and Nanni's experiment (De Lorenzis and Nanni 2001)

	Experimental				Theoretical			
Beam code (1)	V_c, kips (2)	V_s, kips (3)	V_{FRP}, kips (4)	V_n, kips (5)	V_c, kips (6)	V_s, kips (7)	V_{FRP}, kips (8)	V_n, kips (9)
BV	20.3	—	—	20.3	19.7	—	—	19.7
B90-7	20.3*	—	5.6	25.9	19.7	—	2.4	22.1
B90-5	20.3*	—	8.4	28.7	19.7	—	7.1	26.8
B90-5A	20.3*	—	21.5	41.8	19.7	—	16.5	36.2
B45-7	20.3*	—	16.9	37.2	19.7	—	15.1	34.8
B45-5	20.3*	—	19.7	40.0	19.7	—	20.0	39.7
BSV	20.3*	14.2	—	34.5	19.7	11.0	—	30.7
BS90-7A	20.3*	14.2†	12.0	46.5	19.7	11.0	11.8	42.5

V_C, V_S, V_{FRB} are shear resistance that provided by concrete strength, steel stirrups and NSM reinforcement bars, respectively.

2.5.2 Anwarul Islam's Formula

Anwarul Islam (2008) tested four beams having some percentage of steel stirrups and strengthened in shear by using vertical NSM carbon rods. Basically, the results of the experiment were then used to establish a theoretical formula to compute the shear contribution of Near Surface Mounted technique in RC beams. It was actually found that the effective strain in the carbon rods at the shear failure stage in those beams was equal to about 30% from the ultimate strain of the carbon bars. In addition, in this experiment, no shear failures such as debonding and/or fracture of NSM bars were obtained. Therefore, it was assumed that the shear contribution of NSM technique (v_f) when NSM reinforcement bars are used in RC beams can be calculated using equation (2.4):

$$V_f = \frac{1}{3}\frac{A_f \ f_{yf} \ d}{s} \ (sin\theta + cos\theta) \qquad (2.4)$$

Where

f_{yf} : The tensile yield strength of FRP bars

θ: The inclination of the FRP reinforcement and it is measured with respect to the horizontal axis of the beam (degree)

d: The distance from the external compression fiber to centroid of longitudinal tension reinforcement (mm)

A_f: Area of FRP reinforcement in shear (mm^2)

s: The spacing of the FRP reinforcement (mm)

In spite of the fact that this formula showed a reasonable agreement when it was compared to the obtained experimental results, it was built up based on assumptions correspond to a very small experimental data. Furthermore, this model does not consider many of the important variables, which are examined in the previous sections (Islam 2008). Therefore, if it will be used for huge experimental data, insufficient results might be obtained.

2.5.3 Dias and Barross' Model

According to Dias and Barros (2012), an analytical model was established to calculate the shear contribution of NSM technique in RC beams. Fundamentally, this model calculates the shear contribution of NSM technique bases on a similar concept to that of calculating the shear strength provided by steel stirrups. Nevertheless, the concept of using FRP effective strain is adopted instead of using the yield strain of steel stirrups. It is worth to mention this model was developed using the results of 40 tested RC beams taking into account parameters, such as the strength of concrete, the percentage of both steel stirrups and composite material, and the orientation of the NSM reinforcements. A safety factor (γ_s) equal to 1.3 was proposed with this model to make sure that 95% of the tested beams are in the safe side (Dias and Barros, 2012). By using this model, the shear contrition of this technique in RC beams and the FRP effective stain are calculated using equations (2.5) and (2.6).

$$\varepsilon_{fe} = V_f / (h_w \times \frac{A_{fv}}{S_f} \times E_f \times (\cot\alpha + \cot\theta_f) \times \sin\theta_f) \quad (2.5)$$

And

$$\varepsilon_{fe} = \{3.76888 \times e^{(-0.1160261\ \theta f + 0.0010437\ \theta f\text{^}2)} \times [(E_{sw}\rho_{sw} + E_f\rho_f)/(f_{cm}^{2/3})]\text{^} (-0.460679 \times e^{(0.0351199\ \theta f - 0.0003431\ \theta f\text{^}2)})\}/\gamma_s \quad (2.6)$$

Where:

ε_{fe} is the effective strain of FRP laminates. V_f is the shear contribution of NSM technique in RC beams. E_f is the elastic modules of FRP reinforcements. h_w is the web depth of the beam. A_{fv} is the cross sectional area of composite material that is formed by two lateral laminates. α and θ_f are the orientation of both shear failure cracks and composite material, respectively and they are measured with respect to the horizontal axis of the beam. s_f is the spacing of FRP reinforcements. f_{cm} is the concrete strength. ρ_{sw} and ρ_f are the percentage of steel stirrups and composite materials in the strengthened beams, respectively.

When the experimental results of the 40 tested beams were compared to the theoretical reults obtinaed using this model, a reasonable agreement between the two

type of results were achieved especially when a safety factore of 1.3 in stead of 1 was applied in the theoretical model. This is well shown in table(3).

Table (3): Comparison between the experimental and the theoretical outcomes of Dias's and Barros's model (Dias and Barros2012)

Beams	V_f^{exp} [kN]	ε_{fe}^{*} [‰]	$\gamma_f = 1.0$ (using equation (15))			$\gamma_f = 1.3$ (using equation (16))		
			ε_{fe}^{ana} [‰]	V_f^{ana} [kN]	k	ε_{fe}^{ana} [‰]	V_f^{ana} [kN]	k
2S-5LV-A	40.3	4.60	4.73	41.4	0.97	3.64	31.8	1.27
2S-8LV-A	63.7	4.55	4.04	56.6	1.13	3.11	43.5	1.46
2S-3LI45-A	37.9	7.04	8.08	43.6	0.87	6.22	33.5	1.13
2S-5LI45-A	56.5	6.28	6.50	58.4	0.97	5.00	45.0	1.26
2S-8LI45-A	70.3	4.90	5.00	71.8	0.98	3.85	55.2	1.27
2S-3LI60-A	35.4	6.02	7.16	42.1	0.84	5.51	32.4	1.09
2S-5LI60-A	61.3	6.25	5.84	57.3	1.07	4.49	44.0	1.39
2S-7LI60-A	69.7	5.07	4.91	67.5	1.03	3.78	52.0	1.34
2S-7LV-B	57.5	4.81	4.78	57.1	1.01	3.67	43.9	1.31
2S-10LV-B	71.5	4.20	4.18	71.2	1.00	3.21	54.8	1.31
2S-4LI45-B	53.4	7.61	8.74	61.3	0.87	6.72	47.1	1.13
2S-7LI45-B	70.7	5.76	6.59	80.9	0.87	5.07	62.3	1.14
2S-10LI45-B	85.6	4.88	5.26	92.3	0.93	4.05	71.0	1.21
2S-4LI60-B	49.6	6.46	7.77	59.6	0.83	5.98	45.8	1.08
2S-6LI60-B	54.4	4.73	6.47	74.3	0.73	4.97	57.2	0.95
2S-9LI60-B	65.3	3.79	5.14	88.7	0.74	3.95	68.2	0.96
4S-4LV-B	31.9	4.21	4.38	33.2	0.96	3.37	25.5	1.25
4S-4LVa-B	40.7	5.37	4.38	33.2	1.23	3.37	25.5	1.59
4S-7LV-B	33.6	2.81	3.95	47.3	0.71	3.04	36.4	0.92
4S-4LI45-B	42.7	6.08	5.95	41.7	1.02	4.57	32.1	1.33
4S-7LI45-B	64.0	5.21	4.83	59.4	1.08	3.72	45.7	1.40
4S-4LI60-B	43.5	5.67	5.27	40.4	1.08	4.05	31.1	1.40
4S-6LI60-B	51.7	4.50	4.61	53.0	0.98	3.55	40.8	1.27
2S-7LV-C	43.6	3.57	3.37	41.1	1.06	2.59	31.6	1.38
2S-4LI45-C	33.9	4.74	4.93	35.2	0.96	3.79	27.1	1.25
2S-7LI45-C	48.0	3.83	3.70	46.4	1.03	2.85	35.7	1.34
2S-4LI60-C	33.1	4.23	4.42	34.6	0.96	3.40	26.6	1.24
2S-6LI60-C	42.7	3.64	3.67	43.0	0.99	2.82	33.1	1.29
4S-4LI45-C	26.0	3.64	3.36	24.0	1.08	2.59	18.5	1.41
4S-7LI45-C	31.6	2.52	2.72	34.1	0.92	2.10	26.3	1.20
4S-4LI60-C	25.1	3.21	3.00	23.5	1.07	2.31	18.0	1.39
4S-6LI60-C	35.1	2.99	2.62	30.8	1.14	2.02	23.7	1.48
3S-6LV-D	44.7	5.79	6.56	50.7	0.88	5.04	39.0	1.15
3S-10LV-D	81.5	6.68	5.69	69.4	1.17	4.37	53.4	1.53
3S-5LI45-D	81.7	11.42	11.70	83.7	0.98	9.00	64.4	1.27
3S-9LI45-D	117.4	9.37	8.79	110.2	1.07	6.76	84.7	1.39
3S-5LI45F1-D	85.8	11.99	11.70	83.7	1.02	9.00	64.4	1.33
3S-5LI45F2-D	80.9	11.31	11.70	83.7	0.97	9.00	64.4	1.26
3S-5LI60-D	84.6	10.82	10.37	81.1	1.04	7.98	62.4	1.36
3S-8LI60-D	127.9	10.90	8.61	100.9	1.27	6.62	77.6	1.65
5S-5LI45-D	74.9	10.47	8.68	62.1	1.21	6.68	47.8	1.57
5S-9LI45-D	108.9	8.69	6.93	86.9	1.25	5.33	66.8	1.63
5S-5LI60-D	73.4	9.38	7.66	59.9	1.22	5.90	46.1	1.59
5S-5LI60F-D	72.6	9.28	7.66	59.9	1.21	5.90	46.1	1.57

2.5.4 Barros, Bianco and Montis' Model

This model was developed based on the fact that the FRP reinforcement might fail along their available bond length by concrete tensile fracture, debonding or tensile rupture of the FRP reinforcement. Barros, Bianco and Monti (2009) in fact stated that **"**the different and asymmetric geometrical features support the assumption that, in the case of the strips glued into thin slits in the concrete web face, the concrete fracture surface, envelope of the principal tensile stresses induced in the surrounding concrete, has a semi-conical shape propagating from the inner tip of the strip embedded length. The concrete average tensile strength, f_{ctm}, is distributed throughout each of the resulting semi-conical surfaces orthogonally to them in each point. The NSM shear contribution in RC beams, V_f, could be calculated by adding the contribution of each strip, V_{fi}, parallel to its orientation, and projecting the resulting force orthogonally to the beam axis**"** (Barros, Bianco and Monti 2009). Based on this concept, equation (2.7) was proposed

$$V_f = 2 \sin\beta \sum_{i=1}^{N_f} V_{fi}^{P} \qquad (2.7)$$

Where

N_f: The number of the strips crossing the shear crack.

V_{fi}^{P}: The shear contribution provided by each strip. This can be assumed as the minimum value among three possible contributions ascribed respectively to deboning failure, $V_{fi}^{P.db}$, tensile rupture of the FRP reinforcement, $V_{fi}^{P.tr}$, or concrete tensile fracture, $V_{fi}^{P.cf}$, i.e.:

$$V_{fi}^{P} = \min \{V_{fi}^{P.db}; V_{fi}^{P.tr}; V_{fi}^{P.cf}\} \qquad (2.8)$$

Where

$$V_{fi}^{P.db} = 2 \times (a_f + b_f) \times \tau_b(L_f) \times L_f \qquad (2.9)$$

$$V_{fi}^{P.tr} = a_f \times b_f \times f_{fu} \qquad (2.10)$$

$$V_{fi}^{P.cf} = \int_{Cfi\ (L_{fi;}\ \alpha_{fi})} (f_{ctm} \times \sin\alpha_{fi}) \times d \times C_{fi} \quad (2.11)$$

Where

$\tau_b(L_f)$: The length dependent value of the average bond strength (MPa)

f_{fu}: The ultimate tensile strength of FRP reinforcement (MPa)

a_f and b_f: The dimensions of the FRP strips

$Cfi\ (L_{fi;}\ \alpha_{fi})$: The semi-conical surface associated to the i-th strip

α_{fi}: The angle between the generatrices and the axis of the semi-con attributed to the i-th strip (it has a length dependency with the available bond length)

This model is a very complex one. This is because this model assumes the possible failure mechanisms in the NSM shear strengthened beams, which are the tensile rupture of the FRP reinforcements, debonding and the concrete fracture, and allows the interaction between the FRP reinforcements to be accounted for (Barros, Bianco and Monti 2009). In addition to this, the average bond stress and the bond length of the FRP reinforcement need to be available to calculate the two terms; $V_{fi}^{P.db}$ and $V_{fi}^{P.tr}$. Furthermore, to find the semi-conical surface associated to the i-th strip, $Cfi\ (L_{fi;}\ \alpha_{fi})$, a very complex and long procedure need to be applied (Barros, Bianco and Monti 2009). This procedure is not mentioned here, but it can be found in the original reference used in this section.

2.6 Summery

Near Surface Mounted technique in shear strengthening of RC beams is analysed in this chapter. Examining the significant parameters that influence the shear failure modes in the strengthened beams, the efficiency of such technique, and the enhancement in the shear capacity of RC beams was the main concern of the literature review. In this chapter, the current theoretical models, which were proposed to compute the shear contribution of such strengthening technique in RC beams, were also examined. From analysing the information in this chapter, the following conclusion was drawn.

- The NSM shear strengthening technique shows better performance compared to EFRP technique in terms of the load carrying capacity, deflection behaviour of RC beams, preventing early debonding failure, and increasing the tensile strain of NSM reinforcements.
- It is seemed to be that there are not noticeable differences between using steel stirrups, and NSM techniques for shear strengthening in RC beams in terms of the enhancement in the shear strengthen of RC beams. Nevertheless, the NSM shear strengthened beams appear to have better deflection performance.
- Using inclined NSM reinforcements (bars/laminates) (especially the arrangement of 45^{o}) with close spacing is more effective than using the vertical arrangement with close spacing, regarding the improvement in the shear contribution of NSM technique in RC beams, and also preventing debonding failure.
- The presence of the high percentage of existing steel stirrups in the NSM shear strengthened beams illustrated a fall in the efficiency of this technique. However, using certain amount of it seems to be very helpful in improving the shear contribution of NSM technique in RC beams.
- The type and material of Near Surface Mounted FRP reinforcements are important factors in increasing both the effectiveness of this technique, and the tensile strain of NSM FRP reinforcements.
- IT was found that increasing the percentage of composite materials in the NSM shear strengthened beams decreases the shear contribution of NSM technique in RC beams. Also it changes the mode of failure in the strengthened beams from debonding of the NSM reinforcements to be by splitting the concrete cover along the longitudinal flexural bars.
- The compressive strength of concrete appears to be a significant variable that by raising it, the effectiveness of this technique can improve.

- The anchorage of NSM reinforcements can changes the shear failure mode from debonding of the NSM FRP reinforcements to a separation of the concrete cover, and increase the shear capacity of the beams.
- Three main modes of failures can be observed in the NSM shear strengthened beams. Once the debonding failure, which is the first kind, is prevented, splitting the concrete cover (the second type) is more likely to occur. Anchorage the NSM reinforcements, using high strength concrete, and using close spacing with inclined FRP reinforcements can be used as solutions to prevent the debonding failure. The third failure mode is the tensile rapture of the FRP reinforcements, and it is affected mainly by the properties of the FRP reinforcements.

Finally, it was concluded that, although there are few theoretical models were proposed to compute the shear contribution of such technique, such as those considered in section (2.5), all of them based on small experimental data. In addition to this, they do not consider the influences of all the parameters and failure modes. Furthermore, it was found that these models differ in their way in evaluating the term (V_f). Finally, it was found that there is not a final model to compute the contribution of this technique in RC beams accurately. Based on that, the aim and objectives of this project, which are mentioned in chapter one, were built up.

3 EVALUATIONS OF THE CURRENT THEORETICAL MODELS

This chapter deals mainly with the evaluations of the current theoretical models that were proposed previously to calculate the analytical shear contribution of NSM technique in RC beams. This will help later to select the best theoretical model to be then used to establish a design-oriented equation to calculate the shear contribution of NSM technique in RC beams accurately. A brief overview of the shear design in the RC beams and the difference in this design when NSM technique is used in shear strengthening is also considered in the first section. The selection of the current theoretical models, as well as the generation of the experimental database, which is used in this project for the evaluation and modification works, are also considered in this chapter. The last section will be the discussion of the results of evaluation of the three evaluated models.

3.1 Shear Design of Reinforced Concrete Beams

Based on the design codes of reinforced concrete structures, the shear capacity of the reinforced concrete beams can be calculated as the summation of two terms. The first term basically accounts for the action of mechanisms, such as the interlock of aggregate, the dowel action of the bending reinforcements, and also the uncracked concrete in the compression zone (Triantafillou 1998). The second term accounts for the impacts of shear reinforcements such as steel stirrups and/or inclined bars. This term is modelled by using the truss analogy approach. An upper bound to the shear capacity of RC beams is achieved by considering the compression crushing of the concrete blocks, which are formed between the diagonal shear cracks (Triantafillou 1998). For example, according to Eurocode2, the theoretical shear capacity (V_{Rd}) of a reinforced concrete (RC) beam is given in equation (3.1).

$$V_{Rd} = \min\left(V_{cd} + V_{Wd}, V_{Rd2}\right) \tag{3.1}$$

Where

$$V_{cd} = \tau_{Rd} \min\left(2, 1.2+40\rho_{\ell}\right) \max\left(1, 1.6-d\right)\ b_w d \tag{3.2}$$

$$V_{wd} = \left(\frac{A_{sw}}{S\ bw}\right) f_{ywd}\ \ 0.9\ b_w d\ (1+\cot\alpha)\sin\alpha \tag{3.3}$$

$$V_{Rd2} = 0.5 \max\left(0.5,\ 0.7 - \frac{fck}{200}\right) f_{cd}\, 0.9\, b_w\, d\, (1+\cot\alpha) \qquad (3.4)$$

Where

τ_{Rd}: the basic design shear strength = $0.25 f_{ck}/\gamma_c$, f_{ck}: characteristic compressive cylinder strength of concrete at 28 days, γ_c: partial safety factor for concrete equal to 1.5, ρl: longitudinal reinforcement ratio (percentage), d: effective depth of beam cross section, b_w: minimum width of beam cross section over the effective depth, A_{sw}: cross sectional area of shear reinforcement (steel stirrups), s: spacing of shear reinforcement measured along the longitudinal axis, f_{ywd} : design yield strength of steel shear reinforcement, α :angle of the shear reinforcement to the longitudinal axis of the RC member, and f_{cd}: design value of concrete cylinder compressive strength = f_{ck}/γ_c.

It should be mentioned that, the value of (V_{cd}) above should be reduced to be ($r_s \times V_{cd}$) for the case of the design under seismic loading. r_s here is a reduction factor, which depends on the ductility demand; in other word on the ductility class of the RC structures (Triantafillou 1998). It is also stated if the strengthening of the RC beams is carrying out in the absence of full repair, which is in the case of damaged beams (beams with diagonally cracks), (V_{cd}) in equation (3.1) above should be reduced. In fact, it is mentioned this reduction depends on the level of deterioration of the damaged beams, and it can only be calculated on a case by case basis (Triantafillou 1998).

As far as NSM technique is concerned, the only difference in the shear design of RC beams when NSM technique is used in shear strengthening of RC beams is that, a new term has been added to the shear capacity equation of RC beams. This term is assumed to be additive to both the shear strengths provided by the concrete and the steel stirrups, and it is referred to by(V_f). V_f here represents the shear contribution of NSM technique in the strengthened beams. The issue with the determination of this contribution is that it is not yet achieved. On the other hand, both the determinations of the shear contributions of concrete and steel stirrups in RC beams are well established in many design codes, such as Eurocode2 as mentioned above, British standards and many others. Therefore, the works, which are presented in this chapter and the following one, are to achieve a design oriented equation to calculate the new term V_f accurately in the NSM shear strengthened beams.

3.2 The Selection of the Current Theoretical Models

Three of the current theoretical models are selected and evaluated in this project. The reason behind this as mentioned previously is the fact that, the best model from the evaluation will be then modified in chapter (4). Both the evaluation, and the modification processes in this chapter and the following chapter of the dissertation are based on experimental database, which is shown and explained in the next section.

It is important to emphasise that, the available experimental data has contributed in the selection of the three evaluated models in this project, which are the ones that proposed by **A.K.M Anwarul Islam, (Dias and Barros) and T.C. Triantafillou**, respectively. In fact, the absence of some of the information in the available experimental data prevented from considering the other models, that have been examined in chapter two, such as the models of (De Loresnziz and Nanni), or the one of (Barros, Bianco and Monti). These models for example need the average bond stress as well as the bond length of the FRP reinforcement in the calculation of the term (V_f). The average bond stress in its turn needs a bond test to be carried out in order to find it, and most of the experimental studies did not carry it out. The complexity of these two models was also being taken into account as a secondary reason. However, the first reason was the main factor that contributed in ignoring these two models, since (V_f) cannot be calculated using the available experimental data, and therefore these models cannot be calibrated later.

It is also significant to state that the three selected models were developed using the well-known approach, which is the truss analogy one, assuming that the contribution of this technique in the strengthened beams to be additive to the contributions of concrete and steel stirrups. This approach was established long time ago, and it is used to calculate the shear contribution of steel stirrups in RC beams in many designs codes. The use of such approach in such strengthening technique also means the designers and researchers in this field will be so familiar with it, and with the work presented in this dissertation. Therefore, this reason was also taken into consideration in the selection of the models.

In the evaluation of the three models, all the principles, assumptions, details, derivation steps and the approach that were used in the development of these models are included. This will help basically in comparing these models not only in terms of their accuracy in the estimation of the shear contribution of this technique in RC beams, but also in terms of the considered parameters in the development of the analytical

formulations, and the degree of sophistication, and the effects of the latter on the effectiveness of this technique in shear strengthening. In addition, including all of these details are important, since the best model based on the evaluation will be then modified in this dissertation, and finally proposed. Therefore, the details of the proposed model will be required to be stated with it. Given that, the best model is not yet known, including the complete details of all the evaluated models will be therefore required.. The detailed evaluations of the three selected models based on the created database are presented in the next sections.

3.3 The Generation of the Experimental Database

The works presented in this project in particular in chapter three and four are based on experimental database, which was generated for the purposes of these two chapters. This database was collected using all the available technical papers that contain experimental data. This includes 24 papers that have been published during the last 12 years. However, it is important to state that not all of these papers have new data, as some of them used previous data of other researchers in their studies. As a result, the database of this project was selected in a way that the repetition of the data was avoided. Furthermore, the experimental database was organised in terms of the parameters, which were examined in the included experimental studies. **Table (A)** in **appendix (A)** shows this database. All the information that is needed to carry out the evaluation and the modification processes in the dissertation is presented in the database. Therefore, in some occasions in this project, referring to this table for clarity purposes was made.

This table consists of 136 samples (RC beams), and 22 columns. Each one of these columns represents one parameter of the created database. The table is continued on few pages. See notices at the end of this table as well as notation list at the beginning of the dissertation for the definitions of the parameters. Also, note the numbering of the columns and rows in this table.

3.4 The Evaluation of A.K.M Anwarul Islam's Model

According to Islam (2008), this model was built up based on an experimental program. Four rectangular beams were tested and one of these beams was used as a control beam. Carbon FRP (CFRP) bars were used as strengthening reinforcements. Different spacing and one angle of inclination equal to 90^o were considered in the tested beams. Some percentage of steel stirrups was also used in the tested beams. No debonding or fracture of CFRP bars was observed at the failure stage of the beams. In addition to this, the ratio of the effective strain to ultimate strain of CFRP bars in the three beams at failure was almost noticed to be equal to (1/3). In other word, on average at failure of the beams, one third of the ultimate strain of the CFRP reinforcements was observed to be effective in the NSM shear strengthened beams. Based on that, the following formula was proposed to calculate the nominal shear contribution of NSM CFRP reinforcements used in shear strengthening of RC beams. This equation is in fact similar to that is used in calculating the shear contribution of steel stirrups in RC beams in the American Concrete Institute (ACI 318) code. However, instead of using the yield stress of the steel shear reinforcements, the concept of the effective FRP strain was adopted, and in this equation it is equal to (1/3).

$$V_f = \frac{1}{3}\frac{A_f\ f_{yf}\ d}{s}\ (sin\theta + cos\theta) \qquad (3.5)$$

Where

V_f: The shear contribution of NSM technique in RC beams

f_{yf}: Tensile yield strength of FRP reinforcement (MPa)

θ: The inclination of the FRP reinforcements and it is measured with respect to the horizontal axis of the beam (degree)

d: The distance from the external compression fiber to centroid of longitudinal tension reinforcement (mm)

A_f: Area of FRP reinforcement in shear (mm^2)

s: The spacing of the FRP reinforcement (mm)

As far as the evaluation of this model is concerned, this model was evaluated using the generated database. Basically, by substituting all the terms of equation (3.5) using the information in table (A) in appendix (A), the values of (V_f) theoretically were obtained for the whole experimental data. It is important to notice that, this formula was used in this project to estimate the nominal theoretical shear contribution of NSM

technique in RC beams strengthened using FRP laminates and/or FRP bars. This is well illustrated in table (4).

According to the results of the evaluation, this model shows insufficient results. In fact, by obtaining the ratio (K) which represents the ratio between (V_f) experimentally (reported in the created database) and (V_f) theoretically (obtained using this formula), it was found that only 27% of the estimated values of (V_f) is in the safe side. In other word, 27% of the whole beams in table (4) have (K) values equal or greater than unity. Given that, K≥1 represents a safe condition, since it means the theoretical shear contributions of NSM technique in RC beams are not greater than the experimental values. The average value of the ratio K is equal to about (0.79). The low values of the K ratios obtained using this model as shown in table (4); basically reflect a bad agreement with the experimental results. It also demonstrates this formula overestimates the theoretical (V_f). In other word, it means that the experimental values of (V_f) are less than the theoretical ones. This in fact can be very dangerous, as this formula estimated values, which cannot be reached in reality in many beams. Consequently, it can be said using this formula in practice may lead to serious issues in the strengthened beams. Figure (9) shows the relationship between (V_f) experimentally and (V_f) theoretically.

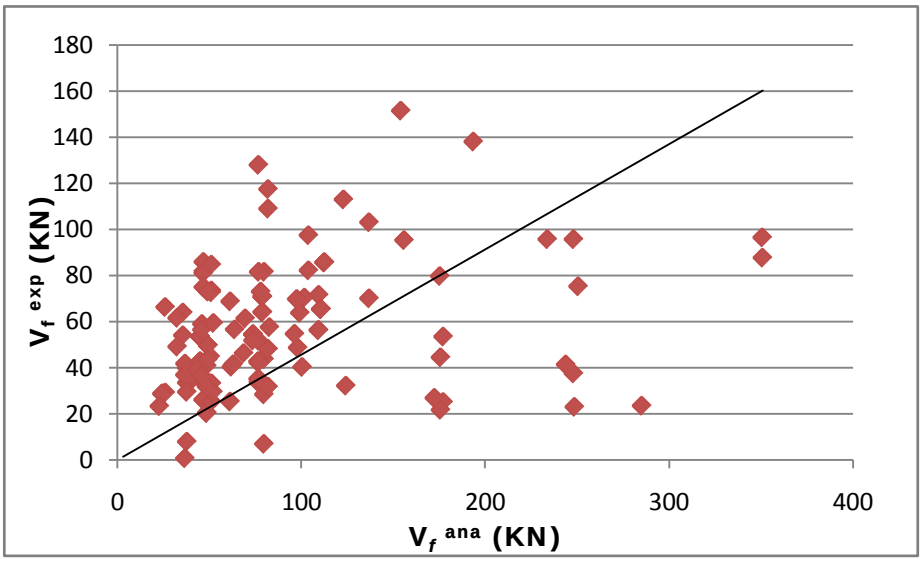

Figure (9): The relationship between (V_f) experimentally and (V_f) analytically calculated using A.K.M Anwarul Islam's model

It can be seen from this figure that many points fall under the diagonal line, and this basically confirms the bad agreement between the theoretical and the experimental results. The evaluation results of this formula were in fact expected, since this equation

is a simple one. In addition, it was developed based on very few experimental specimens. Furthermore, few parameters examined in chapter two were considered in the development of this model. Finally, no failure mode was observed in the tested beams. Therefore, when it was used with such huge data, insufficient results were obtained. Section **(3.7)** later will discuss the obtained results, and compare them with others of the other models in more details.

3.5 The Evaluation of Dias and Barross' Model

This theoretical model was built up using the results of 40 T-section reinforced concrete beams strengthened using Carbon FRP (CFRP) laminates. Various parameters, such as percentage of existing steel stirrups and composite material, angle of inclination of the FRP reinforcements, spacing, and concrete strength, were considered in the tested beams. The three failure modes examined in chapter two were also observed at the shear failure stage in the NSM shear strengthened beams. These failure modes were debonding, tensile rapture of the FRP reinforcement, and fracture of the concrete. The experimental shear contribution of FRP laminates in this experiment was obtained by subcontracting the shear capacity of the control beams from the shear resistance of the strengthened beams. It was in fact assumed in this approach that the steel stirrups give the same contribution in the strengthened and in the corresponding control beams (Dias and Barros 2012).

Regarding the development of this model, it was fundamentally developed using a similar approach to that of calculating the shear contribution of steel shear reinforcements in RC beams, but instead of using the strain at yield initiation of the steel stirrups, the concept of effective strain in the FRP reinforcements (ε_{fe}) was adopted (Dias and Barros 2012). Following this concept, the force resulting from the tensile stress in the CFRP laminates crossing the shear failure crack (F_f) was defined as shown in equation (3.6).

$$F_f = n_f \times A_{fv} \times f_{fe} \qquad (3.6)$$

Where

f_{fe} is the effective stress in the FRP reinforcements and is obtained by multiplying the elastic modulus of the FRP reinforcements (E_f), by the FRP effective strain (ε_{fe}).

Given that,

$$A_{fv} = 2 \times a_f \times b_f \quad (3.7)$$

Where

A_{fv} is the cross sectional area of the FRP reinforcements (mm^2).

a_f and b_f are the dimensions of the FRP laminate cross section.

By also using the triangular geometry shown in figure (10), equation (3.8) was written as below.

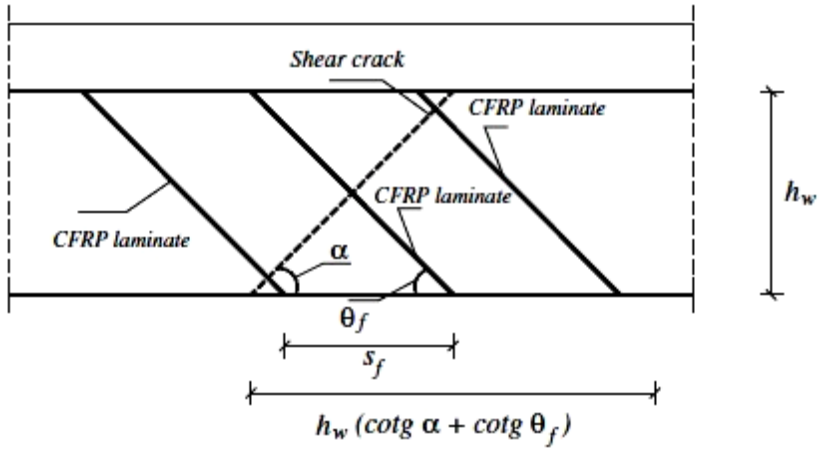

Figure (10): Data for the theoretical definition of the FRP effective strain in a T-beam (Dias and Barros 2012)

$$n_f = \frac{h_w\ (\cot\ \alpha + \cot\ \theta_f)}{S_f} \quad (3.8)$$

Where

n_f is the number of FRP reinforcements crossed by the shear failure crack.

h_w is the web depth of the beam (mm).

α is the orientation of the shear failure crack (degree).

S_f is the spacing of the FRP reinforcements (mm).

θ_f is the inclination of the CFRP laminates with respect to the beam axis (degree).

Then, the shear contribution of the FRP reinforcement in RC beam (V_f) was defined as the vertical projection of the force (F_f) as shown in equation (3.9).

$$V_f = F_f \times \sin \theta_f \quad (3.9)$$

Thereafter, by substituting equations (3.6), (3.7) and (3.8) in equation (3.9), and knowing that (f_{fe}) is obtained by multiplying the elastic modulus of the CFRP (E_f), by the FRP effective strain (ε_{fe}), (V_f) was written as in equation (3.10).

$$V_f = h_w \times \frac{Afv}{Sf} \times \varepsilon_{fe} \times E_f \times \left(\cot \alpha + \cot \theta_f\right) \times \sin\theta_f \quad (3.10)$$

And as a result; the (ε_{fe}) can be written as following,

$$\varepsilon_{fe} = V_f / \left(h_w \times \frac{Afv}{Sf} \times E_f \times \left(\cot \alpha + \cot \theta_f\right) \times \sin\theta_f \right) \quad (3.11)$$

Then, for each inclination of the FRP reinforcement (θ_f); (45º, 60º and 90º); it was defined the equation that relates ε_{fe} with the product ($E_{sw}\,\rho_{sw} + E_f\,\rho_f$)/ ($f_{cm}^{2/3}$). This dependency relationship was established based on the experimental program that was carried out. Basically, four parameters according to their experimental results were found to be having high influences on the behaviour of the NSM shear strengthened beams. These parameters are the angle of inclination of the FRP reinforcement (θ_f), the concrete strength in terms of the average value of the concrete compressive strength in cylinders (f_{cm}), the percentage of both the existing steel stirrups (ρ_{sw}) and composite material (ρ_f). Therefore, these four factors were taken into consideration in the development of this analytical formulation throughout the established dependency relationship mentioned above. The three equations of the three FRP reinforcement arrangements correspond to the best fit of the values of (ε_{fe}) (determined using equation (3.11)), considering the experimental results of V_f (for the 40 tested beams), and 45º for the orientation of the shear failure crack (α) (Dias and Barros 2012).

These equations are:

1- For FRP laminates at 90º

$$\varepsilon_{fe} = 0.5162 \times (E_{sw}\,\rho_{sw} + E_f\,\rho_f)/(f_{cm}^{2/3})^{-0.675} \quad (3.12)$$

2- For FRP laminates at 60°

$$\varepsilon_{fe} = 0.153 \times (E_{sw}\rho_{sw} + E_f\rho_f)/(f_{cm}^{2/3})^{-1.102} \quad (3.13)$$

3- For FRP laminates at 45°

$$\varepsilon_{fe} = 0.1685 \times (E_{sw}\rho_{sw} + E_f\rho_f)/(f_{cm}^{2/3})^{-1.117} \quad (3.14)$$

Noticed: The modulus of elasticity of steel stirrups (E_{sw}) = 200 GPa

By then using equations (3.12), (3.13) and (3.14), it was defined a general form of equation that allows estimating ε_{fe} from the parameter $[(E_{sw}\rho_{sw} + E_f\rho_f)/(f_{cm}^{2/3})]$ and the FRP orientation (θ_f).

$$\varepsilon_{fe} = [3.76888 \times e^{(-0.1160261\,\theta_f + 0.0010437\,\theta_f\wedge 2)} \times [(E_{sw}\rho_{sw} + E_f\rho_f)/(f_{cm}^{2/3})]\wedge(-0.460679 \times e^{(0.0351199\,\theta_f - 0.0003431\,\theta_f\wedge 2)})]/\gamma_s \quad (3.15)$$

Where

ρ_f: The percentage of the composite material (FRP reinforcement) in the strengthened beams
ρ_{sw}: The percentage of the steel stirrups in the strengthened beams
E_f: The tension modulus of elasticity of FRP reinforcement (GPa)
E_{sw}: The modulus of elasticity of steel stirrups (200 GPa)
f_{cm}: The tensile strengthen of the concrete (MPa)
γ_s: A factor of safety equal to (1.3), and it is equal to the average value of the K ratios of the 40 tested beams.

Regarding the evaluation of this model, the created database was used to evaluate this model. By basically using equations (3.10) and (3.15), both the theoretical FRP effective strain and the theoretical shear contribution of NSM technique were calculated for the 136 beams of the database. The ratio, K, between (V_f) experimentally and (V_f) theoretically (obtained using this model) for the 136 beams was also found. This is shown in table (4). The results of evaluation of this model in this table and in figure (11) illustrate a better performance compared to A.K.M Anwarul Islam's formula. In fact, 68.6% of the obtained results are in the safe side. In other word, 68.6% of the 136 beams have K ratio equal or greater than one, where K≥1 represents a safe condition.

Additionally, the values of the K ratios in table (4) demonstrate this model has better agreement with the experimental results. The better agreement here means that the values of the K ratios are near to unity and at the same time in the safe side. The average value of the ratio (K) of the 136 samples is equal to 1.268. This is also greater than that obtained by using the first evaluated model.

The better behaviour of this theoretical model can be due to the fact that, this model is more sophisticated compared to A.K.M Anwarul Islam's equation. This is because the FRP effective strain in this model is calculated using equations, which were defined using the dependency relationship mentioned above. This relationship was established based on the outcomes of 40 tested beams taking into account the influences of the four important parameters stated above. In fact, according to chapter two of this dissertation, the influences of the these four parameters were discovered in many research programs to be able to increase the effectiveness of this technique by means of shear strengthening technique in RC beams. Therefore, the better prediction ability of this model was also expected. More reasons and comparisons will be examined in more details in section **(3.7)**.

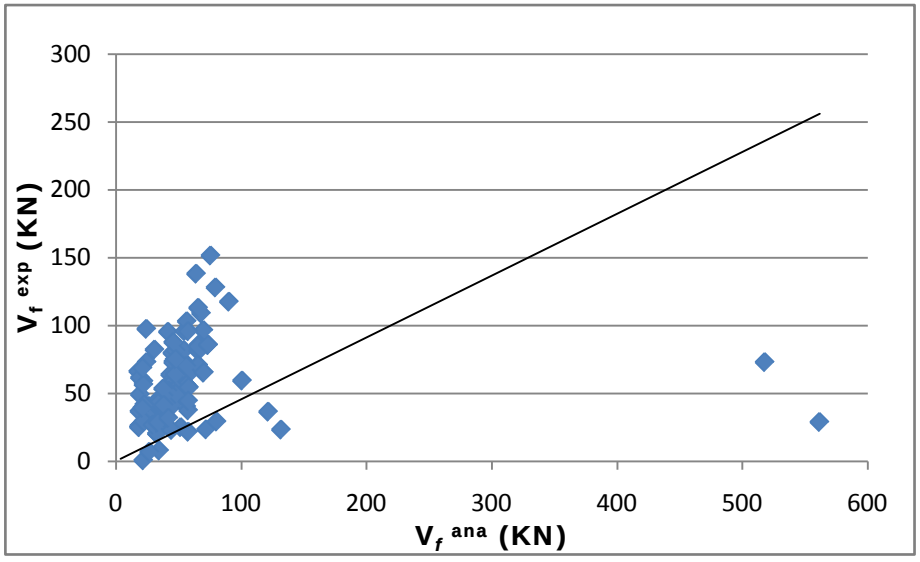

Figure (11): The relationship between V_f experimentally and V_f analytically calculated using Dias and Barross' model

Table (4): Comparison between the experimental and analytical values of both Anwarul Islam's model and Dias and Barross' model

		Anwarul Islam's model		Dias and Barross' model		
Sample No.	V_f^{exp} **(KN)**	V_f^{ana} **(KN)**	**K**	ε^{ana}	V_f^{ana} **(KN)**	**K**
Beam 1 (DB12)	40.3	62.06088	0.649362	4.740249514	31.892646	1.264
Beam 2 (DB12)	63.7	99.297408	0.641507	4.028486244	43.366185	1.469
Beam 3 (DB12)	37.9	38.26368967	0.990495	8.347129065	34.625511	1.095
Beam 4 (DB12)	56.5	63.83079141	0.885153	6.671475829	46.166225	1.224
Beam 5 (DB12)	70.3	101.7592327	0.690846	5.096415673	56.222595	1.25
Beam 6 (DB12)	35.4	41.73624057	0.848184	7.18197603	32.495954	1.089
Beam 7 (DB12)	61.3	69.56040095	0.881249	6.060348916	45.701632	1.341
Beam 8 (DB12)	69.7	97.58473515	0.714251	5.00130257	52.90991	1.317
Beam 9 (DB12)	57.5	82.74784	0.694882	4.85338622	44.662189	1.287
Beam 10 (DB12)	71.5	109.5153787	0.652876	4.291652377	56.277469	1.27
Beam 11 (DB12)	53.4	45.05545712	1.185206	8.900076737	48.014992	1.112
Beam 12 (DB12)	70.7	78.91879432	0.895858	6.937092154	65.553157	1.079
Beam 13 (DB12)	85.6	112.6386428	0.759952	5.455719837	73.582608	1.163
Beam 14 (DB12)	49.6	49.25128869	1.00708	8.09587275	47.743776	1.039
Beam 15 (DB12)	54.4	73.87693304	0.73636	6.559345227	58.023623	0.938
Beam 16 (DB12)	65.3	110.8153996	0.589268	5.281387605	70.078315	0.932
Beam 17 (DB12)	31.9	48.67350164	0.655387	4.45296089	25.952332	1.229
Beam 18 (DB12)	40.7	48.67350164	0.836184	4.45296089	25.952332	1.568
Beam 19 (DB12)	33.6	76.85289733	0.437199	3.991518961	36.731051	0.915
Beam 20 (DB12)	42.7	45.05545712	0.947721	6.015596709	32.453521	1.316
Beam 21 (DB12)	64	78.91879432	0.81096	5.019238554	47.430094	1.349
Beam 22 (DB12)	43.5	49.25128869	0.883226	5.408204025	31.893792	1.364
Beam 23 (DB12)	51.7	76.73856279	0.673716	4.654418442	41.991859	1.231
Beam 24 (DB12)	43.6	79.82980133	0.546162	3.450792689	32.386898	1.346
Beam 25 (DB12)	33.9	46.80068437	0.724348	5.060715327	27.8452	1.217
Beam 26 (DB12)	48	81.97572102	0.585539	3.944533247	38.016059	1.263
Beam 27 (DB12)	33.1	51.15904186	0.647002	4.638631379	27.899619	1.186
Beam 28 (DB12)	42.7	76.73856279	0.556435	3.758258749	33.906765	1.259
Beam 29 (DB12)	26	46.80068437	0.555547	3.420557302	18.82068	1.381
Beam 30 (DB12)	31.6	81.97572102	0.38548	2.854013311	27.506002	1.149
Beam 31 (DB12)	25.1	51.15904186	0.490627	3.098698024	18.637501	1.347
Beam 32 (DB12)	35.1	76.73856279	0.457397	2.666807163	24.05976	1.459
Beam 33 (DB12)	44.7	50.55887418	0.884118	6.763097051	40.200221	1.112
Beam 34 (DB12)	81.5	79.82980133	1.020922	5.817910371	54.603126	1.493
Beam 35 (DB12)	81.7	46.80068437	1.745701	12.01425007	66.10512	1.236
Beam 36 (DB12)	117.4	81.97572102	1.432131	9.364409136	90.250965	1.301
Beam 37 (DB12)	85.8	46.80068437	1.833307	12.01425007	66.10512	1.298
Beam 38 (DB12)	80.9	46.80068437	1.728607	12.01425007	66.10512	1.224
Beam 39 (DB12)	84.6	51.15904186	1.653667	10.88450097	65.466171	1.292

Table (4): continued

		Anwarul Islam's model		Dias and Barross' model		
Sample No.	V_f^{exp} **(KN)**	V_f^{ana} **(KN)**	**K**	ε^{ana}	V_f^{ana} **(KN)**	**K**
Beam 40 (DB12)	127.9	76.73856279	1.666698	8.818715624	79.561876	1.608
Beam 41 (DB12)	74.9	46.80068437	1.600404	8.521684223	46.888233	1.597
Beam 42 (DB12)	108.9	81.97572102	1.328442	7.05816655	68.02419	1.601
Beam 43 (DB12)	73.4	51.15904186	1.434741	7.638887491	45.945029	1.598
Beam 44 (DB12)	72.6	51.15904186	1.419104	7.638887491	45.945029	1.58
Beam 45 (DB09)	20.2	48.61948	0.415471	5.641874821	32.881449	0.614
Beam 46 (DB09)	42.2	76.7676	0.549711	4.85338622	44.662189	0.945
Beam 47 (DB09)	56.2	109.39383	0.51374	4.291652377	56.277469	0.999
Beam 48 (DB09)	53.4	45.00545106	1.186523	8.900076737	48.014992	1.112
Beam 49 (DB09)	70.7	78.83120409	0.896853	6.937092154	65.553157	1.079
Beam 50 (DB09)	85.6	112.5136277	0.760797	5.455719837	73.582608	1.163
Beam 51 (DB09)	49.6	49.19662578	1.008199	8.09587275	47.743776	1.039
Beam 52 (DB09)	54.4	73.79493867	0.737178	6.559345227	58.023623	0.938
Beam 53 (DB09)	65.3	110.692408	0.589923	5.281387605	70.078315	0.932
Beam 54 (JSCA12)	33.41	37.8075	0.883687	5.636981662	38.212091	0.874
Beam 55 (JSCA12)	53.94	35.64525284	1.513245	9.10214296	58.173122	0.927
Beam 56 (JSCA12)	39.88	37.8075	1.054817	5.636981662	38.212091	1.044
Beam 57 (JSCA12)	63.82	35.64525284	1.790421	9.10214296	58.173122	1.097
Beam 58 (JSCA12)	29.4	37.8075	0.777623	5.636981662	38.212091	0.769
Beam 59 (DB08)	0.6	36.736	0.016333	5.42742635	21.882252	0.027
Beam 60 (DB08)	25.2	61.3032	0.411072	4.740249514	31.892646	0.79
Beam 61 (DB08)	48.6	98.08512	0.495488	4.028486244	43.366185	1.121
Beam 62 (DB08)	7.8	37.79654141	0.206368	8.347129065	34.625511	0.225
Beam 63 (DB08)	41.4	63.05150317	0.656606	6.671475829	46.166225	0.897
Beam 64 (DB08)	40.2	100.5168891	0.399933	5.096415673	56.222595	0.715
Beam 65 (DB08)	35.4	41.22669712	0.858667	7.18197603	32.495954	1.089
Beam 66 (DB08)	46.2	68.71116187	0.67238	6.060348916	45.701632	1.011
Beam 67 (DB08)	54.6	96.39335659	0.566429	5.00130257	52.90991	1.032
Beam 68 (DB11)	20.4	48.61948	0.419585	5.641874821	32.881449	0.62
Beam 69 (DB11)	42.18	76.7676	0.549451	4.85338622	44.662189	0.944
Beam 70 (DB11)	56.22	109.39383	0.513923	4.291652377	56.277469	0.999
Beam 71 (DB11)	53.4	45.00545106	1.186523	8.900076737	48.014992	1.112
Beam 72 (DB11)	70.74	78.83120409	0.89736	6.937092154	65.553157	1.079
Beam 73 (DB11)	85.62	112.5136277	0.760974	5.455719837	73.582608	1.164
Beam 74 (DB11)	49.56	49.19662578	1.007386	8.09587275	47.743776	1.038
Beam 75 (DB11)	54.36	73.79493867	0.736636	6.559345227	58.023623	0.937
Beam 76 (DB11)	65.34	110.692408	0.590284	5.281387605	70.078315	0.932
Beam 77 (DB11)	31.86	48.61948	0.655293	4.45296089	25.952332	1.228
Beam 78 (DB11)	33.6	76.7676	0.437685	3.991518961	36.731051	0.915
Beam 79 (DB11)	42.66	45.00545106	0.947885	6.015596709	32.453521	1.314

Table (4): Continued

		Anwarul Islam's model		Dias and Barross' model		
Sample No.	V_f^{exp} **(KN)**	V_f^{ana} **(KN)**	**K**	ε^{ana}	V_f^{ana} **(KN)**	**K**
Beam 80 (DB11)	64.02	78.83120409	0.812115	5.019238554	47.430094	1.35
Beam 81 (DB11)	43.44	49.19662578	0.882987	5.408204025	31.893792	1.362
Beam 82 (DB11)	51.72	73.79493867	0.700861	4.654418442	41.172741	1.256
Beam 83 (DB10)	28.32	79.7412	0.355149	3.450792689	32.386898	0.874
Beam 84 (DB10)	33.9	46.74874132	0.725153	5.060715327	27.8452	1.217
Beam 85 (DB10)	48	81.88473798	0.58619	3.944533247	38.016059	1.263
Beam 86 (DB10)	33.06	51.10226157	0.646938	4.638631379	27.899619	1.185
Beam 87 (DB10)	42.72	76.65339236	0.557314	3.758258749	33.906765	1.26
Beam 88 (DB10)	6.84	79.7412	0.085777	2.837998838	26.635613	0.257
Beam 89 (DB10)	26.04	46.74874132	0.55702	3.420557302	18.82068	1.384
Beam 90 (DB10)	31.56	81.88473798	0.38542	2.854013311	27.506002	1.147
Beam 91 (DB10)	25.08	51.10226157	0.490781	3.098698024	18.637501	1.346
Beam 92 (DB10)	35.1	76.65339236	0.457905	2.666807163	24.05976	1.459
Beam 93 (T10)	72.92	77.9636	0.935308	2.083691851	24.586171	2.966
Beam 94 (T10)	82.13	103.9514667	0.79008	1.960838912	30.848785	2.662
Beam 95 (T10)	95.24	155.9272	0.610798	1.763224188	41.609734	2.289
Beam 96 (T10)	79.65	175.3664	0.454192	1.699815133	45.114235	1.766
Beam 97 (T10)	95.64	233.8218667	0.409029	1.549774058	54.842726	1.744
Beam 98 (T10)	96.42	350.7328	0.27491	1.317482088	69.933719	1.379
Beam 99 (T10)	97.38	103.9514667	0.936783	1.546982311	24.33781	4.001
Beam 100 (I08)	151.4	154.1538356	0.982136	3.027613502	75.563317	2.004
Beam 101 (I08)	81.5	76.87461617	1.060168	3.829587127	47.664074	1.71
Beam 102 (I08)	112.9	122.9993859	0.917891	3.299555046	65.707443	1.718
Beam 103 (RR10)	70	136.88835	0.511366	2.929752214	56.186672	1.246
Beam 104 (RR10)	103	136.88835	0.752438	2.950867551	56.591621	1.82
Beam 105 (RR10)	138	193.5893611	0.712849	2.362295579	64.069664	2.154
Beam 106 (RS12)	36.78	36.7815	0.999959	3.851749324	18.832763	1.953
Beam 107 (RS12)	29.43	52.01689614	0.565778	3.212951195	22.216516	1.325
Beam 108 (RS12)	49.05	32.55	1.506912	3.700426968	19.213685	2.553
Beam 109 (RS12)	58.86	46.03265146	1.278658	3.006720002	22.078401	2.666
Beam 110 (RS12)	66.21	26.04	2.542627	4.301743387	17.868715	3.705
Beam 111 (RS12)	41.69	36.82612116	1.132077	3.857736513	22.661944	1.84
Beam 112 (RS12)	61.51	32.55	1.889708	3.700426968	19.213685	3.201
Beam 113 (RS12)	56.4	46.03265146	1.225217	3.006720002	22.078401	2.555
Beam 114 (RS12)	39.24	43.4	0.904147	3.047516269	21.098112	1.86
Beam 115 (RS12)	68.67	61.37686861	1.118825	2.180458898	21.3482	3.217
Beam 116 (DN01)	25	177.2	0.141084	2.639363473	51.741299	0.483
Beam 117 (DN01)	37.4	248.08	0.150758	2.103271527	57.724676	0.648
Beam 118 (DN01)	95.64	248.08	0.385521	2.103271527	57.724676	1.657
Beam 119 (DN01)	75.2	250.5986433	0.300081	1.718637739	47.647296	1.578

Table (4): Continued

		Anwarul Islam's model		Dias and Barross' model		
Sample No.	V_f^{exp} **(KN)**	V_f^{ana} **(KN)**	**K**	ε^{ana}	V_f^{ana} **(KN)**	**K**
Beam 120 (DN01)	87.63	350.8381006	0.249773	1.180246614	45.809412	1.913
Beam 121 (DN01)	53.4	177.2	0.301354	1.924592057	37.729132	1.415
Beam 122 (RD07)	44.4	175.7703699	0.252602	1.782520853	57.757943	0.769
Beam 123 (RD07)	21.6	175.7703699	0.122888	1.782520853	57.757943	0.374
Beam 124 (RD07)	23.4	285.1386	0.082065	1.371009147	72.065566	0.325
Beam 125 (RD07)	32.1	124.2884205	0.25827	1.754050087	40.188786	0.799
Beam 126 (RD07)	22.9	248.5768409	0.092124	0.972173607	44.548873	0.514
Beam 127 (RD07)	41.3	243.8367854	0.169376	2.216270071	38.135586	1.083
Beam 128 (RD07)	26.8	172.4186445	0.155436	2.429294113	29.557904	0.907
Beam 129 (DB)	29.1	26.13333333	1.11352	16.59141197	80.40424	0.362
Beam 130 (DB)	28.8	24.63874295	1.168891	122.9036394	561.54541	0.051
Beam 131 (DB)	59.3	52.26666667	1.134566	10.3933412	100.73509	0.589
Beam 132 (DB)	72.9	49.27748591	1.479377	56.66852573	517.83577	0.141
Beam 133 (DB)	28.6	24.26666667	1.178571	6.912187099	33.497399	0.854
Beam 134 (DB)	23.2	22.87883274	1.014038	28.84933725	131.81231	0.176
Beam 135 (DB)	31.8	48.53333333	0.65522	4.329994279	41.967483	0.758
Beam 136 (DB)	36.4	45.75766548	0.795495	13.30187957	121.55229	0.299

3.6 The Evaluation of Thanasis C. Triantafillou's Model

This model is in fact used to calculate the theoretical shear contribution of RC beams, which are strengthened in shear using externally FRPs (EFRP) bonded laminates. However, this model was built up using an approach, which can be also used in developing an analytical design guidance to calculate the shear contribution of NSM technique in RC beams. This approach is explained in details down in this section. It should be mentioned that NSM technique is a relatively new FRP-based strengthening technique, as well as it works in a similar manner to that EFRP technique regarding shear strengthening of RC beams. However, the main differences between NSM and EFRP techniques are the NSM technique provides larger bond area for the FRP reinforcements, and higher confinement provided by the concrete that surround the NSM FRP reinforcements. This is due to the fact that the NSM FRP reinforcements are embedded in grooves that are introduced into the surface of the RC members (See chapter two for more details and differences). These two factors basically play an important role in preventing the earlier debonding failure of FRP reinforcement from taking place in the NSM shear strengthened beams, and therefore increase its effectiveness in shear strengthening. As a result, if this model shows a good result and sufficient agreement with the experimental derived results of the generated database, it can be adopted. Then, this model can be modified such that it can be used to calculate the shear contribution of NSM technique in RC beams.

According to Triantafillou (2000), this model was developed following the concept that at the ultimate limit state, the effectiveness of the strengthening reinforcements, which is the load carried by the FRP reinforcements, depends on the failure mechanism, which in fact depends on different factors. The failure of the FRP reinforcements might happen either by debonding, or by tensile rupture of the FRP reinforcements. The latter failure may happen at a stress, which could be lower than the tensile strength of the FRP reinforcements. This is because of the stress concentrations at debonded areas or at rounded corners, etc. Whether debonding or fracture failures will take place first in the strengthened beams depends on the bond conditions, the available anchorage length and/or the type of attachment at the FRP ends, the thickness of the laminates and others factors (Triantafillou 2000). In fact, it was mentioned that the actual failure mode of the FRP reinforcements can be a combination of FRP debonding at certain areas of the RC beam and fracture of the FRP reinforcements at others. It was also stated that at the beam's ultimate limit state, the load carried by FRP reinforcement is rather impossible to quantify based on rigorous analysis (Triantafillou 2000). Therefore, the contribution of

the FRP laminates in the strengthened beams by using this model is calculated through a semi-quantitative description of the problem. First of all, the case of epoxy-bonded laminates, or FRP laminates without any anchorage and with the strong material direction (the principal fiber orientation) at an angle (β) to the longitudinal axis of the RC beam was considered. A qualitative description of the FRP load bearing mechanisms at ultimate shear capacity is shown in Figure (12a). This figure indicates regions in the strengthened beams of full debonding, full shear transfer and limited shear transfer (Triantafillou 2000).

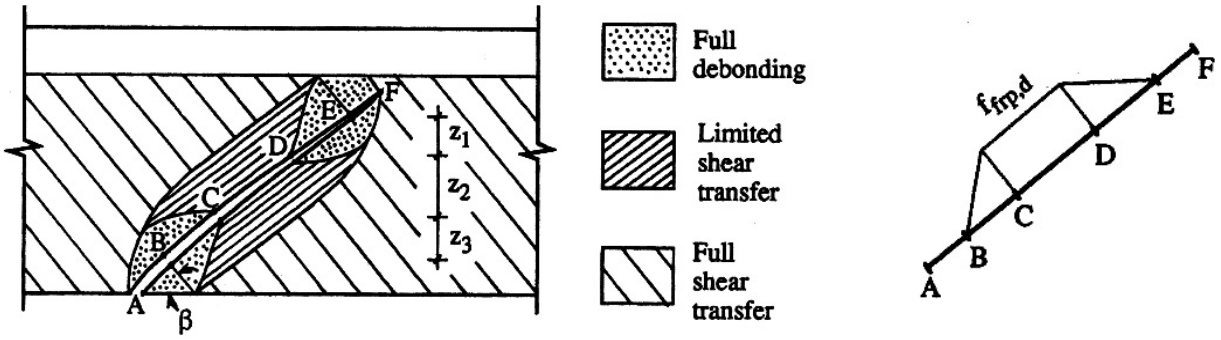

Figure (12): (a) Schematic representation of FRP stress bearing mechanism
(b) Simplified normal stress along diagonal crack (Triantafillou 1998)

A simplification of the associated tensile stresses in the FRP reinforcements is shown in Figure (12b), where only a portion of the reinforcement is stressed to its tensile capacity, $f_{frp,d}$. Using the classical truss analogy approach, which is similar to that used with steel stirrups, and based on the geometry of Figure (12a) and the simplified stress distribution of Figure (12b), the contribution of external FRP laminates in the EFRP shear strengthened beams was defined as shown in equation (3.16). This equation was built up in accordance to Eurocode2.

$$Vfrp,d = \frac{2\,t}{bw}\, f_{frp,d}\,(\frac{z1}{2} + z2 + \frac{z3}{2})(1 + cot\beta)\,\sin\beta \qquad (3.16)$$

Where

t: Thickness of FRP laminate on each side of the RC beam. By defining the FRP percentage of composite material as p_{frp} = 2t/bw, equation (3.16) above was written as following,

$$Vfrp,d = p_{frp}\ \mathrm{E}_{frp}\ 0.9\ b_w\ d\ (r_1 \frac{\varepsilon_{frp,u}}{\gamma_{frp}})(1 + cot\beta\ )\ \sin\beta \quad (3.17)$$

Where

E_{frp}: FRP elastic modulus, $\varepsilon_{frp,u}$: ultimate strain of FRP in the principal material direction, γ_{frp}: partial safety factor for FRP in uniaxial tension (equal to 1.15, 1.20 and 1.25 for Carbon FRP, aramid FRP and Glass FRP, respectively) and r_1: FRP reinforcement efficiency factor, which depends on the failure mode of the FRP laminates, and is equal to:

$$r_1 = \frac{\frac{z_1}{2} + z_2 + \frac{z_3}{2}}{0.9\ d} \quad (3.18)$$

Triantafillou (2000) stated that in the case of perfect anchorage of the FRP reinforcements, the only difference is that r_1 should be replaced by r_2. This has the meaning of a FRP strength reduction factor due to stress concentrations. Therefore, the contribution of FRP laminates in RC beams strengthened in shear using EFRP technique was finally written as shown in equation (3.19):

$$Vfrp,d = \frac{0.9}{\gamma_{frp}}\ p_{frp}\,\mathrm{E}_{frp}\ b_w\ d\ \ \varepsilon_{fk,e}(1 + cot\beta\ )\ \sin\beta \quad (3.19)$$

Where

$\varepsilon_{fk,e}$ is the characteristic value of the effective FRP strain, and it equals to (0.8 x effective FRP strain ($\varepsilon_{frp,e}$))

It should be mentioned that the above model is a descriptive one, and not an exact model relating the FRP effective strain with the geometric parameters z_1, z_2, and z_3 (shown in figure 12a). The effective FRP strain in this model was obtained based on the fact that $\varepsilon_{frp,e}$ was found experimentally to depend heavily on the bond area between the FRP reinforcements and concrete. In other word, it depends on the FRP development length, which is defined as the required length to reach FRP tensile fracture before debonding. The development length was found experimentally in its turn to depend on the FRP axial rigidity, which is expressed by the product ($E_f\ P_f$), and to be inversely proportional to the tensile strength of concrete. Nowadays, it is well-known in many design codes such as Eurocode2 that the tensile strength of concrete is proportional to

($f_c^{2/3}$). (f_c) here represents the compressive strength of concrete. Therefore, it was finally argued that the FRP effective strain ($\varepsilon_{frp,e}$) depends on the product ($E_f P_f / f_c^{2/3}$) (Triantafillou 2000). It is important to mention this dependence was confirmed later by many other experimental studies in the field of using NSM and EFRP techniques in shear strengthening of RC beams. Then, by using this dependency relationship, three equations, which relates the FRP effective strain (ε_{fe}) with the quantity [($E_f \rho_f$)/ ($f_{cm}^{2/3}$)], were proposed. These equations were proposed in accordance to the failure type of EFRP shear strengthened beams, and the material type of the FRP laminates. Each of these equations corresponds to the best fit of power type curves, that describe the relationship between ε_{fe} experimentally (obtained using experimental results of 70 tested beams strengthened using EFRP technique), and the product [($E_f \rho_f$)/ ($f_{cm}^{2/3}$)] for the three cases as shown below (Triantafillou 2000).

1-Premature shear failure due to debonding (for Carbon FRP (CFRP) only):

$$\varepsilon_{fe} = 0.65 \times [(E_f \rho_f)/(f_{cm}^{2/3})]^{-0.30} \quad (3.20)$$

2-Shear failure combined with or followed by Carbon FRP (CFRP) fracture:

$$\frac{\varepsilon_{fe}}{\varepsilon_{fu}} = 0.17 \times [(E_f \rho_f)/(f_{cm}^{2/3})]^{-0.56} \quad (3.21)$$

3- Shear failure combined with or followed by aramid FRP (AFRP) fracture:

$$\frac{\varepsilon_{fe}}{\varepsilon_{fu}} = 0.048 \times [(E_f \rho_f)/(f_{cm}^{2/3})]^{-0.47} \quad (3.22)$$

Note that in all equations and figures above, f_c is in MPa and E_f is in GPa.

Regarding the evaluation of this model, the created database (shown in table A) was also used to evaluate this model. However, not all of the samples of the database were considered. Only, those beams that were strengthened in shear using either FRP laminates or strips, and they experienced either debonding or FRP tensile fracture failures were considered in the evaluation of this model. This is due to the fact this theoretical model was developed to be valid in these cases, as it is originally used for beams strengthened in shear using only externally bonded FRP **laminates**. Therefore, considering other beams such as those strengthened using FRP bars, and/or others with fracture of concrete failure type is not a right case to be considered in the evaluation.

This is because this can lead to incorrect results, which can cause a misunderstanding of the evaluation of this model. It is significant to note that, the percentage of the composite material in the NSM shear strengthened beams was calculated from (ρ_f = (2 x a_f x b_f)/ (b_w x s_f x sinθ_f) x 100%) not (ρ_{frp} = 2t/b_w). Following the restrictions above, the evaluation was based on only 19 samples (beams) of the database. The analytical strain (ε^{ana}) for the considered beams was calculated using equations (3.20), (3.21) and (3.22) above taking into account the material type of FRP laminates and the observed failure mode in the strengthened beams. Then, (V_f) theoretically was calculated for each beam using equation (3.19). The ratio (K) which is as mentioned before equal to ((V_f) experimentally / (V_f) analytically) was also found. This is shown in table (5) down.

Based on the results of evaluation of this model, the values of K ratios of all the considered beams are equal of greater than one. This basically represents safe conditions in the NSM shear strengthened beams. In fact, this model shows a 100% safe prediction percentage with average value of K ratio being equal to 2.27. This means this model did not overestimate the theoretical shear contribution of NSM technique, since all of the 19 beams have K value greater than unity. It should be also mentioned that this model is rather more sophisticate one compared to the first as well as the second evaluated models. This is because it was built up by adopting the classic truss analogy approach, and considering the geometry of the FRP reinforcement bearing mechanisms, and the simplified stress distribution along diagonal crack shown in figure (12). In addition to this, it is a destructive model that links the geometric parameters shown in figure (12b) with the FRP effective strain, and relates the latter to the development length of the FRP reinforcement. This was achieved throughout the established dependency relationship stated above. In this relationship, it can be noticed that the effects of both the percentage of composite material and the concrete strength parameters are considered. Both of which are significant factors, which influence the effectiveness of this technique as a shear strengthening technique in RC beams. Beside this, they affect the shear failure mode of the FRP-based shear strengthened beams, which in its turn affects the effectiveness of the FRP reinforcements. See section (**3.7**) for the detailed discussion and comparisons of the obtained results.

Nevertheless, Triantafillou (2000) stated that **"**one drawback of the qualitative approach explained above is that the FRP bonded length is not taken explicitly into account. However, this could be partially justified by the following arguments: (1) For the real size structures, the effective bond length is a small part of an RC element's depth; hence, the partially ineffective FRP comprises a small fraction of the total; (2) the effect of short FRP bonded lengths may be taken into account to a certain extent through

the experimental data fitting and calibration procedure, and (3) Adding more complexity to an approach that is meant to be as simple as possible for the purpose of design calculations might not be wanted" (Triantafillou 2000).

Table (5): Comparison between the experimental and theoretical results of Triantafillou's model

		Triantafillou's model		
Sample No.	V_f^{exp} **(KN)**	ε^{ana}	V_f^{ana} **(KN)**	**K**
Beam 33 (DB12)	44.7	0.0075	33.9	1.317
Beam 34 (DB12)	81.5	0.00571	42	1.94
Beam 35 (DB12)	81.7	0.00905	57.88	1.414
Beam 36 (DB12)	117.4	0.00782	81.3	1.4438
Beam 37 (DB12)	85.8	0.00905	57.88	1.48225
Beam 38 (DB12)	80.9	0.00905	57.88	1.4
Beam 39 (DB12)	84.6	0.00942	50.92	1.66
Beam 40 (DB12)	127.9	0.00823	69.87	1.83
Beam 41 (DB12)	74.9	0.00905	57.884	1.23
Beam 42 (DB12)	108.9	0.00782	81.3	1.34
Beam 43 (DB12)	73.4	0.00942	50.923	1.44
Beam 44 (DB12)	72.6	0.00942	50.93	1.425
Beam 45 (DB09)	20.2	0.00262	11.6	1.74
Beam 49 (DB09)	53.4	0.00652	40.87	1.306
Beam 52 (DB09)	49.6	0.00703	32.23	1.332
Beam 112 (RS12)	61.51	0.00106	5.1	8.18
Beam 114(RS12)	56.4	0.00099	5.95	9.46
Beam 130(DB)	29.1	0.0123	21.76	1.33
Beam 132(DB)	59.3	0.00837	29.53	2

3.7 Discussion of the Results of Evaluation

The detailed discussion of the evaluation results, which were obtained in the last three sections, is examined here. Based on this discussion, a decision regarding the selection of the best model for the modification processes in this project was made in chapter four.

As far as A.K.M Anwarul Islam's formula is concerned, the evaluation of this model basically proved that this model is not that reliable. In other word, it is not worth using it to calculate the theoretical shear conurbation of NSM technique in RC beams. This is due to the fact that by using this formula; only few numbers of the RC beams have analytical (V_f) in the safe side. It can be in fact noticed that most of the beams in the evaluation of this model in table (4) about 73% of them have K ratio by far less than unity. This result and the bad agreement with the experimental derived (V_f) can be because this formula is a very simple one compared to the other evaluated models. Additionally, it does not take into consideration the effects of many parameters, which have been found according to the findings of chapter two to influence the effectiveness of this technique. The effective strain in this formula was also found according to only the results of three tested beams. If many samples beams were used in the development of this model, the (1/3), which the proposed ratio (value) of the FRP effective stain, was unlikely to be achieved. In particular, if FRP tensile fracture or debonding of the FRP reinforcement failure modes were observed in these beams, which is the case in the beams of the database, such a constant ratio would be impossible to be observed. Therefore, using this constant ratio of the FRP effective stain is not a real case, since the ratio between the FRP effective stain and the ultimate FRP stain can be varied in the different beams of the experimental database shown in table (A). On the other hand, dependency relationships were proposed with the other two models, and then were used to establish equations to calculate the FRP effective strain. These dependency relationships were based on testing many beams, and they reflect the impacts of different parameters as mentioned before on the effectiveness of this technique in more realistic manner. Therefore, it is a normal case this model was not able to offer a safe and realistic prediction of the theoretical results compared to the other two models. Based on the reasons mentioned above, this model will not be considered in chapter four.

Regarding the evaluation of Dias and Barross' model, this model showed better results in terms of the agreement with the experimental results and the safe prediction

of the theoretical results compared to that of the first evaluated formula. 68.6% of the considered beams in the evaluation of it in table (4) have k ratio equal or greater than one. This represents a percentage of safe prediction greater than that of A.K.M Anwarul Islam's formula by about 2.5 times. Knowing that, the percentage of safe prediction is the percentage ratio obtained by comparing the numbers of beams that have K ratios equal or greater than one, with the total considered samples in the evaluation. The better performance of this model can be linked to the fact that the impacts of many variables, such as the concrete strength, the percentage of both the composite material and existing steel stirrups, the orientation of FRP reinforcements were introduced to this model. This was achieved by establishing a dependency relationship that takes into consideration these effects, and then used it to produce three equations to calculate the FRP effective strain. This clearly is more sophisticated step compared to the constant ratio, which was proposed with the first evaluated model. It is important to note that the same approach, which is the truss analogy one, was used in the development of these two models. However, three equations that relate the (ε_{fe}) with the product ($E_{sw}\,\rho_{sw} + E_f\,\rho_f$)/ ($f_{cm}^{2/3}$), and (1/3) were used instead of the yield stain of the steel stirrups in the second and first evaluated models, respectively. Another factor contributed in the better results, the development of this model was based on 40 beams, and different failure modes were observed in the experimental program, which was not the case in A.K.M Anwarul Islam's formula. Developing a model using more data is believed to be more effective, as this can help to reflect the real situations, which might be faced in reality, on the behaviour of the theoretical model. Finally, a safety factor equal to 1.3 was originally proposed with this model. This basically contributed in reducing the theoretical results of (V_f), and thus increase the safe prediction percentage, as more beams became in the safe side. Therefore, it can be said this model is more reliable compared to the first formula due to the factors mentioned above.

Regarding the evaluation of Thanasis C. Triantafillou's model, this analytical model was evaluated using only 19 beams of the generated database for reasons related to the validity of using it. Interestingly, all of the 19 beams have K ratio as shown in table (5) equal or greater than unity. It is however important to note that beams 112 and 114 in the same table have a very high values of the K ratio. This still shows a safe condition, but it shows at the same time insufficient agreement with the experimental results. The very high percentage of composite material and the no clear FRP failure modes in these two beams as shown in table (A) can justify the obtained results in them. These two factors basically resulted in obtaining small values of the theoretical derived results of (V_f) compared to the experimental obtained results, which in its turn led to obtain high values of the ratio K in these two beams.

Based on the evaluations of the three models, the last evaluated one seems to be the best model among the others, as all the considered beams in the evaluation of it are in the safe side. Many factors in fact can be the reasons behind stating this, and behind the obtained results of this model. First factor, this model is a rather more sophisticated one compared to the other two. This is because it was built up by adopting the classic truss analogy approach, and using the geometry of the FRP reinforcement bearing mechanisms, and the simplified stress distribution along diagonal crack shown in figure (12). Another reason, this model is a destructive one that links the geometric parameters shown in figure (12b) with the FRP effective strain, and relates the latter to the development length of the FRP reinforcement, which was found experimentally to have a dependency relationship with the product ($E_f \rho_f$ / $f_c^{2/3}$). It should be stated that this dependency relationship has been approved by many experimental programs including those carried out in the field of shear strengthening of RC by NSM technique. Adding to this, this dependency relationship take into account the effects of the percentage of composite materials, and the concrete strength. Both of these factors according to chapter two are important, as they can play a role in increasing the efficiency of NSM FRP reinforcement, and they can also change the failure modes in these reinforcements. Furthermore, this model takes into account the failure mechanism of the FRP reinforcement (laminates), which affects the load carrying capacity of the FRP reinforcement, and as a result the effectiveness of both NSM and EFRP techniques. Another factor, different safety factors were proposed to increase the safe prediction ability of this model. A final important factor to be mentioned, the use of the characteristic value of the effective FRP strain plays an important role in increasing the efficiency of this model. In fact, the FRP effective stain in this model is not used directly, but it should be firstly lowered by multiplying it by (0.8). This in its turn led to increase the safe prediction ability of this model by decreasing the analytical values of the shear contribution of NSM technique in RC beams. The use of the characteristic value of FRP effective strain has the meaning of using another safety factor with this model.

4 THE CALIBRATION OF MODELS

According to the final results of the evaluations of the three models in the previous chapter, the theoretical model that was proposed by Thanasis C. Triantafillou showed a sufficient agreement with the experimental results, and all the considered beams in the evaluation of it have K ratio equal or greater than unity. 100% safe prediction as mentioned before was achieved by using this model. The reasons behind this are already mentioned in chapter three. Although this model was evaluated using few samples of the generated data base, it is believed that by modifying it using the database of the project more sufficient results can be achieved. In addition, by modifying this model, no restrictions on the use of it will be there anymore, and it can be then used for the whole collected database. Therefore, the modification of this model is considered in section (4.1). The discussion of the obtained results of this model is examined in section (4.2)

Despite this, the modification of Dias and Barross' model is also considered in this project for some reasons. Firstly, someone might argue that this model was originally developed to be used for NSM shear strengthened beams. In addition, different factors, which affect the effectiveness of this technique by means of shear strengthening technique in RC beams, were taking into account when it was built up. Furthermore, according to the evaluation of this model in section (3.5), 68.6% of the considered beams of the generated database have K values equal or greater than one. This percentage is by far greater than that obtained using A.K.M Anwarul Islam's model (section 3.4). At the same time, this percentage was obtained considering all the beams of the database, which was not the case when Thanasis C. Triantafillou's model was evaluated. Thus, it might be argued that the 68.6% is a reasonable percentage, and better results can be obtained by calibrating it. Finally, it might be thought that modifying this model can show better performance than that will be obtained after modifying Thanasis C. Triantafillou's model. Following this argument, the modification of Dias and Barros model is illustrated in section (4.3) to justify this argument and compare the results of the two modified models. The final comparison between the results of the two modified models is presented in the last section of this chapter. It is important to state that, even after modifying Dias and Barross' model; Thanasis C. Triantafillou's model still shows higher safe prediction percentage and sufficient agreement with the experimental results.

4.1 The Modification of Thanasis C. Triantafillou's Model

4.1.1 Strategy for the Modification of the Analytical Model

The theoretical shear contribution (v_f) of NSM technique in RC beams can be calculated using the model of Thanasis C. Triantafillou by using the following equation.

$$v_f = \frac{0.9}{\gamma_s}\, p_f\, \mathrm{E}_f\ \mathrm{b}_w\, \mathrm{d}\ \varepsilon_{fk,e}\left(1+\cot\theta_f\right)\sin\theta_f \qquad (4.1)$$

Where

$\varepsilon_{fk,e}$: The characteristic value of the effective FRP strain and it equals to (0.8 x effective FRP strain (ε_{fe})).
E_f: FRP elastic modulus (GPa).
p_f: The percentage of the composite material (FRP reinforcement) in the NSM shear strengthened beams.
b_w: beam web width (mm)
d: The distance from the external compression fiber to centroid of longitudinal tension reinforcement (mm)
θ_f: The inclination of the FRP reinforcement and it is measured with respect to the horizontal axis of the beam (degree).
γ_s: Partial safety factor

The principles and the approach that were used to develop this model are explained in details in section (3.6) above. Referring back to the same section in chapter three, Thanasis C. Triantafillou's model is a descriptive one relating the FRP effective strain with the geometric parameters of the FRP stress bearing mechanisms shown in figure (12b). Therefore, the only unknown yet in equation (4.1), in which by finding it this model will be valid to use in the NSM shear strengthened beams without restrictions, is the FRP effective strain (ε_{fe}). This unknown will be found by establishing equations using the dependency relationship found by Thanasis C. Triantafillou, and proved by many others. This dependency as stated before relates the FRP effective strain with the product ($E_f\ \rho_f$) / ($f_{cm}^{2/3}$). Many scenarios were applied to achieve the equations that describe the best fit of this dependency relationship in this dissertation. However, only

the one that showed the best results is examined in details in this chapter, while others are also mentioned briefly in section (4.1.2). The equations, which relate the FRP effective strain with the product ($E_f \rho_f$) / ($f_{cm}^{2/3}$) for the best scenario, were obtained following the next strategy (procedure):

1- For each inclination (θ_f) of the FRP reinforcements; (45º, 60º and 90º), it was defined the equation that relates ε_{fe} (experimentally) with the product [($E_f \rho_f$) / ($f_{cm}^{2/3}$)]. This was achieved by first obtaining the values of ε_{fe} (experimentally), and then plotting these values against the product ($E_f \rho_f$) / ($f_{cm}^{2/3}$) for the three arrangements of FRP reinforcements separately. The experimental values of the FRP effective strain were obtained by substituting the experimental shear contribution of NSM technique for each beam of the generated database (shown in table (A)) in equation (4.2) below. Each of the three proposed equations corresponds to the best fit of power-type curves that describe the dependency relationship mentioned above.

$$v_f^{exp} = 0.9\ p_f\ \mathrm{E}_f\ b_w\ \mathrm{d}\ \varepsilon_{fe}\ (1 + \cot\theta_f)\ \sin\theta_f \qquad (4.2)$$

Where

v_f^{exp}: Experimentally derived contribution of FRP reinforcement to shear capacity of RC beams

ε_{fe}: FRP effective strain

2- By considering the equations defined in the step (1) and using equation (4.1) above, it was possible to calculate the theoretical value (v_f) for each beam of the experimental database described in this project, and considered in this analysis. The comparison between experimental and analytical values of (v_f) was done, and safety factors were defined in order to insure that the modified analytical formulation provides safety predictions for 94% of the considered beams of the database in this analysis. Maximum limits for the FRP effective stain were also defined to maintain the aggregate interlock and control the shear cracks in the NSM shear strengthened beams. It is important to mention that, a similar scenario that is explained in points one and two was used in the development of Dias and Barros's model.

4.1.2 Development of the Analytical Formulation

Figure (13) illustrates the relationships between the FRP effective strain (ε_{fe}), which was calculated following point one of the strategy explained above, and the product [($E_f \rho_f$) / ($f_{cm}^{2/3}$)] for the arrangements of FRP reinforcement; 45°, 60° and 90°. The relationships represent the best fit of power-type curves. It is important to notice that some of the RC beams were not considered in this analysis. For example, beams 96, 97, 98, 99 and 124 were not considered for the case of θ_f = 90°, as it is reported that the failure mode in these beams were a shear and flexural failure mode (See table (A) for more details). Furthermore, it is stated in the original papers that the data was taken from, due to some test defects, the experimental shear contribution of NSM technique of beams 50, 88 for the arrangement 90°, and beams 62 and 105 for the arrangement 45° are odd values. Therefore, these beams as well as few others were ignored in obtaining the best fit of the FRP effective strain versus [($E_f \rho_f$) / ($f_{cm}^{2/3}$)] relationships for the arrangements 90° and 45°. This is due to the fact that considering these beams can affect the obtained results and lead to some errors. The best fit power-type expressions for the three relationships shown in figure (13) are defined as following:

1- For the FRP reinforcement at 45° (See figure13a)

$$\varepsilon_{fe} = 0.306 \times [(E_f \rho_f)/(f_{cm}^{2/3})]^{-0.61} \quad (4.3)$$

2- For the FRP reinforcement at 60° (See figure13b)

$$\varepsilon_{fe} = 1.104 \times [(E_f \rho_f)/(f_{cm}^{2/3})]^{-0.31} \quad (4.4)$$

3- For the FRP reinforcement at 90° (See figure 13c)

$$\varepsilon_{fe} = 0.222 \times [(E_f \rho_f)/(f_{cm}^{2/3})]^{-0.75} \quad (4.5)$$

It is important to mention that other scenarios to obtain the best fit of the FRP effective strain versus [($E_f \rho_f$) / ($f_{cm}^{2/3}$)] relationships were tried. For example, the whole collected data were used to obtain one relationship that links the ε_{fe} with the product [($E_f \rho_f$) / ($f_{cm}^{2/3}$)]. However, this trial showed not sufficient results regarding estimating the theoretical (v_f). Furthermore, these expressions were also calibrated using the same

scenario used originally in the development of this model (i.e considering the type of failure in the NSM shear strengthened beams). Similarly, this scenario was not that good compared to the scenario, which was used to obtain equation (4.3), (4.4) and (4.5). The calculations of the considered scenario (shown in figure 13) are only presented in the dissertation. The three plots; a, b and c; of figure (13) were plotted using the calculations presented in tables B1, B2 and B3 in **Appendix (B)**, respectively.

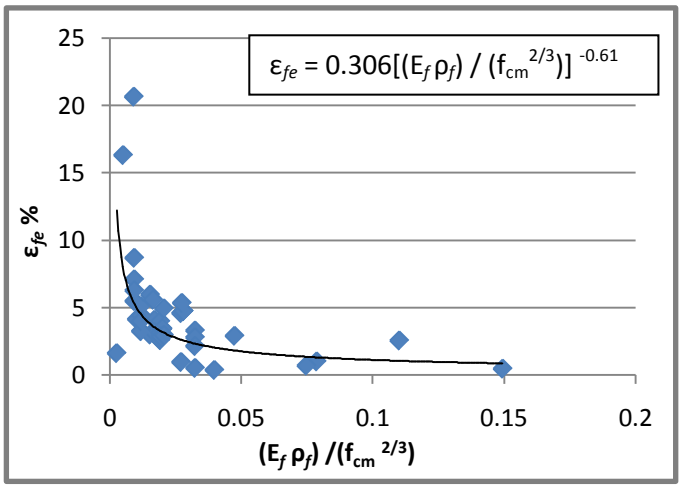

(a) FRP reinforcement at 45°

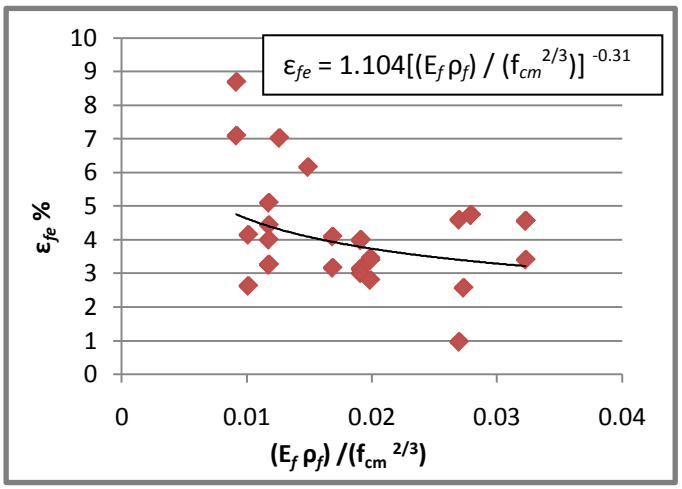

(b) FRP reinforcement at 60°

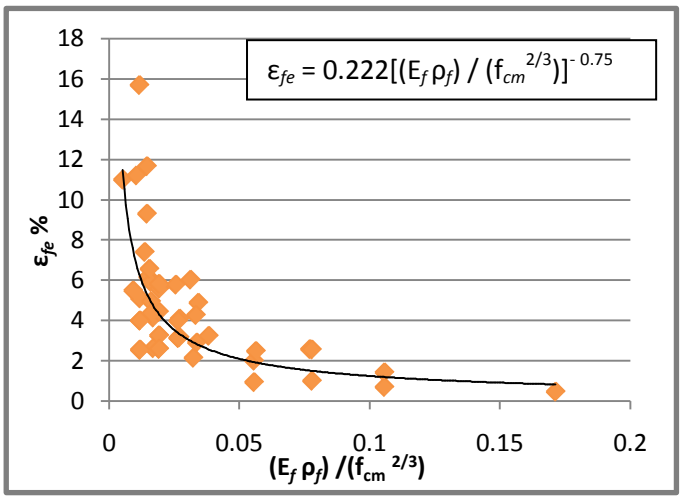

(c) FRP reinforcement at 90°

Figure (13): Effective strain of FRP reinforcement *versus* $[(E_f \rho_f) / (f_{cm}^{2/3})]$

In agreement with the qualitative argument made above during the development of this model, it can be noticed that the three diagrams that are presented in figure (13) are decreasing relationships. Basically, as the term $[(E_f \rho_f) / (f_{cm}^{2/3})]$ increase the FRP effective strain decrease.

It is also significant to note that, the three plots of figure (13) and equations (4.3), (4.4) and (4.5) were obtained considering the RC beams strengthened using different FRP materials and types of FRP reinforcement, such as Carbon FRP laminates, Carbon FRP rod/bars, Glass FRP laminates and Glass FRP bars/rods. However, the beams strengthened using the last two types of FRP reinforcement made form Glass FRP were not many. An important point to be mentioned regarding this, when debonding of NSM FRP reinforcement is the dominate failure type in the NSM strengthened beams, ε_{fe} is not affected by the FRP reinforcement material type for reasons mentioned above. In contrast, if fracture of NSM FRP reinforcement is the dominate failure type; ε_{fe} can be influenced by the material kind of the FRP reinforcement. This is because of the different fracture strains of the FRP materials. On the other hand, the strength of concrete is the main factor that can lead to the fracture of the concrete failure type in the strengthened beams, so this type of failure also does not depend heavily on the FRP reinforcement material. Therefore, in the future, when more experimental data in which other types and materials of FRP reinforcement are used, the three proposed expressions above can be improved more. This will basically help in reflecting the effects of the different materials and types of FRP reinforcements on the efficiency of this model in a very rich picture.

A final point to be pointed out in this analysis, the maximum value of FRP effective strain should be limited to the average value of the FRP ultimate strain. Doing so was reported by many that can contribute significantly in maintaining the aggregate interlock in the concrete, improving the shear behaviour of the strengthened beams and controlling the shear cracks in the NSM shear strengthened beams. Therefore, for each type of the FRP reinforcement, an average value of the FRP ultimate strain was calculated using the values reported in the generated database (table A). These values are: ε_{max}= 3.52% for Carbon FRP rods, 8.94% for Carbon FRP laminates, 8% for Glass FRP laminates and 2% for Glass FRP rods.

4.2 Validation of the Modified Thanasis C. Triantafillou's Model and Discussion of the Results

By using equations (4.3), (4.4) and (4.5), the analytical values of the FRP effective strain ($\varepsilon_{fe}{}^{ana}$) were determined for all the considered beams in the analysis shown in table (6). Introducing the ($\varepsilon_{fe}{}^{ana}$) to equation (4.1) and using a partial safety factor equal to one, the theoretical shear contributions of NSM technique in the strengthened beams ($v_f{}^{ana}$) were calculated. Then, by considering the analytical results ($v_f{}^{ana}$) and the experimental results ($v_f{}^{exp}$), the ratio (K) was calculated for the considered beams. This is well illustrated in table (6). It is important to emphasize that, in this analysis; a K ≥ 1 represents a safety condition. 1.38 is the obtained average value of the ratio (K) when the applied partial safety factor in equation (4.1) was equal to one.

It can be noticed that, the values of the ratio K in most of the considered beams of the database in table (6) are close to the unity, evidencing that the analytical model predicts with sufficient accuracy the experimental results. However, as equation (4.1) does not take all the effects that influence the effectiveness of the NSM FRP reinforcements, new uncertainty factors have been proposed. Basically, partial safety factors equal to 1.2 and 1.3 have been proposed for the case of using inclined FRP reinforcements (at 45^o and 60^o), and the vertical arrangement of FRP reinforcements, respectively. As this technique was discovered to be more effective in the case of using inclined FRP reinforcements, the proposed factor of safety for the inclined arrangement was less than that of the vertical arrangement. These two uncertainty factors also were established in a manner such that an increase in the percentage of the safe prediction of the modified model, and sufficient agreement with the experimental results were achieved. It is important to emphasise that, the percentage of safe prediction here represents the percentage ratio between the beams that have K≥1 and the total numbers of the considered beams in the analysis. Using these factors in fact led to have 94% safe prediction. In other word, 94% of the considered beams in the analysis shown in table (6) have (K) ratio equal or greater than one. Furthermore, an average value of the ratio K equal to 1.7 was obtained after using the proposed safety factors. It is important to note that some of the sample beams in table (6), such as beams 45, 60, 68, 116 and 126, are still have K values less than unity even after introducing the uncertainty factors. The observed failure modes in these beams could justify their relatively low experimental values of v_f. In fact, debonding of the FRP reinforcements was the failure mode type that was obtained in these beams. Based on the literature review, the effectiveness of this technique was found to be reduced when such failure

mode was obtained. This is due to the fact that the bound length between the NSM FRP reinforcements and the surrounding concrete will be less in this case. This in its turn reduces the effectiveness of NSM technique by means of shear strengthening technique in RC beams, and leads to have K ratio less than unity.

Furthermore, the K values in some of the beams in table (6) are greater than two. This still shows a safe condition. Nevertheless, the reason behind this can be linked to the high percentage of the used composite materials (FRP reinforcement) in some of these beams. This resulted in reducing the theoretical FRP effective strain, and consequently decreasing the theoretical (v_f), which in its turn resulted in the high K values.

If a safety factor equal to 1.38 is introduced to the equation (4.1) instead of the proposed ones, a very high percentage of safe prediction can be achieved. The 1.38 as mentioned before is the obtained average value of the ratio K when no partial safety factor was considered in the calculation of (v_f^{ana}). In fact, by using such factor of safety, more than 97% of the considered beams in table (6) can have K ratio greater than one. However, this is not recommended to be used, as this means huge uncertainty is introduced to the model. In addition, doing so will lead to the fact that many of the samples beams will have K ratio greater than two causing an insufficient agreement with experimental results.

Finally, by comparing the obtained results of the modified model to that were obtained from the evaluation of A.K.M Anwarul Islam's, and Dias and Barross' models, the modified model shows by far a very good results, and close agreement with the experimental results. In fact, only few beams as shown in table (6) have (k) values less than unity. The corresponding percentage of the safe prediction of this model after the modifying, and introducing safety factors to it is 94%. This is actually greater than 27% and 68.6%, that were obtained from using A.K.M Anwarul Islam's, and Dias and Barross' models, respectively. This percentage is also obtained considering all the beams, not few numbers of them, as it was the case when the modified model was evaluated in chapter three. Therefore, the 94% is even a very high percentage compared to that obtained in the evaluation of this model. The reasons behind the high ability of this model in predicting the shear contribution of NSM technique in RC beams have been already mentioned in section (3.7) above, and this ability has been now increased after modifying this model. The modification (calibration) of this model basically contributed firstly in removing the restrictions on using this model for RC beams strengthened in shear using NSM technique. It also resulted in making this model predicts the analytical results in more realistic and accurate way, and showing sufficient agreement with the

experimental results. This is based on the fact that the more considered data in the calibration of the three power-type expressions of the FRP effective stain, the better performance of the theoretical model is. The performance of Thanasis C. Triantafillou's model is clearly improved dramatically after calibrating the three power type expressions of the FRP effective stain. These three equations; (4.3), (4.4) and (4.5); were calibrated in this project using the database, which consists of 136 RC beams. Various FRP materials, FRP types, FRP arrangements, FRP spacing, percentage of composite material, percentage of steel stirrups, percentage of flexural reinforcements, concrete strengths, anchorage system, shear span (a/d), cross sectional type of RC beams and shear failure modes are considered in the calibrations of these three equations, since these parameters differ in the different samples of the database. This basically resulted in making equations (4.3), (4.4) and (4.5) predicts the theoretical FRP strain of the FRP reinforcements in more accurate, sufficient and realistic way, and this in its turn increased the efficiency of this model.

Table (6): Comparison between the experimental and analytical results using the modified Thanasis C. Triantafillou's model

			γ_s=1		γ_s= **1.2** for inclined FRP and **1.3** for vertical FRP reinforcement	
Sample No.	v_f^{exp} **(KN)**	ε^{ana} **%**	v_f^{ana} **(KN)**	**K**	v_f^{ana} **(KN)**	**K**
Beam 1 (DB12)	40.3	3.618039775	35.19233887	1.145	27.0710299	1.4887
Beam 2 (DB12)	63.7	2.669788888	41.55006406	1.533	31.96158774	1.993
Beam 3 (DB12)	37.9	4.036205725	33.31304536	1.138	27.76087114	1.3652
Beam 4 (DB12)	56.5	2.955599312	40.65700176	1.39	33.8808348	1.6676
Beam 5 (DB12)	70.3	2.218872601	48.83623128	1.44	40.6968594	1.7274
Beam 6 (DB12)	35.4	3.669583188	29.25509803	1.21	24.37924835	1.4521
Beam 7 (DB12)	61.3	3.132157736	37.45585407	1.637	31.21321172	1.9639
Beam 8 (DB12)	69.7	2.707487314	46.7674136	1.49	38.97284466	1.7884
Beam 9 (DB12)	57.5	3.457993348	43.72625668	1.315	33.63558206	1.7095
Beam 10 (DB12)	71.5	2.709114052	48.65658828	1.469	37.42814483	1.9103
Beam 11 (DB12)	53.4	3.682380561	41.56956823	1.285	31.97659094	1.67
Beam 12 (DB12)	70.7	2.738470812	50.23522203	1.407	41.86268503	1.6889
Beam 13 (DB12)	85.6	2.172570432	58.24844328	1.47	48.5403694	1.7635
Beam 14 (DB12)	49.6	3.502416819	33.41692664	1.484	27.84743886	1.7811
Beam 15 (DB12)	54.4	3.013028825	45.17483834	1.204	37.64569862	1.4451
Beam 16 (DB12)	65.3	2.678626181	58.41612266	1.118	48.68010222	1.3414
Beam 17 (DB12)	31.9	4.976960312	39.72793797	0.803	30.55995228	1.0438
Beam 18 (DB12)	40.7	4.976960312	39.72793797	1.024	30.55995228	1.3318
Beam 19 (DB12)	33.6	3.457993348	44.85484553	0.749	33.22581151	1.0113
Beam 20 (DB12)	42.7	3.682380561	41.56956823	1.027	34.64130686	1.2326
Beam 21 (DB12)	64	2.738470812	50.23522203	1.274	41.86268503	1.5288
Beam 22 (DB12)	43.5	3.013028825	28.7476244	1.513	23.95635367	1.8158
Beam 23 (DB12)	51.7	3.502416819	52.51231329	0.985	43.76026107	1.1814
Beam 25 (DB12)	33.9	2.673029259	30.77555413	1.102	25.64629511	1.3218
Beam 26 (DB12)	48	1.987847939	37.19107176	1.291	30.9925598	1.5488
Beam 27 (DB12)	33.1	2.560356498	24.91462986	1.329	19.16509989	1.7271
Beam 28 (DB12)	42.7	2.976219672	45.51071179	0.938	37.92559316	1.1259
Beam 29 (DB12)	26	2.673029259	30.77555413	0.845	25.64629511	1.0138
Beam 30 (DB12)	31.6	1.987847939	37.19107176	0.85	30.9925598	1.0196
Beam 31 (DB12)	25.1	2.696442393	26.23887112	0.957	21.86572593	1.1479
Beam 32 (DB12)	35.1	2.976219672	45.51071179	0.771	35.00823984	1.0026
Beam 33 (DB12)	44.7	5.998541301	48.83518354	0.915	37.5655258	1.1899
Beam 34 (DB12)	81.5	4.167788091	55.13738508	1.478	42.41337314	1.9216
Beam 35 (DB12)	81.7	4.286224716	49.34885778	1.656	41.12404815	1.9867

Table (6): Continued

			γ_s **=1**		γ_s **=1.2**for inclined FRP and **1.3** for vertical FRP reinforcement	
Sample No.	v_f^{exp} **(KN)**	ε^{ana} **%**	v_f^{ana} **(KN)**	**K**	v_f^{ana} **(KN)**	**K**
Beam 37$^{(DB12)}$	85.8	4.286224716	49.34885778	1.739	41.12404815	2.0864
Beam 38$^{(DB12)}$	80.9	4.286224716	49.34885778	1.639	41.12404815	1.9672
Beam 39$^{(DB12)}$	84.6	3.25474496	31.67166995	2.671	26.39305829	3.2054
Beam 40$^{(DB12)}$	127.9	3.783393439	57.85356841	2.211	48.21130701	2.6529
Beam 41$^{(DB12)}$	74.9	4.286224716	49.34885778	1.518	41.12404815	1.8213
Beam 43 $^{(DB12)}$	73.4	3.427738401	33.35505567	2.201	27.79587973	2.6407
Beam 44 $^{(DB12)}$	72.6	3.783393439	36.81590717	1.972	30.67992264	2.3664
Beam 45 $^{(DB09)}$	20.2	4.976960312	39.68384481	0.509	30.52603447	0.6617
Beam 46 $^{(DB09)}$	42.2	3.457993348	44.80506213	0.942	34.46543241	1.2244
Beam 47 $^{(DB09)}$	56.2	2.709114052	48.60258541	1.156	37.38660416	1.5032
Beam 48 $^{(DB09)}$	53.4	3.682380561	41.52343108	1.286	34.60285924	1.5432
Beam 49 $^{(DB09)}$	70.7	2.738470812	50.17946707	1.409	41.81622256	1.6907
Beam 50 $^{(DB09)}$	85.6	2.172570432	58.18379461	1.471	48.48649551	1.7654
Beam 51 $^{(DB09)}$	49.6	3.502416819	33.37983793	1.486	27.81653161	1.7831
Beam 52 $^{(DB09)}$	54.4	3.013028825	45.12469979	1.206	37.60391649	1.4467
Beam 53 $^{(DB09)}$	65.3	2.678626181	58.3512879	1.119	48.62607325	1.3429
Beam 54 $^{(JSCA12)}$	33.41	3.939098212	26.61816073	1.255	20.47550826	1.6317
Beam 55 $^{(JSCA12)}$	53.94	3.148040571	28.47958379	1.894	23.7329865	2.2728
Beam 56 $^{(JSCA12)}$	39.88	3.939098212	26.61816073	1.498	20.47550826	1.9477
Beam 57 $^{(JSCA12)}$	63.82	3.148040571	28.47958379	2.241	23.7329865	2.6891
Beam 58 $^{(JSCA12)}$	29.4	3.939098212	26.61816073	1.105	20.47550826	1.4359
Beam 60$^{(DB08)}$	25.2	3.798104487	36.49277738	0.691	28.07136721	0.8977
Beam 61$^{(DB08)}$	48.6	2.669788888	41.04279358	1.184	31.57137968	1.5394
Beam 63 $^{(DB08)}$	41.4	2.955599312	40.16063437	1.031	33.46719531	1.237
Beam 64 $^{(DB08)}$	40.2	2.218872601	48.24000648	0.833	39.54098892	1.0167
Beam 65 $^{(DB08)}$	35.4	3.669583188	28.89793257	1.225	22.2291789	1.5925
Beam 66 $^{(DB08)}$	46.2	3.132157736	36.99856839	1.249	30.83214033	1.4984
Beam 67 $^{(DB08)}$	54.6	2.707487314	46.19644628	1.182	38.49703857	1.4183
Beam 68 $^{(DB11)}$	20.4	4.976960312	39.68384481	0.514	30.52603447	0.6683
Beam 69 $^{(DB11)}$	42.18	3.457993348	44.80506213	0.941	34.46543241	1.2238
Beam 70 $^{(DB11)}$	56.22	2.709114052	48.60258541	1.157	37.38660416	1.5037
Beam 71 $^{(DB11)}$	53.4	3.682380561	41.52343108	1.286	31.94110083	1.6718
Beam 72 $^{(DB11)}$	70.74	2.738470812	50.17946707	1.41	41.81622256	1.6917
Beam 73 $^{(DB11)}$	85.62	2.172570432	58.18379461	1.472	48.48649551	1.7659
Beam 74 $^{(DB11)}$	49.56	3.502416819	33.37983793	1.485	27.81653161	1.7817
Beam 75 $^{(DB11)}$	54.36	3.013028825	45.12469979	1.205	37.60391649	1.4456

Table(6): Continued

			γ_s=1		γ_s=1.2 for inclined FRP and 1.3 for vertical FRP reinforcement	
Sample No.	v_f^{exp} **(KN)**	**ε ana %**	v_f^{ana} **(KN)**	**K**	v_f^{ana} **(KN)**	**K**
Beam 76 (DB11)	65.34	2.678626181	58.3512879	1.12	48.62607325	1.3437
Beam 77 (DB11)	31.86	4.976960312	39.68384481	0.803	30.52603447	1.0437
Beam 78 (DB11)	33.6	3.457993348	44.80506213	0.75	33.18893491	1.0124
Beam 79 (DB11)	42.66	3.682380561	41.52343108	1.027	34.60285924	1.2328
Beam 80 (DB11)	64.02	2.738470812	50.17946707	1.276	41.81622256	1.531
Beam 82 (DB11)	51.72	3.502416819	52.45403103	0.986	43.71169253	1.1832
Beam 83 (DB10)	28.32	2.332216583	30.81960964	0.919	23.70739203	1.1946
Beam 84 (DB10)	33.9	2.673029259	30.74139702	1.103	25.61783085	1.3233
Beam 85 (DB10)	48	1.987847939	37.14979421	1.292	30.95816184	1.5505
Beam 86 (DB10)	33.06	2.560356498	24.88697766	1.328	20.73914805	1.5941
Beam 87 (DB10)	42.72	2.976219672	45.46020046	0.94	37.88350038	1.1277
Beam 89 (DB10)	26.04	2.673029259	30.74139702	0.847	25.61783085	1.0165
Beam 90 (DB10)	31.56	1.987847939	37.14979421	0.85	30.95816184	1.0194
Beam 91 (DB10)	25.08	2.560356498	24.88697766	1.008	20.73914805	1.2093
Beam 92 (DB10)	35.1	2.976219672	45.46020046	0.772	34.96938497	1.0037
Beam 93 (T10)	72.92	2.778492245	35.06381638	2.08	26.97216645	2.7035
Beam 94 (T10)	82.13	2.234798031	37.60339105	2.184	28.92568542	2.8393
Beam 99 (T10)	97.38	1.215575705	45.9429269	2.12	35.340713	2.7555
Beam 100 (I08)	151.4	2.394219989	60.14948767	2.517	46.26883667	3.2722
Beam 101 (I08)	81.5	4.062480401	50.43006451	1.616	38.79235732	2.1009
Beam 103 (RR10)	70	2.263291567	54.59323656	1.282	41.99479736	1.6669
Beam 104 (RR10)	103	2.281429282	55.03073944	1.872	42.33133803	2.4332
Beam 106 (RS12)	36.78	4.454854228	22.1362504	1.662	17.02788493	2.16
Beam 107 (RS12)	29.43	2.723759267	27.06876739	1.087	22.55730616	1.3047
Beam 108 (RS12)	49.05	4.26075844	22.46740533	2.183	17.28261949	2.8381
Beam 109 (RS12)	58.86	2.62683926	27.70312133	2.125	23.08593444	2.5496
Beam 110 (RS12)	66.21	5.036970678	21.24836007	3.116	16.34489236	4.0508
Beam 111 (RS12)	41.69	3.009876017	25.39415692	1.642	21.16179744	1.9701
Beam 112 (RS12)	61.51	4.26075844	22.46740533	2.738	17.28261949	3.5591
Beam 113 (RS12)	56.4	2.62683926	27.70312133	2.036	23.08593444	2.443
Beam 114 (RS12)	39.24	3.43386218	24.14279821	1.625	18.57138324	2.1129
Beam 115 (RS12)	68.67	2.204047091	30.99237165	2.216	25.82697638	2.6588
Beam 116 (DN01)	25	1.552433484	41.49699414	0.602	31.92076472	0.7832
Beam 117 (DN01)	37.4	1.206193475	45.13865854	0.829	34.72204503	1.0771
Beam 118 (DN01)	95.64	1.206193475	45.13865854	2.119	34.72204503	2.7544
Beam 119 (DN01)	75.2	1.155601377	61.77900176	1.217	51.48250146	1.4607

Table (6): Continued

			γ_s **=1**		γ_s **=1.2** for inclined FRP and **1.3** for vertical FRP reinforcement	
Sample No.	v_f^{exp} **(KN)**	ε^{ana} **%**	v_f^{ana} **(KN)**	**K**	v_f^{ana} **(KN)**	**K**
Beam 120 (DN01)	87.63	0.94117406	70.44186091	1.244	58.70155076	1.4928
Beam 121 (DN01)	53.4	1.552433484	41.49699414	1.287	31.92076472	1.6729
Beam 122 (RD07)	44.4	0.959014089	29.96028736	1.482	23.04637489	1.9266
Beam 123 (RD07)	21.6	0.959014089	29.96028736	0.721	21.40020526	1.0093
Beam 125 (RD07)	32.1	1.192056289	37.24062427	0.862	31.03385356	1.0344
Beam 126 (RD07)	22.9	0.781031349	48.7998684	0.469	40.666557	0.5631
Beam 127 (RD07)	41.3	1.537641372	25.59779864	1.613	19.69061434	2.0974
Beam 128 (RD07)	26.8	1.753942761	29.09289866	0.921	24.24408221	1.1054
Beam 129 (DB)	29.1	9.153811876	24.22098622	1.201	18.63152786	1.5619
Beam 130 (DB)	28.8	9.56277018	16.86958723	1.707	14.05798935	2.0487
Beam 131 (DB)	59.3	5.442889106	28.80376915	2.059	22.1567455	2.6764
Beam 132 (DB)	72.9	6.265495483	22.10579583	3.298	18.42149652	3.9573
Beam 133 (DB)	28.6	3.458936552	16.99721422	1.683	13.07478017	2.1874
Beam 134 (DB)	23.2	4.333319892	14.19668023	1.634	11.83056686	1.961
Beam 135 (DB)	31.8	2.056695979	20.21320808	1.573	15.5486216	2.0452
Beam 136 (DB)	36.4	2.839176901	18.60323613	1.957	15.50269678	2.348
			$K_{ave.}$=1.38		**$K_{ave.}$= 1.7**	

Note: K ave. = the average value of K

4.3 The Modification of Dias and Barross' Model

Following the argument made at the beginning of this chapter, the modification of Dias and Barros model is illustrated in this section to only justify this argument and compare the results of the two modified models.

The modification of this model was carried out using the same procedure (strategy) that was used in modifying Thanasis C. Triantafillou's model (see section (4.4.1) for more details). However, there are two differences to be noticed. Firstly, in this model, the theoretical shear contribution of NSM technique in RC beams is calculated using equation (4.6) below. The development steps, principles and approach of this equation are explained in details in section (3.5) above.

$$v_f = \frac{h_w}{\gamma_s} \times \frac{A_{fv}}{S_f} \times \varepsilon_{fe} \times E_f \times \left(\cot\alpha + \cot\theta_f\right) \times \sin\theta_f \qquad (4.6)$$

Where:

h_w is the web depth of the beam (mm). α is the orientation of the shear failure crack which is equal to 45°. θ_f is the inclination in degree of the FRP reinforcements and it is measured with respect to the horizontal axis of the beams. S_f is the spacing of FRP reinforcements (mm). A_{fv} is the area of FRP reinforcement in shear (mm^2), E_f is the tension modulus of elasticity of FRP reinforcement (GPa). ε_{fe} is the FRP effective strain. γ_s is a partial safety factor.

Secondly, for each inclination of the FRP reinforcements (θ_f); (45°, 60° and 90°); it was defined the equation that relates ε_{fe} with the product $\mathbf{[(E_{sw}\,\rho_s + E_f\,\rho_f) / (f_{cm}^{2/3})]}$. This was established according to the dependency relationship that was found by only Dias and Barros (see section 3.5 for more details regarding this). It can be notice this relationship is different to that dependency relationship of Thanasis C. Triantafillou. This is because the effect of the steel stirrups in the strengthened beams is also considered in Dias and Barross' dependency relationship.

The experimental values of ε_{fe} for the three cases of FRP orientations were obtained by substituting the experimental values of V_f of the considered beams in equation (4.6) above. Then, by plotting these values against the product [($E_{sw}\,\rho_{sw} + E_f$

$\rho_f)/ (f_{cm}^{2/3})]$ for the three arrangements of FRP reinforcements separately, equations (4.7), (4.8) and (4.9) were obtained. It should be noticed that, the same samples (RC beams) of the database, which were not considered in the modification analysis of Thanasis C. Triantafillou's model, are also not considered in the modification processes of this model for the same reasons (see section 4.1.2 for the reasons).

The calibrated equations are:

1- For FRP reinforcement at 90°(See figure**14a**)

$$\varepsilon_{fe} = 0.5953 \times (E_{sw}\rho_{sw} + E_f\rho_f)/(f_{cm}^{2/3})^{-0.549} \quad (4.7)$$

2- For FRP reinforcement at 60°(See figure **14b**)

$$\varepsilon_{fe} = 0.2134 \times (E_{sw}\rho_{sw} + E_f\rho_f)/(f_{cm}^{2/3})^{-0.974} \quad (4.8)$$

3- For FRP reinforcement at 45°(See figure **14c**)

$$\varepsilon_{fe} = 1.0045 \times (E_{sw}\rho_{sw} + E_f\rho_f)/(f_{cm}^{2/3})^{-0.456} \quad (4.9)$$

These equations correspond to the best fit of power-type curves that describe the relationship between ε_{fe} and the product $[(E_{sw}\rho_{sw} + E_f\rho_f)/ (f_{cm}^{2/3})]$ for each arrangement of the FRP reinforcements.

By using equations (4.7), (4.8) and) (4.9) above, the theoretical FRP effective strain was obtained. Thereafter, by introducing the theoretical FRP effective strain to equation (4.6), the theoretical shear contribution of NSM technique in RC beams was also calculated. Similar to before, the K ratio, which is equal to ($v_f^{\ exp} / v_f^{\ ana}$), was also calculated for the considered beams. This is well shown in table (7). The average value of the K ratio when no safety factor was used in equation (4.6) is equal to (1.1). It is important to emphasise that by introducing the value (1.1) to equation (4.6) above as an uncertainty factor to increase the safe prediction ability of the modified model, the corresponding percentage of the safe prediction is equal to 70%, and the corresponding average K ratio in this case is equal to (1.2). This demonstrates that only 70% of the

considered beams in table (7) are in the safe side, as they have K value equal or greater than unity. This also illustrates a slight improvement to this model, as this model showed 68.8% safe prediction percentage before equations (4.7), (4.8) and (4.9) being calibrated.

Another slight enhancement can be noticed when a safety factor equal to 1.2 is used as shown in table (7). In fact, using this uncertainty factor led to increase the percentage of the safe prediction to be equal to 76% and the corresponding average K ratio to be equal to (1.32). Introducing higher safety factors such as (1.3) to this model might also improve it slightly. However, this is not a real case as doing so means more uncertainty is introduced to this model. This is because of the fact that the safety factors (1.2 and 1.3) are greater than the average value of the K ratio (1.1), which was obtained without introducing a safety factor to this model. In addition, doing so will lead to have a very bad agreement between the experimental and theoretical results of v_f . By this point, this model has been modified.

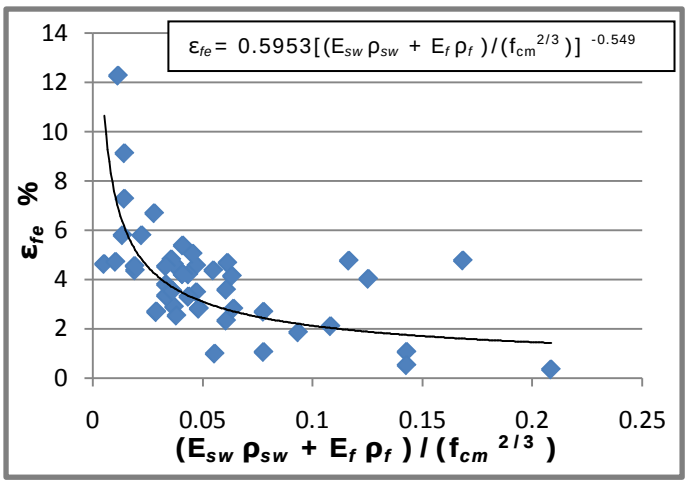

(a) FRP reinforcement at 90°

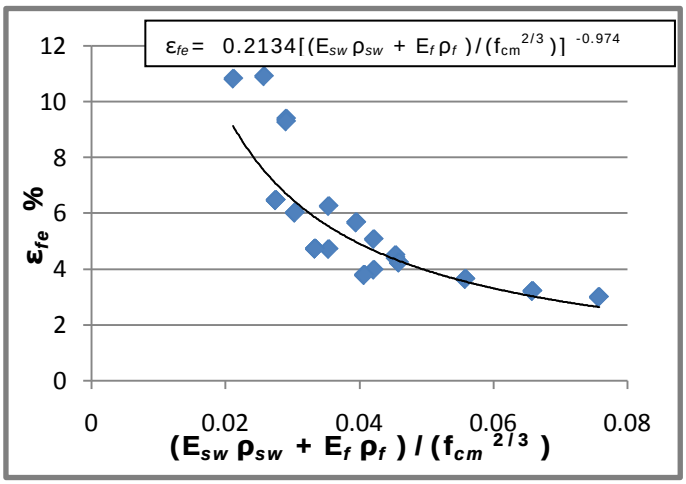

(b) FRP reinforcement at 60°

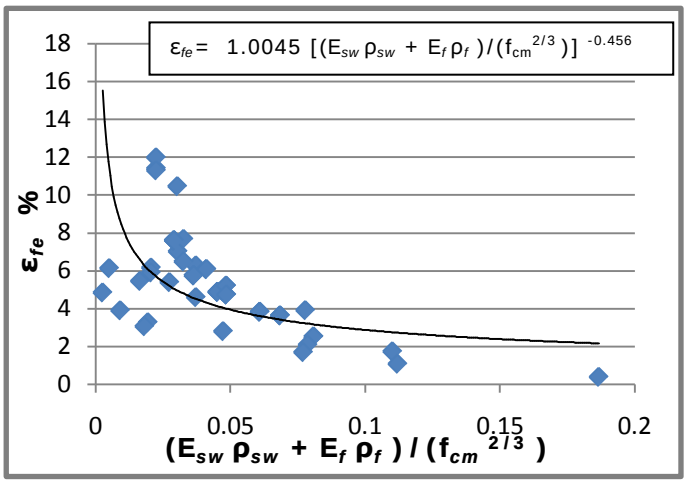

(c) FRP reinforcement at 45°

Figure (14): Effective strain of FRP reinforcement *versus* [($E_{sw}\rho_{sw}$+ $E_f\rho_f$) / ($f_{cm}^{2/3}$)]

Notice that, the three plots; a, b and c; of figure (14) above were plotted using the calculations presented in tables C1, C2 and C3 in **Appendix (C)**, respectively.

4.4 The Results of the Comparison between the Modified Thanasis C. Triantafillou's and Dias and Barross' Models

The comparison between the results of the analysis in table (7) with that in table (6) proves that, the modified Thanasis C. Triantafillou's model is a sufficient theoretical model, which predicts the shear contribution of Near Surface Mounted technique accurately and showing sufficient agreement with the experimental results in RC beams. Adding to this, this examination demonstrates that the selection of Thanasis C. Triantafillou's for the modification processes in this project was the right decision. This is due to the fact that by calibrating this model, 94% of the considered beams in table (6) have K value equal or greater than unity. In other word, by using this model 94% of the NSM shear strengthened beams in this table are in the safe side. This is because the predicted theoretical shear contribution of NSM technique by using this modified model is less than that obtained experimentally. The 94% of safe prediction is basically by far greater than that percentage obtained using Dias and Barross' model after modifying it and introducing different safety factors to it. In fact, 76% was the highest safe prediction percentage, which was obtained using partial safety factor equal to 1.2 with the modified Dias and Barross' model. Using higher safety factors, which are not a real case to be considered as mentioned before, could also improve this percentage slightly. However, it will be by far less than 94%. Based on this, the argument made in the beginning of chapter four has now been justified. Both the factors mentioned in section (3.7) regarding the performance of these two models, and the impacts of the calibration discussed in section (4.2) are reasons contributed in the achieved results in this chapter.

Finally, by reaching this point, it can be said the modified Thanasis C. Triantafillou's model in this dissertation can be now used to estimate the shear contribution of NSM technique in RC beams without any restrictions and with high accuracy. However, it is important to mention that when more experimental data is available; this model can be improved more. This is due to the fact that the more considered data in the modification of this model, the closer to reality the predicted results can be.

Table (7): Comparison between the experimental and analytical results using the modified Dias and Barros's model

			γ_s= 1		γ_s= 1.1		γ_s= 1.2	
Sample No.	v_f^{exp} **(KN)**	ε^{ana} **%**	v_f^{ana} **(KN)**	**K**	v_f^{ana} **(KN)**	**K**	v_f^{ana} **(KN)**	**K**
Beam 1 (DB12)	40.3	3.634	31.782	1.268	28.893	1.395	26.485	1.522
Beam 2 (DB12)	63.7	3.183	44.546	1.43	40.497	1.573	37.122	1.716
Beam 3 (DB12)	37.9	4.945	26.669	1.4211	24.245	1.563	22.224	1.705
Beam 4 (DB12)	56.5	4.513	40.6	1.3916	36.909	1.531	33.833	1.67
Beam 5 (DB12)	70.3	4.043	57.985	1.2124	52.714	1.334	48.321	1.455
Beam 6 (DB12)	35.4	6.424	37.789	0.9368	34.353	1.03	31.491	1.124
Beam 7 (DB12)	61.3	5.529	54.203	1.1309	49.275	1.244	45.169	1.357
Beam 8 (DB12)	69.7	4.666	64.166	1.0862	58.333	1.195	53.472	1.303
Beam 9 (DB12)	57.5	3.704	43.197	1.3311	39.27	1.464	35.997	1.597
Beam 10 (DB12)	71.5	3.323	56.651	1.2621	51.501	1.388	47.209	1.515
Beam 11 (DB12)	53.4	5.053	35.438	1.5068	32.217	1.658	29.532	1.808
Beam 12 (DB12)	70.7	4.558	55.991	1.2627	50.901	1.389	46.659	1.515
Beam 13 (DB12)	85.6	4.128	72.371	1.1828	65.792	1.301	60.309	1.419
Beam 14 (DB12)	49.6	7.076	54.252	0.9143	49.32	1.006	45.21	1.097
Beam 15 (DB12)	54.4	5.859	67.378	0.8074	61.253	0.888	56.149	0.969
Beam 16 (DB12)	65.3	4.827	83.256	0.7843	75.687	0.863	69.38	0.941
Beam 17 (DB12)	31.9	3.44	26.061	1.224	23.692	1.346	21.718	1.469
Beam 18 (DB12)	40.7	3.44	26.061	1.5617	23.692	1.718	21.718	1.874
Beam 19 (DB12)	33.6	3.142	37.589	0.8939	34.171	0.983	31.324	1.073
Beam 20 (DB12)	42.7	4.312	30.243	1.4119	27.493	1.553	25.202	1.694
Beam 21 (DB12)	64	4	49.136	1.3025	44.669	1.433	40.947	1.563
Beam 22 (DB12)	43.5	4.968	38.085	1.1422	34.623	1.256	31.738	1.371
Beam 23 (DB12)	51.7	4.34	49.911	1.0359	45.373	1.139	41.592	1.243
Beam 24 (DB12)	43.6	2.77	33.798	1.29	30.726	1.419	28.165	1.548
Beam 25 (DB12)	33.9	3.998	28.598	1.1854	25.998	1.304	23.832	1.422
Beam 26 (DB12)	48	3.602	45.135	1.0635	41.032	1.17	37.612	1.276
Beam 27 (DB12)	33.1	4.294	33.575	0.9858	30.523	1.084	27.979	1.183
Beam 28 (DB12)	42.7	3.548	41.611	1.0262	37.828	1.129	34.676	1.231
Beam 29 (DB12)	26	3.416	24.431	1.0642	22.21	1.171	20.36	1.277
Beam 30 (DB12)	31.6	3.165	39.656	0.7969	36.051	0.877	33.047	0.956
Beam 31 (DB12)	25.1	3.021	23.622	1.0626	21.474	1.169	19.685	1.275
Beam 32 (DB12)	35.1	2.635	30.9	1.1359	28.091	1.25	25.75	1.363
Beam 33 (DB12)	44.7	4.803	37.118	1.2043	33.743	1.325	30.931	1.445
Beam 34 (DB12)	81.5	4.237	51.697	1.5765	46.997	1.734	43.08	1.892
Beam 35 (DB12)	81.7	5.691	40.704	2.0072	37.004	2.208	33.92	2.409
Beam 37 (DB12)	85.8	5.691	40.704	2.1079	37.004	2.319	33.92	2.529
Beam 38 (DB12)	80.9	5.691	40.704	1.9875	37.004	2.186	33.92	2.385
Beam 39 (DB12)	84.6	9.127	71.361	1.1855	64.874	1.304	59.468	1.423
Beam 40 (DB12)	127.9	7.541	88.44	1.4462	80.4	1.591	73.7	1.735

Table (7): Continued

Sample No.	v_f^{exp} (KN)	ε^{ana} %	$\gamma_s = 1$		$\gamma_s = 1.1$		$\gamma_s = 1.2$	
			v_f^{ana} (KN)	K	v_f^{ana} (KN)	K	v_f^{ana} (KN)	K
Beam 41 (DB12)	74.9	4.957	35.456	2.1125	32.233	2.324	29.546	2.535
Beam 43 (DB12)	73.4	6.704	52.417	1.4003	47.652	1.54	43.681	1.68
Beam 45 (DB09)	20.2	4.163	31.542	0.6404	28.675	0.704	26.285	0.768
Beam 46 (DB09)	42.2	3.677	43.989	0.9593	39.99	1.055	36.657	1.151
Beam 47 (DB09)	56.2	3.323	56.651	0.992	51.501	1.091	47.209	1.19
Beam 48 (DB09)	53.4	5.053	35.438	1.5068	32.217	1.658	29.532	1.808
Beam 49 (DB09)	70.7	4.558	55.991	1.2627	50.901	1.389	46.659	1.515
Beam 50 (DB09)	85.6	4.128	72.371	1.1828	65.792	1.301	60.309	1.419
Beam 51 (DB09)	49.6	7.076	54.252	0.9143	49.32	1.006	45.21	1.097
Beam 52 (DB09)	54.4	5.859	67.378	0.8074	61.253	0.888	56.149	0.969
Beam 53 (DB09)	65.3	4.827	83.256	0.7843	75.687	0.863	69.38	0.941
Beam 54 (JSCA12)	33.41	3.851	33.938	0.9844	30.853	1.083	28.282	1.181
Beam 55 (JSCA12)	53.94	4.793	39.821	1.3546	36.201	1.49	33.184	1.625
Beam 56 (JSCA12)	39.88	3.851	33.938	1.1751	30.853	1.293	28.282	1.41
Beam 57 (JSCA12)	63.82	4.793	39.821	1.6027	36.201	1.763	33.184	1.923
Beam 58 (JSCA12)	29.4	3.851	33.938	0.8663	30.853	0.953	28.282	1.04
Beam 60 (DB08)	25.2	3.634	31.782	0.7929	28.893	0.872	26.485	0.951
Beam 61 (DB08)	48.6	3.183	44.546	1.091	40.497	1.2	37.122	1.309
Beam 63 (DB08)	41.4	4.513	40.6	1.0197	36.909	1.122	33.833	1.224
Beam 64 (DB08)	40.2	4.043	57.985	0.6933	52.714	0.763	48.321	0.832
Beam 65 (DB08)	35.4	6.424	37.789	0.9368	34.353	1.03	31.491	1.124
Beam 66 (DB08)	46.2	5.529	54.203	0.8524	49.275	0.938	45.169	1.023
Beam 67 (DB08)	54.6	4.666	64.166	0.8509	58.333	0.936	53.472	1.021
Beam 68 (DB11)	20.4	4.163	31.542	0.6467	28.675	0.711	26.285	0.776
Beam 69 (DB11)	42.18	3.677	43.989	0.9589	39.99	1.055	36.657	1.151
Beam 70 (DB11)	56.22	3.323	56.651	0.9924	51.501	1.092	47.209	1.191
Beam 71 (DB11)	53.4	5.053	35.438	1.5068	32.217	1.658	29.532	1.808
Beam 72 (DB11)	70.74	4.602	56.535	1.2513	51.395	1.376	47.112	1.502
Beam 73 (DB11)	85.62	4.169	73.106	1.1712	66.46	1.288	60.921	1.405
Beam 74 (DB11)	49.56	7.076	54.252	0.9135	49.32	1.005	45.21	1.096
Beam 75 (DB11)	54.36	5.859	67.378	0.8068	61.253	0.887	56.149	0.968
Beam 76 (DB11)	65.34	4.827	83.256	0.7848	75.687	0.863	69.38	0.942
Beam 77 (DB11)	31.86	3.44	26.061	1.2225	23.692	1.345	21.718	1.467
Beam 78 (DB11)	33.6	3.142	37.589	0.8939	34.171	0.983	31.324	1.073
Beam 79 (DB11)	42.66	4.312	30.243	1.4106	27.493	1.552	25.202	1.693
Beam 80 (DB11)	64.02	4.041	49.642	1.2896	45.129	1.419	41.368	1.548
Beam 81 (DB11)	43.44	4.968	38.085	1.1406	34.623	1.255	31.738	1.369
Beam 82 (DB11)	51.72	4.34	49.911	1.0363	45.373	1.14	41.592	1.244
Beam 83 (DB10)	28.32	3.602	43.953	0.6443	39.958	0.709	36.628	0.773
Beam 84 (DB10)	33.9	4.039	28.892	1.1733	26.266	1.291	24.077	1.408

Table (7): Continued

Sample No.	v_f^{exp} (KN)	ε^{ana} %	$\gamma_s = 1$		$\gamma_s = 1.1$		$\gamma_s = 1.2$	
			v_f^{ana} (KN)	K	v_f^{ana} (KN)	K	v_f^{ana} (KN)	K
Beam 85 (DB10)	48	3.641	45.62	1.0522	41.473	1.157	38.017	1.263
Beam 86 (DB10)	33.06	4.294	33.575	0.9847	30.523	1.083	27.979	1.182
Beam 87 (DB10)	42.72	3.548	41.611	1.0267	37.828	1.129	34.676	1.232
Beam 89 (DB10)	26.04	3.416	24.431	1.0658	22.21	1.172	20.36	1.279
Beam 90 (DB10)	31.56	3.165	39.656	0.7958	36.051	0.875	33.047	0.955
Beam 91 (DB10)	25.08	3.021	23.622	1.0617	21.474	1.168	19.685	1.274
Beam 92 (DB10)	35.1	2.635	30.9	1.1359	28.091	1.25	25.75	1.363
Beam 93 (T10)	72.92	1.937	29.719	2.4536	27.017	2.699	24.766	2.944
Beam 94 (T10)	82.13	1.861	38.064	2.1577	34.604	2.373	31.72	2.589
Beam 95 (T10)	95.24	1.733	53.152	1.7918	48.32	1.971	44.293	2.15
Beam 96 (T10)	79.65	1.689	58.287	1.3665	52.989	1.503	48.573	1.64
Beam 97 (T10)	95.64	1.585	72.924	1.3115	66.295	1.443	60.77	1.574
Beam 98 (T10)	96.42	1.412	97.416	0.9898	88.56	1.089	81.18	1.188
Beam 99 (T10)	97.38	1.583	32.373	3.0081	29.43	3.309	26.977	3.61
Beam 100 (I08)	151.4	2.756	89.425	1.693	81.295	1.862	74.521	2.032
Beam 101 (I08)	81.5	3.245	52.498	1.5524	47.725	1.708	43.748	1.863
Beam 102 (I08)	112.9	2.929	75.815	1.4891	68.923	1.638	63.18	1.787
Beam 103 (RR10)	70	2.69	67.074	1.0436	60.976	1.148	55.895	1.252
Beam 104 (RR10)	103	2.706	67.467	1.5267	61.333	1.679	56.222	1.832
Beam 106 (RS12)	36.78	6.296	40.021	0.919	36.383	1.011	33.351	1.103
Beam 107 (RS12)	29.43	6.083	54.684	0.5382	49.713	0.592	45.57	0.646
Beam 108 (RS12)	49.05	6.094	41.137	1.1924	37.397	1.312	34.281	1.431
Beam 109 (RS12)	58.86	5.921	56.52	1.0414	51.382	1.146	47.1	1.25
Beam 110 (RS12)	66.21	6.889	37.198	1.7799	33.817	1.958	30.999	2.136
Beam 111 (RS12)	41.69	6.555	50.059	0.8328	45.508	0.916	41.716	0.999
Beam 112 (RS12)	61.51	6.094	41.137	1.4953	37.397	1.645	34.281	1.794
Beam 113 (RS12)	56.4	5.921	56.52	0.9979	51.382	1.098	47.1	1.197
Beam 114 (RS12)	39.24	5.204	46.836	0.8378	42.578	0.922	39.03	1.005
Beam 115 (RS12)	68.67	5.193	66.095	1.039	60.086	1.143	55.079	1.247
Beam 116 (DN01)	25	2.91	74.173	0.337	67.43	0.371	61.811	0.404
Beam 117 (DN01)	37.4	2.42	86.328	0.4332	78.48	0.477	71.94	0.52
Beam 118 (DN01)	95.64	2.42	86.328	1.1079	78.48	1.219	71.94	1.329
Beam 119 (DN01)	75.2	3.205	115.5	0.6511	105	0.716	96.251	0.781
Beam 120 (DN01)	87.63	2.749	138.7	0.6318	126.09	0.695	115.58	0.758
Beam 121 (DN01)	53.4	2.018	51.424	1.0384	46.749	1.142	42.853	1.246
Beam 122 (RD07)	44.4	1.733	72.997	0.6082	66.361	0.669	60.831	0.73
Beam 123 (RD07)	21.6	1.733	72.997	0.2959	66.361	0.325	60.831	0.355
Beam 124 (RD07)	32.1	2.727	81.229	0.3952	73.845	0.435	67.691	0.474
Beam 125 (RD07)	22.9	2.16	128.68	0.178	116.99	0.196	107.24	0.214
Beam 126 (RD07)	41.3	2.187	48.913	0.8444	44.466	0.929	40.761	1.013

Table (7): Continued

			$\gamma_s = 1$		$\gamma_s = 1.1$		$\gamma_s = 1.2$	
Sample No.	v_f^{exp} **(KN)**	ε^{ana} **%**	v_f^{ana} **(KN)**	**K**	v_f^{ana} **(KN)**	**K**	v_f^{ana} **(KN)**	**K**
Beam 128 (RD07)	26.8	3.236	51.187	0.5236	46.534	0.576	42.656	0.628
Beam 129 (DB)	29.1	10.67	67.201	0.433	61.092	0.476	56.001	0.52
Beam 130 (DB)	28.8	15.55	92.391	0.3117	83.992	0.343	76.992	0.374
Beam 131 (DB)	59.3	7.291	91.863	0.6455	83.512	0.71	76.553	0.775
Beam 132 (DB)	72.9	11.34	134.71	0.5412	122.46	0.595	112.26	0.649
Beam 133 (DB)	28.6	5.232	32.96	0.8677	29.964	0.954	27.467	1.041
Beam 134 (DB)	23.2	8.608	51.127	0.4538	46.479	0.499	42.606	0.545
Beam 135 (DB)	31.8	3.576	45.056	0.7058	40.96	0.776	37.547	0.847
Beam 136 (DB)	36.4	6.275	74.544	0.4883	67.767	0.537	62.12	0.586

5 CONCLUSIONS

5.1 Summery

This dissertation aimed firstly to study the effects of different parameters on the effectiveness of NSM technique by means of shear strengthening technique in RC beams using the findings of previous experimental tests. Secondly, it aimed to evaluate the current theoretical models in terms of the accuracy in estimating the shear contribution (v_f) of this technique in RC beams, the considered parameters in the development of them, and their degree of sophistication. Finally, by using the generated experimental database and the final results of evaluation of the selected models, it was aimed in this project to propose a modified model, which can be used as a design-oriented equation to calculate the term (v_f) in the NSM shear strengthened beams accurately. This chapter is divided into three aspects according to the aims of the project.

Regarding the influences of the different factors on the effectiveness of NSM technique, it was found that all the studied parameters in chapter two have significant impacts on the effectiveness of this technique in shear strengthening of RC beams. Basically, using inclined NSM FRP reinforcements (bars/laminates) with close spacing was found to be more effective than using these reinforcements with the vertical arrangement and the close spacing, in terms of increasing the shear contribution of NSM technique, and preventing debonding failure from taking place in the strengthened beams. Additionally, the presence of the high percentage of existing steel stirrups in the NSM shear strengthened beams illustrated a fall in the efficiency of this technique. However, using certain amount of it seems to be very helpful in improving the shear contribution of NSM technique in RC beams. The type and material of Near Surface Mounted FRP reinforcements was discovered to be important factors in increasing both the effectiveness of this technique, and the tensile strain of NSM reinforcements. Furthermore, it was discovered that increasing the percentage of composite material in the strengthened beams generally led to a decrease in the shear strength provided by each NSM FRP laminate/bar in the strengthened beams. Also, it changed the mode of failure in the NSM shear strengthened beams from debonding of the NSM reinforcements to be by splitting the concrete cover along the longitudinal flexural bars. It was also found the compressive strength of concrete appears to be a significant variable that by raising it, the effectiveness of this technique can improve. Finally, the anchorage of NSM reinforcements discovered to be able to change the shear failure mode from debonding

of the NSM FRP reinforcements to a separation of the concrete cover, and increase the shear capacity of the strengthened beams.

As far as the evaluation of the current theoretical models is concerned, the availability of the experimental data, and the complexity of some models contributed mainly in considering only three models in this project. Experimental database was generated in this dissertation. This database was then used to evaluate A.K.M Anwarul Islam's, Dias and Barross', Thanasis C. Triantafillou's models, respectively. Despite the fact that the last evaluated model was originally developed to calculate the shear contribution of EFRP technique in RC beams, this model was built up using an approach and principles, which can be also used in developing an analytical design guidance to calculate the shear contribution of NSM technique in RC beams. By examining the degree of sophistication of the three models, it was found that Thanasis C. Triantafillou's model is a rather more sophisticated one compared to the other two. It was basically found that it is a descriptive model, which links the FRP effective strain with the geometric parameters of the FRP stress bearing mechanisms shown in (figure 12), and links the FRP effective stain to the development length of the FRP reinforcement. In fact, a dependency relationship; which links the FRP effective strain with the product ($E_f \rho_f / f_c^{2/3}$); was established with this model based on experimental findings. This relationship was proved later by many others in both the fields of using EFRP and NSM techniques in shear strengthening of RC beams. In addition, the examination of these models showed that A.K.M Anwarul Islam's formula is a very simple one, and it does not take into consideration the impacts of many variables. Furthermore, this comparison illustrated that Dias and Barross' model is a rather more sophisticated compared to A.K.M Anwarul Islam's formula. This is due to a dependency relationship taking into account the effects of different variables was proposed with this model, and then used to establish equations to calculate the FRP effective stain in the NSM shear strengthened beams. From calculating the ratio (K) between the experimental and theoretical shear contribution of this technique in RC beams, Thanasis C. Triantafillou's model showed again the best results among the others. In fact, 27%, 68.6% and 100% were the safe prediction percentages obtained using A.K.M Anwarul Islam's, Dias and Barross', Thanasis C. Triantafillou's models, respectively. It is important to note that the safe prediction percentage here reflects the ability of the theoretical models in predicting the theoretical shear contribution of NSM technique in RC beams accurately, with values less than that obtained experimentally. In addition, this percentage represents the percentage ratio between the number of beams, which have (K) ratio equal or greater than unity, and the total number of the considered beams in the evaluation.

According to the final results of the evaluation of the three models, Thanasis C. Triantafillou's model was the selected one for the modification processes in this project. However, the modification of Dias and Barross' model was also considered in this dissertation. This was for the comparison purposes and the justification of any argument, which might be raised regarding the selection of Thanasis C. Triantafillou's model for the calibration processes. The modifications (calibrations) of the two models were based on the created experimental database. Three equations, which link the FRP effective strain with the product $[(E_f \rho_f)/ (f_{cm}^{2/3})]$ for the three arrangements of FRP reinforcement; (90^o, 60^o and 45^o); were proposed in section (4.1.2). This was achieved using the dependency relationship of Thanasis C. Triantafillou, and following the proposed strategy for the best scenario of calibration of Thanasis C. Triantafillou's model. These three equations can be now used instead of those were proposed with the original version of Thanasis C. Triantafillou's model (in section 3.6). In addition, new uncertainty factors equal to 1.2 and 1.3 for the inclined and vertical arrangements of FRP reinforcements were proposed to be used with the modified model, respectively. These factors were established in order to ensure a safe condition ($K \geq 1$) for 94% of the considered beams of the database in the analysis shown in table (6). A maximum limit for the FRP effective strain for each type of the FRP reinforcement was defined in this project using the database. This was defined in order to maintain the aggregate interlock, and control the shear cracks in the NSM shear strengthened beams. After that, Dias and Barross' model was modified by calibrating the equations, which link the FRP effective strain with the product $(\rho_f E_f + E_{sw} \rho_{sw} / f_{cm}^{2/3})$ for the three arrangements of the FRP reinforcements. Similar to the first modified model, new safety factors were introduced to this model based on the results of the new analysis of it in table (7). This was also carried out to increase the ability of this model in the safe prediction of the analytical values of (v_f). However, 76% was the maximum safe prediction percentage, which was obtained using a safety factor equal to 1.2 with this model.

By comparing the results obtained using the two modified models in terms of the percentage of the safe prediction, and the close agreement with the experimental results, the modified Thanasis C. Triantafillou's model showed by far better results. In fact, even by introducing different safety factors to the second modified model, the percentage of safe prediction of it did not exceed 76%. Finally, this comparison proved that the modified Thanasis C. Triantafillou's model is a sufficient theoretical model, which can predict the shear contribution of NSM technique in the NSM shear beams accurately, and showing sufficient agreement with the experimental results. Therefore, Thanasis C. Triantafillou's model has been adopted, and it can be now used in the NSM shear strengthened beams as a design-oriented equation to calculate the term (v_f). It is

important to note this modified model is compatible with Eurocode2, as the original model was built up in accordance to this design code.

5.2 Recommendation for Future Researches

Despite the investigations in this project, there are some other fields that might still need more examination and work. For example, when more experimental data is available, the three proposed expressions that link the FRP effective strain with the product $[(E_f \rho_f)/ (f_{cm}^{2/3})]$ can be improve more. This is due to the fact that the more considered data in the calibration of these expressions, the more accurate results, and the closer agreement between the theoretical and the experimental results can be. Another considerable area is the investigation of new parameters, which may affect the effectiveness of this technique by means of shear strengthening technique in RC beams. This can be achieved by carrying out more experimental tests to study the new factors. If such new factors exist, the impacts of them might be tried to introduce to the modified Thanasis C. Triantafillou's model in this dissertation.

LIST OF REFERENCES

- Anwarul Islam, A. K. M. (2008) 'Effective method of using CFRP bars in shear strengthening of concrete girders'. *Engineering Structures* **31**(3), 709-714

- Barros, J. A. O., Bianco, V., and Monti, G. (2009) 'NSM CFRP Strips for Shear Strengthening of RC Beams: Tests and Mechanical Model' *The Open Construction and Building Technology Journal***3**(2009), 12-32

- Barros, J.A.O., and Dias, S.J.E. (2006) 'Near surface mounted CFRP laminates for shear strengthening of concrete beams' *Cement and Concrete Composites* **28**(3), 276-292

- Cameron, R. (2012) *Strengthening of RC Beams with Externally Bounded Anchored FRP Laminate* [Online] MA dissertation. Mc Master University. Available form<http://digitalcommons.mcmaster.ca/cgi/viewcontent.cgi?article=8054&context=opendissertations> [Accessed 24 October 2012]

- De Lorenzis, L., and Nanni, A. (2000) *Strengthening of RC Structures with Near Surface Mounted FRP Rods. United States: University of Missouri-Rolla*

- De Lorenzis, L., and Nanni, A. (2001) 'Shear Strengthening of Reinforced Concrete Beams with Near-Surface Mounted Fiber-Reinforced Polymer Rods'. *ACI Structural Journal* **98** (1), 60-68

- Dias, S.J.E., and Barros, J.A.O. (2005) 'Experimental Research of a New CFRP-Based Shear Strengthening Technique for Reinforced Concrete Beams'. *IBRACON Structural Journal* **1**(2), 103-126

- Dias, S.J.E., and Barros, J.A.O. (2006) 'Near Surface Mounted CFRP Laminates for Shear Strengthening of Concrete Beams'. *Cement and Concrete Composites* **28**(2006), 276-292

- Dias, S.J.E., Barros, J.A.O., and Lima, J.L.T. (2006) 'Efficacy of CFRP-based techniques for flexural and shear strengthening of concrete beams'. *Cement and Concrete Composites* **29(**2007), 203-217

- Dias, S.J.E., and Barros, J.A.O. (2008) 'Shear Strengthening of T Cross Section Reinforced Concrete Beams by Near-Surface Mounted Technique'. *Journal of Composites for Construction* **12**(3), 300-311

- Dias, S.J.E., and Barros, J.A.O. (2009) 'Performance of reinforced concrete T beams strengthened in shear with NSM CFRP laminates'. *Engineering Structures* **32**(2010), 373-384

- Dias, S.J.E., and Barros, J.A.O. (2010) 'Shear strengthening of RC T-section beams with low strength concrete using NSM CFRP laminates'. *Cement and Concrete Composite* **33**(2), 334-3405

- Dias, S.J.E., and Barros, J.A.O. (2011) 'Experimental Behaviour of RC Beams Shear Strengthening with NSM CFRP Laminates'. *Strain* **48**(1), 88-100

- Dias, S.J.E., and Barros, J.A.O. (2012) 'Shear strengthening of RC beams with NSM CFRP laminates: Experimental Research and Analytical Formulation'. *Composite structural* in Press (2012), 1-32

- Dias, S.J.E., and Barros, J.A.O. '*Shear Strengthening of RC Beams with Near-Surface-Mounted CFRP Laminates'* [Online] Available from <http://repositorium.sdum.uminho.pt/bitstream/1822/5013/1/Barros_CI_5_2005.pdf> [Accessed 30June 2013]

- Ehsani, M. (2005) 'Strengthening of Concrete and Masonry Structures with Reinforced Polymers (FRP)'. 'Our World in Concrete and Structures'. held 23-24 August 2005 at Singapore. USA: University of Arizona

- Federation International du Beton, fib (2001) '*Externally bonded FRP reinforcement for RC structures'*, Bulletine 24. Lausanne

- Jalali, M., Kazem Sharbatdar, M., Chen, J., and Alaee, F. (2012) 'Shear strengthening of RC beams using innovative manually made NSM FRP bars'. *Construction and Building Materials* **36** (November 2012), 990-1000

- Rahal, K.N., and Rumaih, H. A. (2010) 'Test on reinforced concrete beams strengthened in shear using near surface mounted CRFP and steel bars'. *Engineering Structures* **33**(1), 53-62

- Raj, S.D., and Surumi, R.S. (2012) 'Shear Strengthening of Reinforced Concrete Beams Using Near Surface Mounted Glass Fibre Reinforced Polymer'. *Asian Journal of Civil Engineering (Building and Housing)* **13**(5), 679-690

- Rizzo, A., and De Lorenzis, L., (2007) 'Behaviour and Capacity of RC Beams Strengthened in Shear with NSM FRP Reinforcement'. *Construction and Building Materials* **23**(2009), 1555–1567

- Tanaslan, H.M. (2010) 'The effects of NSM CFRP reinforcements for improving the shear capacity of RC beam'. *Construction and Building Materials* **25**(5), 2663-2673

- Teng, J.G., Chen, J.F., Smith, S.T., and Lam, L. (2002) *FRP Strengthened RC Structures.* England: John Wily and Sons

- Transportation Research Board of The National Academies (2011) *Design of FRP Systems for Strengthening Concrete Girders in Shear* project no.678. United States: The American Association of State Highway and Transportation offices and Federal Highway Administration

- Triantafillou, C. T. (1998) 'Shear Strengthening of Reinforced Concrete Beams Using Epoxy-Bonded FRP Composites'. *ACI Structural Journal* **95**(2), 107-115

– Triantafillou, C. T. (2000) ‘Design of Concrete Flexural Members Strengthening in Shear with FRP’. *Journal of Composite Construction* **4**(4), 198-20

APPENDIX (A): THE CREATED EXPERIMENTAL DATABASE

Table (A): The created experimental database on shear strengthening of RC beams with NSM FRP reinforcements

Sample No.(1)	f_{cm} (MPa) (2)	ρ_f % (3)	E_f (GPa) (4)	ε_{fu} % (5)	Tensile strength of FRP reinforcement (MPa) (6)	ρ_{sw} % (7)	ρ_{sl} % (8)	a/d (9)	S_f (mm) (10)
Beam 1[DB12]	31.1	0.1	166.6	17.1	2952	0.1	2.9	2.5	160
Beam 2[DB12]	31.1	0.16	166.6	17.1	2952	0.1	2.9	2.5	100
Beam 3[DB12]	31.1	0.06	166.6	17.1	2952	0.1	2.9	2.5	367
Beam 4[DB12]	31.1	0.1	166.6	17.1	2952	0.1	2.9	2.5	220
Beam 5[DB12]	31.1	0.16	166.6	17.1	2952	0.1	2.9	2.5	138
Beam 6[DB12]	31.1	0.06	166.6	17.1	2952	0.1	2.9	2.5	325
Beam 7[DB12]	31.1	0.09	166.6	17.1	2952	0.1	2.9	2.5	195
Beam 8[DB12]	31.1	0.13	166.6	17.1	2952	0.1	2.9	2.5	139
Beam 9[DB12]	39.7	0.13	170.9	16	2952	0.1	2.8	2.5	114
Beam 10[DB12]	39.7	0.18	170.9	16	2741.7	0.1	2.8	2.5	80
Beam 11[DB12]	39.7	0.08	170.9	16	2741.7	0.1	2.8	2.5	275
Beam 12[DB12]	39.7	0.13	170.9	16	2741.7	0.1	2.8	2.5	157
Beam 13[DB12]	39.7	0.19	170.9	16	2741.7	0.1	2.8	2.5	110
Beam 14[DB12]	39.7	0.07	170.9	16	2741.7	0.1	2.8	2.5	243
Beam 15[DB12]	39.7	0.11	170.9	16	2741.7	0.1	2.8	2.5	162
Beam 16[DB12]	39.7	0.16	170.9	16	2741.7	0.1	2.8	2.5	108
Beam 17[DB12]	39.7	0.08	170.9	16	2741.7	0.17	2.8	2.5	180
Beam 18[DB12]	39.7	0.08	170.9	16	2741.7	0.17	2.8	2.5	180
Beam 19[DB12]	39.7	0.13	170.9	16	2741.7	0.17	2.8	2.5	114
Beam 20[DB12]	39.7	0.08	170.9	16	2741.7	0.17	2.8	2.5	275
Beam 21[DB12]	39.7	0.13	170.9	16	2741.7	0.17	2.8	2.5	157
Beam 22[DB12]	39.7	0.07	170.9	16	2741.7	0.17	2.8	2.5	243
Beam 23[DB12]	39.7	0.11	174.3	16	2847.9	0.17	2.8	2.5	162
Beam 24[DB12]	18.6	0.13	174.3	16.3	2847.9	0.1	2.8	2.5	114
Beam 25[DB12]	18.6	0.08	174.3	16.3	2847.9	0.1	2.8	2.5	275
Beam 26[DB12]	18.6	0.13	174.3	16.3	2847.9	0.1	2.8	2.5	157
Beam 27[DB12]	18.6	0.07	174.3	16.3	2847.9	0.1	2.8	2.5	243
Beam 28[DB12]	18.6	0.11	174.3	16.3	2847.9	0.1	2.8	2.5	162
Beam 29[DB12]	18.6	0.08	174.3	16.3	2847.9	0.17	2.8	2.5	275
Beam 30[DB12]	18.6	0.13	174.3	16.3	2847.9	0.17	2.8	2.5	157
Beam 31[DB12]	18.6	0.07	174.3	16.3	2847.9	0.17	2.8	2.5	243
Beam 32[DB12]	18.6	0.11	174.3	16.3	2847.9	0.17	2.8	2.5	162
Beam 33[DB12]	59.4	0.08	174.3	16.3	2847.9	0.1	3.1	3.3	180
Beam 34[DB12]	59.4	0.13	174.3	16.3	2847.9	0.1	3.1	3.3	114
Beam 35[DB12]	59.4	0.08	174.3	16.3	2847.9	0.1	3.1	3.3	275
Beam 36[DB12]	59.4	0.13	174.3	16.3	2847.9	0.1	3.1	3.3	157

Table (A): Continued

Sample No.(1)	f_{cm} (MPa) (2)	ρ_f % (3)	E_f (GPa) (4)	ε_{fu}% (5)	Tensile strength of FRP reinforcement (MPa) (6)	ρ_{sw} % (7)	ρ_{sl}% (8)	a/d (9)	S_f (mm) (10)
Beam 37[DB12]	59.4	0.08	174.3	16.3	2847.9	0.1	3.1	3.3	275
Beam 38[DB12]	59.4	0.08	174.3	16.3	2847.9	0.1	3.1	3.3	275
Beam 39[DB12]	59.4	0.07	174.3	16.3	2847.9	0.1	3.1	3.3	243
Beam 40[DB12]	59.4	0.11	174.3	16.3	2847.9	0.1	3.1	3.3	162
Beam 41[DB12]	59.4	0.08	174.3	16.3	2847.9	0.16	3.1	3.3	275
Beam 42[DB12]	59.4	0.13	174.3	16.3	2847.9	0.16	3.1	3.3	157
Beam 43[DB12]	59.4	0.07	174.3	16.3	2847.9	0.16	3.1	3.3	243
Beam 44[DB12]	59.4	0.07	174.3	16.3	2847.9	0.16	3.1	3.3	243
Beam 45[DB09]	39.7	0.08	170.9	1.6	2741.7	0.1	2.8	2.5	180
Beam 46[DB09]	39.7	0.13	170.9	1.6	2741.7	0.1	2.8	2.5	114
Beam 47[DB09]	39.7	0.18	170.9	1.6	2741.7	0.1	2.8	2.5	80
Beam 48[DB09]	39.7	0.08	170.9	1.6	2741.7	0.1	2.8	2.5	275
Beam 49[DB09]	39.7	0.13	170.9	1.6	2741.7	0.1	2.8	2.5	157
Beam 50[DB09]	39.7	0.19	170.9	1.6	2741.7	0.1	2.8	2.5	110
Beam 51[DB09]	39.7	0.07	170.9	1.6	2741.7	0.1	2.8	2.5	243
Beam 52[DB09]	39.7	0.11	170.9	1.6	2741.7	0.1	2.8	2.5	162
Beam 53[DB09]	39.7	0.16	170.9	1.6	2741.7	0.1	2.8	2.5	108
Beam 54[JSCA12]	36.4	0.075	235	1.5	3550	0.095	2.8	3.1	160
Beam 55[JSCA12]	36.4	0.071	235	1.5	3550	0.095	2.8	3.1	240
Beam 56[JSCA12]	36.4	0.075	235	1.5	3550	0.095	2.8	3.1	160
Beam 57[JSCA12]	36.4	0.071	235	1.5	3550	0.095	2.8	3.1	240
Beam 58[JSCA12]	36.4	0.075	235	1.5	3550	0.095	2.8	3.1	160
Beam 59[DB08]	31.1	0.06	166.6	1.77	2952	0.1	2.9	2.5	267
Beam 60[DB08]	31.1	0.1	166.6	1.77	2952	0.1	2.9	2.5	160
Beam 61[DB08]	31.1	0.16	166.6	1.77	2952	0.1	2.9	2.5	100
Beam 62[DB08]	31.1	0.06	166.6	1.77	2952	0.1	2.9	2.5	367
Beam 63[DB08]	31.1	0.1	166.6	1.77	2952	0.1	2.9	2.5	220
Beam 64[DB08]	31.1	0.16	166.6	1.77	2952	0.1	2.9	2.5	138
Beam 65[DB08]	31.1	0.06	166.6	1.77	2952	0.1	2.9	2.5	325
Beam 66[DB08]	31.1	0.09	166.6	1.77	2952	0.1	2.9	2.5	195
Beam 67[DB08]	31.1	0.13	166.6	1.77	2952	0.1	2.9	2.5	139
Beam 68[DB11]	39.7	0.08	170.9	1.6	2741.7	0.1	2.8	2.5	180
Beam 69[DB11]	39.7	0.13	170.9	1.6	2741.7	0.1	2.8	2.5	114
Beam 70[DB11]	39.7	0.18	170.9	1.6	2741.7	0.1	2.8	2.5	80
Beam 71[DB11]	39.7	0.08	170.9	1.6	2741.7	0.1	2.8	2.5	275
Beam 72[DB11]	39.7	0.13	170.9	1.6	2741.7	0.1	2.8	2.5	157
Beam 73[DB11]	39.7	0.19	170.9	1.6	2741.7	0.1	2.8	2.5	110
Beam 74[DB11]	39.7	0.07	170.9	1.6	2741.7	0.1	2.8	2.5	243
Beam 75[DB11]	39.7	0.11	170.9	1.6	2741.7	0.1	2.8	2.5	162
Beam 76[DB11]	39.7	0.16	170.9	1.6	2741.7	0.1	2.8	2.5	108

Table (A): Continued

Sample No.(1)	f_{cm} (MPa) (2)	ρ_f % (3)	E_f (GPa) (4)	ε_{fu} % (5)	Tensile strength of FRP reinforcement (MPa) (6)	ρ_{sw} % (7)	ρ_{sl} % (8)	a / d (9)	S_f (mm) (10)
Beam 77(DB11)	39.7	0.08	170.9	1.6	2741.7	0.17	2.8	2.5	180
Beam 78(DB11)	39.7	0.13	170.9	1.6	2741.7	0.17	2.8	2.5	114
Beam 79(DB11)	39.7	0.08	170.9	1.6	2741.7	0.17	2.8	2.5	275
Beam 80(DB11)	39.7	0.13	170.9	1.6	2741.7	0.17	2.8	2.5	157
Beam 81(DB11)	39.7	0.07	170.9	1.6	2741.7	0.17	2.8	2.5	243
Beam 82(DB11)	39.7	0.11	170.9	1.6	2741.7	0.17	2.8	2.5	162
Beam 83(DB10)	18.6	0.13	174.3	1.63	2847.9	0.1	3.1	2.5	114
Beam 84(DB10)	18.6	0.08	174.3	1.63	2847.9	0.1	3.1	2.5	275
Beam 85(DB10)	18.6	0.13	174.3	1.63	2847.9	0.1	3.1	2.5	157
Beam 86(DB10)	18.6	0.07	174.3	1.63	2847.9	0.1	3.1	2.5	243
Beam 87(DB10)	18.6	0.11	174.3	1.63	2847.9	0.1	3.1	2.5	162
Beam 88(DB10)	18.6	0.13	174.3	1.63	2847.9	0.17	3.1	2.5	114
Beam 89(DB10)	18.6	0.08	174.3	1.63	2847.9	0.17	3.1	2.5	275
Beam 90(DB10)	18.6	0.13	174.3	1.63	2847.9	0.17	3.1	2.5	157
Beam 91(DB10)	18.6	0.07	174.3	1.63	2847.9	0.17	3.1	2.5	243
Beam 92(DB10)	18.6	0.11	174.3	1.63	2847.9	0.17	3.1	2.5	162
Beam 93(T10)	25.1	0.1767	124	1.7	2068	0.39	1.48	5	160
Beam 94(T10)	25	0.2356	124	1.7	2068	0.39	1.48	5	120
Beam 95(T10)	24.9	0.3534	124	1.7	2068	0.39	1.48	5	80
Beam 96(T10)	24.8	0.3969	124	1.7	2068	0.39	1.48	5	160
Beam 97(T10)	25	0.5292	124	1.7	2068	0.39	1.48	5	120
Beam 98(T10)	24.8	0.7938	124	1.7	2068	0.39	1.48	5	80
Beam 99(T10)	24.9	0.5292	124	1.7	2068	0.39	1.48	5	120
Beam 100(I08)	49.75	0.34	124	16.7	2068	0.204	1.7	2.34	152
Beam 101(I08)	49.75	0.168	124	16.7	2068	0.204	1.7	2.34	304.8
Beam 102(I08)	49.75	0.27	124	16.7	2068	0.204	1.7	2.34	190.5
Beam 103(RR10)	43.5	0.3351	124	1.53	1900	0.1886	2.36	3	200
Beam 104(RR10)	44.2	0.3351	124	1.53	1900	0.1886	2.36	3	200
Beam 105(RR10)	43.8	0.474	124	1.53	1900	0.1886	2.36	3	200
Beam 106(RS12)	34.88	0.3231	45	2	900	0	1.6	two-point loading	100
Beam 107(RS12)	34.88	0.4569	45	2	900	0	1.6	two-point loading	100
Beam 108(RS12)	34.88	0.3429	45	2	750	0	1.6	two-point loading	100
Beam 109(RS12)	34.88	0.4849	45	2	750	0	1.6	two-point loading	100
Beam 110(RS12)	34.88	0.2743	45	2	750	0	1.6	two-point loading	125
Beam 111(RS12)	34.88	0.3879	45	2	750	0	1.6	two-point loading	125
Beam 112(RS12)	34.88	0.3429	45	2	750	0	1.6	two-point loading	100
Beam 113(RS12)	34.88	0.4849	45	2	750	0	1.6	two-point loading	100
Beam 114(RS12)	34.88	0.4571	45	2	750	0	1.6	two-point loading	75
Beam 115(RS12)	34.88	0.6465	45	2	750	0	1.6	two-point loading	75
Beam 116(DN01)	31	0.5229	104.8	1.8	1875	0	0.24	3	177.8

Table (A): Continued

Sample No.(1)	f_{cm} (MPa) (2)	ρ_f % (3)	E_f (GPa) (4)	ε_{fu} % (5)	Tensile strength of FRP reinforcement (MPa) (6)	ρ_{sw} % (7)	ρ_{sl} % (8)	a/d (9)	S_f (mm) (10)
Beam 117(DN01)	31	0.7321	104.8	1.8	1875	0	0.24	3	127
Beam 118(DN01)	31	0.7321	104.8	1.8	1875	0	0.24	3	127
Beam 119(DN01)	31	0.7395	104.8	1.8	1875	0	0.24	3	177.8
Beam 120(DN01)	31	1.0354	104.8	1.8	1875	0	0.24	3	127
Beam 121(DN01)	31	0.5229	104.8	1.8	1875	0.26	0.24	3	177.8
Beam 122(RD07)	29.3	0.6886	145.7	1.52	2214	0.177	4.4	3	73
Beam 123(RD07)	29.3	0.6886	145.7	1.52	2214	0.177	4.4	3	73
Beam 124(RD07)	29.3	1.117	145.7	1.52	2214	0.177	4.4	3	45
Beam 125(RD07)	29.3	0.4869	145.7	1.52	2214	0.177	4.4	3	146
Beam 126(RD07)	29.3	0.9738	145.7	1.52	2214	0.177	4.4	3	73
Beam 127(RD07)	29.3	0.44	121.5	1.52	4823	0.177	4.4	3	73
Beam 128(RD07)	29.3	0.31	121.5	1.52	4823	0.177	4.4	3	146
Beam 129(DB)	49.2	0.0467	150	14	2000	0	1.6	2	200
Beam 130(DB)	49.2	0.022	150	14	2000	0	1.6	2	300
Beam 131(DB)	49.2	0.0933	150	14	2000	0	2.32	2	100
Beam 132(DB)	49.2	0.044	150	14	2000	0	2.32	2	150
Beam 133(DB)	56.2	0.1867	150	14	2000	0	0.75	2	100
Beam 134(DB)	56.2	0.088	150	14	2000	0	0.75	2	150
Beam 135(DB)	56.2	0.3733	150	14	2000	0	1.08	2	50
Beam 136(DB)	**56.2**	**0.176**	**150**	**14**	**2000**	**0**	**1.08**	**2**	**75**

Table (A): Continued

Sample No.(1)	θ_f (degree) (11)	FRP reinforcement type (12)	a_f x b_f (mm^2) (13)	A_f (mm^2) (14)	F_{max} (KN) (15)	V_f^{exp} (KN) (16)	Beam section type (17)	h_w (mm) (18)
Beam 1(DB12)	90	CFRP laminates	14	28	357	40.3	T- beam	300
Beam 2(DB12)	90	CFRP laminates	14	28	396	63.7	T- beam	300
Beam 3(DB12)	45	CFRP laminates	14	28	328	37.9	T- beam	300
Beam 4(DB12)	45	CFRP laminates	14	28	384	56.5	T- beam	300
Beam 5(DB12)	45	CFRP laminates	14	28	382	70.3	T- beam	300
Beam 6(DB12)	60	CFRP laminates	14	28	374	35.4	T- beam	300
Beam 7(DB12)	60	CFRP laminates	14	28	392	61.3	T- beam	300
Beam 8(DB12)	60	CFRP laminates	14	28	406	69.7	T- beam	300
Beam 9(DB12)	90	CFRP laminates	13.3	26.6	374.1	57.5	T- beam	300
Beam 10(DB12)	90	CFRP laminates	13.3	26.6	397.5	71.5	T- beam	300
Beam 11(DB12)	45	CFRP laminates	13.3	26.6	392.8	53.4	T- beam	300
Beam 12(DB12)	45	CFRP laminates	13.3	26.6	421.7	70.7	T- beam	300
Beam 13(DB12)	45	CFRP laminates	13.3	26.6	446.5	85.6	T- beam	300
Beam 14(DB12)	60	CFRP laminates	13.3	26.6	386.4	49.6	T- beam	300

Table (A): Continued

Sample No.(1)	θ_f (degree) (11)	FRP reinforcement type (12)	a_f x b_f (mm^2) (13)	A_f (mm^2) (14)	F_{max} (KN) (15)	V_f^{exp} (KN) (16)	Beam section type (17)	h_w (mm) (18)
Beam 15[DB12]	60	CFRP laminates	13.3	26.6	394.4	54.4	T- beam	300
Beam 16[DB12]	60	CFRP laminates	13.3	26.6	412.7	65.3	T- beam	300
Beam 17[DB12]	90	CFRP laminates	13.3	26.6	424.5	31.9	T- beam	300
Beam 18[DB12]	90	CFRP laminates	13.3	26.6	439.2	40.7	T- beam	300
Beam 19[DB12]	90	CFRP laminates	13.3	26.6	427.4	33.6	T- beam	300
Beam 20[DB12]	45	CFRP laminates	13.3	26.6	442.5	42.7	T- beam	300
Beam 21[DB12]	45	CFRP laminates	13.3	26.6	478.1	64	T- beam	300
Beam 22[DB12]	60	CFRP laminates	13.3	26.6	443.9	43.5	T- beam	300
Beam 23[DB12]	60	CFRP laminates	13.3	26.6	457.6	51.7	T- beam	300
Beam 24[DB12]	90	CFRP laminates	13.3	26.6	273.7	43.6	T- beam	300
Beam 25[DB12]	45	CFRP laminates	13.3	26.6	283	33.9	T- beam	300
Beam 26[DB12]	45	CFRP laminates	13.3	26.6	306.5	48	T- beam	300
Beam 27[DB12]	60	CFRP laminates	13.3	26.6	281.6	33.1	T- beam	300
Beam 28[DB12]	60	CFRP laminates	13.3	26.6	297.7	42.7	T- beam	300
Beam 29[DB12]	45	CFRP laminates	13.3	26.6	327.2	26	T- beam	300
Beam 30[DB12]	45	CFRP laminates	13.3	26.6	356.4	31.6	T- beam	300
Beam 31[DB12]	60	CFRP laminates	13.3	26.6	345.6	25.1	T- beam	300
Beam 32[DB12]	60	CFRP laminates	13.3	26.6	362.3	35.1	T- beam	300
Beam 33[DB12]	90	CFRP laminates	13.3	26.6	387	44.7	T- beam	300
Beam 34[DB12]	90	CFRP laminates	13.3	26.6	491.7	81.5	T- beam	300
Beam 35[DB12]	45	CFRP laminates	13.3	26.6	492.1	81.7	T- beam	300
Beam 36[DB12]	45	CFRP laminates	13.3	26.6	563.6	117.4	T- beam	300
Beam 37[DB12]	45	CFRP laminates	13.3	26.6	531.4	85.8	T- beam	300
Beam 38[DB12]	45	CFRP laminates	13.3	26.6	490.6	80.9	T- beam	300
Beam 39[DB12]	60	CFRP laminates	13.3	26.6	497.9	84.6	T- beam	300
Beam 40[DB12]	60	CFRP laminates	13.3	26.6	584.5	127.9	T- beam	300
Beam 41[DB12]	45	CFRP laminates	13.3	26.6	559.5	74.9	T- beam	300
Beam 42[DB12]	45	CFRP laminates	13.3	26.6	627.5	108.9	T- beam	300
Beam 43[DB12]	60	CFRP laminates	13.3	26.6	556.4	73.4	T- beam	300
Beam 44[DB12]	60	CFRP laminates	13.3	26.6	277.4	72.6	T- beam	300
Beam 45[DB09]	90	CFRP laminates	1.4 x 9.5	26.6	337.4	20.2	T- beam	300
Beam 46[DB09]	90	CFRP laminates	1.4 x 9.5	26.6	374.1	42.2	T- beam	300
Beam 47[DB09]	90	CFRP laminates	1.4 x 9.5	26.6	397.5	56.2	T- beam	300
Beam 48[DB09]	45	CFRP laminates	1.4 x 9.5	26.6	392.8	53.4	T- beam	300
Beam 49[DB09]	45	CFRP laminates	1.4 x9.5	26.6	421.7	70.7	T- beam	300
Beam 50[DB09]	45	CFRP laminates	1.4 x 9.5	26.6	446.5	85.6	T- beam	300
Beam 51[DB09]	60	CFRP laminates	1.4 x 9.5	26.6	386.4	49.6	T- beam	300
Beam 52[DB09]	60	CFRP laminates	1.4 x 9.5	26.6	394.4	54.4	T- beam	300
Beam 53[DB09]	60	CFRP laminates	1.4 x 9.5	26.6	412.7	65.3	T- beam	300
Beam 54[JSCA12]	90	CFRP rods	12	24	48	33.41	Rectangular beam	250
Beam 55[JSCA12]	45	CFRP rods	12	24	40	53.94	Rectangular beam	250

Table (A): Continued

Sample No.(1)	θ_f (degree) (11)	FRP reinforcement type (12)	a_f x b_f (mm^2) (13)	A_f (mm^2) (14)	F_{max} (KN) (15)	V_f^{exp} (KN) (16)	Beam section type (17)	h_w (mm) (18)
Beam 56[JSCA12]	90	CFRP rods	12	24	77	39.88	Rectangular beam	250
Beam 57[JSCA12]	45	CFRP rods	12	24	50	63.82	Rectangular beam	250
Beam 58[JSCA12]	90	CFRP rods	12	24	48	29.4	Rectangular beam	250
Beam 59[DB08]	90	CFRP laminates	1.4 x 10	28	316	0.6	T- beam	300
Beam 60[DB08]	90	CFRP laminates	1.4 x 10	28	257	25.2	T- beam	300
Beam 61[DB08]	90	CFRP laminates	1.4 x 10	28	396	48.6	T- beam	300
Beam 62[DB08]	45	CFRP laminates	1.4 x 10	28	328	7.8	T- beam	300
Beam 63[DB08]	45	CFRP laminates	1.4 x 10	28	384	41.4	T- beam	300
Beam 64[DB08]	45	CFRP laminates	1.4 x 10	28	282	40.2	T- beam	300
Beam 65[DB08]	60	CFRP laminates	1.4 x 10	28	374	35.4	T- beam	300
Beam 66[DB08]	60	CFRP laminates	1.4 x 10	28	392	46.2	T- beam	300
Beam 67[DB08]	60	CFRP laminates	1.4 x 10	28	406	54.6	T- beam	300
Beam 68[DB11]	90	CFRP laminates	1.4 x 9.5	26.6	337.4	20.4	T- beam	300
Beam 69[DB11]	90	CFRP laminates	1.4 x 9.5	26.6	374.1	42.18	T- beam	300
Beam 70[DB11]	90	CFRP laminates	1.4 x 9.5	26.6	397.5	56.22	T- beam	300
Beam 71[DB11]	45	CFRP laminates	1.4 x 9.5	26.6	392.8	53.4	T- beam	300
Beam 72[DB11]	45	CFRP laminates	1.4 x 9.5	26.6	421.7	70.74	T- beam	300
Beam 73[DB11]	45	CFRP laminates	1.4 x 9.5	26.6	446.5	85.62	T- beam	300
Beam 74[DB11]	60	CFRP laminates	1.4 x 9.5	26.6	386.4	49.56	T- beam	300
Beam 75[DB11]	60	CFRP laminates	1.4 x 9.5	26.6	394.4	54.36	T- beam	300
Beam 76[DB11]	60	CFRP laminates	1.4 x 9.5	26.6	412.7	65.34	T- beam	300
Beam 77[DB11]	90	CFRP laminates	1.4 x 9.5	26.6	424.5	31.86	T- beam	300
Beam 78[DB11]	90	CFRP laminates	1.4 x 9.5	26.6	427.4	33.6	T- beam	300
Beam 79[DB11]	45	CFRP laminates	1.4 x 9.5	26.6	442.5	42.66	T- beam	300
Beam 80[DB11]	45	CFRP laminates	1.4 x 9.5	26.6	478.1	64.02	T- beam	300
Beam 81[DB11]	60	CFRP laminates	1.4 x 9.5	26.6	443.8	43.44	T- beam	300
Beam 82[DB11]	60	CFRP laminates	1.4 x 9.5	26.6	457.6	51.72	T- beam	300
Beam 83[DB10]	90	CFRP laminates	1.4 x 9.5	26.6	387	28.32	T- beam	300
Beam 84[DB10]	45	CFRP laminates	1.4 x 9.5	26.6	491.7	33.9	T- beam	300
Beam 85[DB10]	45	CFRP laminates	1.4 x 9.5	26.6	492.1	48	T- beam	300
Beam 86[DB10]	60	CFRP laminates	1.4 x 9.5	26.6	563.6	33.06	T- beam	300
Beam 87[DB10]	60	CFRP laminates	1.4 x 9.5	26.6	497.9	42.72	T- beam	300
Beam 88[DB10]	90	CFRP laminates	1.4 x 9.5	26.6	584.5	6.84	T- beam	300
Beam 89[DB10]	45	CFRP laminates	1.4 x 9.5	26.6	559.5	26.04	T- beam	300
Beam 90[DB10]	45	CFRP laminates	1.4 x 9.5	26.6	627.5	31.56	T- beam	300
Beam 91[DB10]	60	CFRP laminates	1.4 x 9.5	26.6	556.4	25.08	T- beam	300
Beam 92[DB10]	60	CFRP laminates	1.4 x 9.5	26.6	654.6	35.1	T- beam	300
Beam 93[T10]	90	CFRP rods	Dia.6	56.55	72.1	72.92	Rectangular beam	350
Beam 94[T10]	90	CFRP rods	Dia.6	56.55	82.1	82.13	Rectangular beam	350
Beam 95[T10]	90	CFRP rods	Dia.6	56.55	93.1	95.24	Rectangular beam	350
Beam 96[T10]	90	CFRP rods	Dia.9	127.2	79.6	79.65	Rectangular beam	350

Table (A): Continued

Sample No.(1)	θ_f (degree) (11)	FRP reinforcement type (12)	a_f x b_f (mm^2) (13)	A_f (mm^2) (14)	F_{max} (KN) (15)	V_f^{exp} (KN) (16)	Beam section type (17)	h_w (mm) (18)
Beam 97[T10]	90	CFRP rods	Dia.9	127.2	95.5	95.64	Rectangular beam	350
Beam 98[T10]	90	CFRP rods	Dia.9	127.2	89.3	96.42	Rectangular beam	350
Beam 99[T10]	90	CFRP rods	Dia.6	56.55	-80.1	97.38	Rectangular beam	350
Beam 100[I08]	90	CFRP bars	65.2	130.4	454	151.4	Rectangular beam	305
Beam 101[I08]	90	CFRP bars	65.2	130.4	427	81.5	Rectangular beam	305
Beam 102[I08]	90	CFRP bars	65.2	130.4	436	112.9	Rectangular beam	305
Beam 103[RR10]	90	CFRP bars	Dia.8	100.53	440	70	T- beam	400
Beam 104[RR10]	90	CFRP bars	Dia.8	100.53	506	103	T- beam	400
Beam 105[RR10]	45	CFRP bars	Dia.8	100.53	576	138	T- beam	400
Beam 106[RS12]	90	GFRP rods	Dia.6	56.5	235.44	36.78	Rectangular beam	250
Beam 107[RS12]	45	GFRP rods	Dia.6	56.5	220.73	29.43	Rectangular beam	250
Beam 108[RS12]	90	GFRP strip	3 x 10	60	259.97	49.05	Rectangular beam	250
Beam 109[RS12]	45	GFRP strip	3 x 10	60	279.59	58.86	Rectangular beam	250
Beam 110[RS12]	90	GFRP strip	3 x 10	60	294.3	66.21	Rectangular beam	250
Beam 111[RS12]	45	GFRP strip	3 x 10	60	245.25	41.69	Rectangular beam	250
Beam 112[RS12]	90	GFRP strip	3 x 10	60	284.89	61.51	Rectangular beam	250
Beam 113[RS12]	45	GFRP strip	3 x 10	60	274.68	56.4	Rectangular beam	250
Beam 114[RS12]	90	GFRP strip	3 x 10	60	240.35	39.24	Rectangular beam	250
Beam 115[RS12]	45	GFRP strip	3 x 10	60	299.21	68.67	Rectangular beam	250
Beam 116[DN01]	90	CFRP rods	Dia.9.5	141.76	228.2	25	T- beam	305
Beam 117[DN01]	90	CFRP rods	Dia.9.5	141.76	255.3	37.4	T- beam	305
Beam 118[DN01]	90	CFRP rods	Dia.9.5	141.76	371.4	95.64	T- beam	305
Beam 119[DN01]	45	CFRP rods	Dia.9.5	141.76	331	75.2	T- beam	305
Beam 120[DN01]	45	CFRP rods	Dia.9.5	141.76	355.8	87.63	T- beam	305
Beam 121[DN01]	90	CFRP rods	Dia.9.5	141.76	413.7	53.4	T- beam	305
Beam 122[RD07]	90	CFRP rods	Dia.9.5	100.5	352.8	44.4	Rectangular beam	210
Beam 123[RD07]	90	CFRP rods	Dia.8	100.5	297.1	21.6	Rectangular beam	210
Beam 124[RD07]	90	CFRP rods	Dia.8	100.5	301.5	23.4	Rectangular beam	210
Beam 125[RD07]	45	CFRP rods	Dia.8	100.5	322.6	32.1	Rectangular beam	210
Beam 126[RD07]	45	CFRP rods	Dia.8	100.5	300.3	22.9	Rectangular beam	210
Beam 127[RD07]	90	CFRP strip	2 x 16	64	345.3	41.3	Rectangular beam	210
Beam 128[RD07]	45	CFRP strip	2 x 16	64	309.7	26.8	Rectangular beam	210
Beam 129[DB]	90	CFRP laminates	1.4 x 10	28	158.64	29.1	Rectangular beam	300
Beam 130[DB]	45	CFRP laminates	1.4 x 10	28	157.9	28.8	Rectangular beam	300
Beam 131[DB]	90	CFRP laminates	1.4 x 10	28	235.11	59.3	Rectangular beam	300
Beam 132[DB]	45	CFRP laminates	1.4 x 10	28	262.38	72.9	Rectangular beam	300
Beam 133[DB]	90	CFRP laminates	1.4 x 10	28	131.22	28.6	Rectangular beam	150
Beam 134[DB]	45	CFRP laminates	1.4 x 10	28	120.44	23.2	Rectangular beam	150
Beam 135[DB]	90	CFRP laminates	1.4 x 10	28	139.2	31.8	Rectangular beam	150
Beam 136[DB]	**45**	**CFRP laminates**	**1.4 x 10**	**28**	**148.5**	**36.4**	**Rectangular beam**	**150**

Table (A): Continued

Sample No.(1)	b_w (mm) (19)	d (mm) (20)	End anchorage (21)	Failure type (22)
Beam 1(DB12)	180	360.4	No	Concrete Fracture
Beam 2(DB12)	180	360.4	No	Concrete Fracture
Beam 3(DB12)	180	360.4	No	Concrete Fracture
Beam 4(DB12)	180	360.4	No	Concrete Fracture
Beam 5(DB12)	180	360.4	No	Concrete Fracture
Beam 6(DB12)	180	360.4	No	Concrete Fracture
Beam 7(DB12)	180	360.4	No	Concrete Fracture
Beam 8(DB12)	180	360.4	No	Concrete Fracture
Beam 9(DB12)	180	360.4	No	Concrete Fracture
Beam 10(DB12)	180	360.4	No	Concrete Fracture
Beam 11(DB12)	180	360.4	No	Concrete Fracture
Beam 12(DB12)	180	360.4	No	Concrete Fracture
Beam 13(DB12)	180	360.4	No	Concrete Fracture
Beam 14(DB12)	180	360.4	No	Concrete Fracture
Beam 15(DB12)	180	360.4	No	Concrete Fracture
Beam 16(DB12)	180	360.4	No	Concrete Fracture
Beam 17(DB12)	180	360.4	No	Concrete Fracture
Beam 18(DB12)	180	360.4	No	Concrete Fracture
Beam 19(DB12)	180	360.4	No	Concrete Fracture
Beam 20(DB12)	180	360.4	No	Concrete Fracture
Beam 21(DB12)	180	360.4	No	Concrete Fracture
Beam 22(DB12)	180	360.4	No	Concrete Fracture
Beam 23(DB12)	180	360.4	No	Concrete Fracture
Beam 24(DB12)	180	360.4	No	Concrete Fracture
Beam 25(DB12)	180	360.4	No	Concrete Fracture
Beam 26(DB12)	180	360.4	No	Concrete Fracture
Beam 27(DB12)	180	360.4	No	Concrete Fracture
Beam 28(DB12)	180	360.4	No	Concrete Fracture
Beam 29(DB12)	180	360.4	No	Concrete Fracture
Beam 30(DB12)	180	360.4	No	Concrete Fracture
Beam 31(DB12)	180	360.4	No	Concrete Fracture
Beam 32(DB12)	180	360.4	No	Concrete Fracture
Beam 33(DB12)	180	360.4	No	Debonding
Beam 34(DB12)	180	360.4	No	Debonding
Beam 35(DB12)	180	360.4	No	FRP Rupture
Beam 36(DB12)	180	360.4	No	FRP Rupture
Beam 37(DB12)	180	360.4	No	FRP Rupture
Beam 38(DB12)	180	360.4	No	FRP Rupture
Beam 39(DB12)	180	360.4	No	FRP Rupture
Beam 40(DB12)	180	360.4	No	FRP Rupture

Table (A): Continued

Sample No.(1)	b_w (mm) (19)	d (mm) (20)	End anchorage (21)	Failure type (22)
Beam 41[DB12]	180	360.4	No	FRP Rupture
Beam 42[DB12]	180	360.4	No	FRP Rupture
Beam 43[DB12]	180	360.4	No	FRP Rupture
Beam 44[DB12]	180	360.4	No	FRP Rupture
Beam 45[DB09]	180	360	No	Debonding
Beam 46[DB09]	180	360	No	Concrete Fracture
Beam 47[DB09]	180	360	No	Concrete Fracture
Beam 48[DB09]	180	360	No	Debonding
Beam 49[DB09]	180	360	No	Concrete Fracture
Beam 50[DB09]	180	360	No	Concrete Fracture
Beam 51[DB09]	180	360	No	Debonding
Beam 52[DB09]	180	360	No	Concrete Fracture
Beam 53[DB09]	180	360	No	Concrete Fracture
Beam 54[JSCA12]	200	213	No	Debonding
Beam 55[JSCA12]	200	213	No	Debonding
Beam 56[JSCA12]	200	213	Yes	Concrete Fracture
Beam 57[JSCA12]	200	213	Yes	Concrete Fracture
Beam 58[JSCA12]	200	213	Yes	FRP Rupture
Beam 59[DB08]	180	356	No	Debonding + Concrete Fracture
Beam 60[DB08]	180	356	No	Debonding + Concrete Fracture
Beam 61[DB08]	180	356	No	Debonding + Concrete Fracture
Beam 62[DB08]	180	356	No	Debonding + Concrete Fracture
Beam 63[DB08]	180	356	No	Debonding + Concrete Fracture
Beam 64[DB08]	180	356	No	Debonding + Concrete Fracture
Beam 65[DB08]	180	356	No	Debonding + Concrete Fracture
Beam 66[DB08]	180	356	No	Debonding + Concrete Fracture
Beam 67[DB08]	180	356	No	Debonding + Concrete Fracture
Beam 68[DB11]	180	360	No	Debonding + Concrete Fracture
Beam 69[DB11]	180	360	No	Concrete Fracture
Beam 70[DB11]	180	360	No	Concrete Fracture
Beam 71[DB11]	180	360	No	Debonding + Concrete Fracture
Beam 72[DB11]	180	360	No	Concrete Fracture
Beam 73[DB11]	180	360	No	Concrete Fracture
Beam 74[DB11]	180	360	No	Debonding + Concrete Fracture
Beam 75[DB11]	180	360	No	Concrete Fracture
Beam 76[DB11]	180	360	No	Concrete Fracture
Beam 77[DB11]	180	360	No	Debonding + Concrete Fracture
Beam 78[DB11]	180	360	No	Concrete Fracture
Beam 79[DB11]	180	360	No	Debonding + Concrete Fracture
Beam 80[DB11]	180	360	No	Concrete Fracture
Beam 81[DB11]	180	360	No	Debonding + Concrete Fracture

Table (A): Continued

Sample No.(1)	b_w (mm) (19)	d (mm) (20)	End anchorage (21)	Failure type (22)
Beam 82(DB11)	180	360	No	Concrete Fracture
Beam 83(DB10)	180	360	No	Concrete Fracture
Beam 84(DB10)	180	360	No	Debonding + Concrete Fracture
Beam 85(DB10)	180	360	No	Concrete Fracture
Beam 86(DB10)	180	360	No	Debonding + Concrete Fracture
Beam 87(DB10)	180	360	No	Concrete Fracture
Beam 88(DB10)	180	360	No	Concrete Fracture
Beam 89(DB10)	180	360	No	Debonding + Concrete Fracture
Beam 90(DB10)	180	360	No	Concrete Fracture
Beam 91(DB10)	180	360	No	Concrete Fracture
Beam 92(DB10)	180	360	No	Concrete Fracture
Beam 93(T10)	200	320	No	Shear Failure
Beam 94(T10)	200	320	No	Shear Failure
Beam 95(T10)	200	320	No	Flexural + Shear Failure
Beam 96(T10)	200	320	No	Shear Failure
Beam 97(T10)	200	320	No	Flexural + Shear Failure
Beam 98(T10)	200	320	No	Flexural + Shear Failure
Beam 99(T10)	200	320	No	Flexural + Shear Failure
Beam 100(I08)	254	260.67	No	Flexural + Shear Failure
Beam 101(I08)	254	260.67	No	Flexural + Shear Failure
Beam 102(I08)	254	260.67	No	Flexural + Shear Failure
Beam 103(RR10)	150	430	No	Debonding + Concrete Fracture
Beam 104(RR10)	150	430	No	Shear Failure
Beam 105(RR10)	150	430	No	Shear Failure
Beam 106(RS12)	175	217	No	Shear Failure
Beam 107(RS12)	175	217	No	Debonding
Beam 108(RS12)	175	217	No	Rapture of FRP
Beam 109(RS12)	175	217	No	Shear Failure
Beam 110(RS12)	175	217	No	Concrete Rapture
Beam 111(RS12)	175	217	No	Rapture of FRP
Beam 112(RS12)	175	217	No	Shear Failure
Beam 113(RS12)	175	217	No	Rapture of FRP
Beam 114(RS12)	175	217	No	Shear Failure
Beam 115(RS12)	175	217	No	Concrete Rapture
Beam 116(DN01)	152.4	355.6	No	Debonding
Beam 117(DN01)	152.4	355.6	No	Debonding
Beam 118(DN01)	152.4	355.6	Yes	Concrete Rapture
Beam 119(DN01)	152.4	355.6	No	Debonding
Beam 120(DN01)	152.4	355.6	No	Debonding
Beam 121(DN01)	152.4	355.6	Yes	Concrete Fracture
Beam 122(RD07)	200	173	No	Shear Failure

Table (A): Continued

Sample No.(1)	b_w (mm) (19)	d (mm) (20)	End anchorage (21)	Failure type (22)
Beam 123(RD07)	200	173	No	Shear Failure
Beam 124(RD07)	200	173	No	Shear Failure
Beam 125(RD07)	200	173	No	Shear Failure
Beam 126(RD07)	200	173	No	Shear Failure
Beam 127(RD07)	200	173	No	Shear Failure
Beam 128(RD07)	200	173	No	Shear Failure
Beam 129(DB)	150	280	No	Debonding
Beam 130(DB)	150	280	No	Rupture of Beam (Flexural Failure)
Beam 131(DB)	150	280	No	Debonding
Beam 132(DB)	150	280	No	Rupture of Beam (Flexural Failure)
Beam 133(DB)	150	130	No	N.A.
Beam 134(DB)	150	130	No	Concrete Fracture
Beam 135(DB)	150	130	No	Concrete Fracture
Beam 136(DB)	**150**	**130**	**No**	**Concrete Fracture**

In column (1) of table (A) above, (DB12) = (Dias and Barros 2012); (DB09) = (Dias and Barros 2009); (JSCA12) = (Jalali, Sharrbatdar, Chen and Alaee 2012); (DB08) = (Dias and Barros 2008); (DB11) = (Dias and Barros 2011); (DB10) = (Dias and Barros 2010); (T10) = (Tanarslan 2010); (I08) = (Islam 2008); (RR10) = (Rahal and Rumaith 2010); (RS12) = (Raj and Surumi 2012); (DN01) = (De Lorenzis and Nanni 2001); (RD07)= (Rizzo and De Lorenzis 2007); (DB) = (Dias and Barros). See **list of references** for the complete details of each reference.

Notice that:

ρ_f = (2 x a_f x b_f)/ (b_w x S_f x sinθ_f) x100% (For FRP laminates); ρ_f = (2 x area of FRP bar)/ (b_w x S_f x sinθ_f) x100% (For FRP bars/rods); ρ_{sw}= (A_{sw} /(b_w × S_w)) ×100; ρ_{sl} = (A_{sl}/(b_w × d)) ×100; A_f = 2 x a_f x b_f (For FRP laminates and strips); A_f = 2 x area of FRP bar (For FRP rods/bars). In column (9), a/d represents the shear span ratio, which is equal to the length of the monitored span in the strengthened beam divided by the effective depth of the RC beam. In Column (12), CFRP and GFRP refer to Carbon and Glass FRP reinforcement, respectively. In column (13) of table (A) above, if FRP laminates are used, (a_f x b_f) represents the dimensions of the FRP laminates. However, if FRP rods or bars are used, the diameters of the FRP rods or bars (Dia.) are given instead of the product (a_f x b_f). For some samples, only one square number is given in the same column, and it represents the cross sectional area of the FRP reinforcement in that sample. In column (21), (Yes) refers to the use of the anchorage system in that sample, while (No) means this system was not used in that beam. For column (22), it is recommended to see section (2.4) and figure (7) for more details if that is needed. However, in this column, 22, (N.A.) means the shear failure mode in that sample (RC beam) was not reported in the reference, or not observed in some beams. If the failure mode in the same column is reported as (Shear Failure), it means that the failure mode in the strengthened beams was a shear failure mode, but it was not mentioned which one of the three types mentioned in section (2.4) occurred in those samples. Rapture of the beam failure refers to flexural failure in the NSM shear strengthened beams.

APPENDIX (B): THE CALCULATIONS OF CALIBRATION OF THANASIS C. TRIANTAFILLOU'S MODEL

TableB1: The Calculations of Figure **13A**

Sample No.	θ_f	V_f^{exp} (KN)	E_f (GPa)	ρ_f %	f_{cm} (MPa)	$(E_f * \rho_f) / (f_c^{2/3})$	ε^{exp} %
Beam 3 (DB12)	45°	37.9	166.6	0.06	31.1	0.010107707	4.143146
Beam 4 (DB12)	45°	56.5	166.6	0.1	31.1	0.016846179	4.093027
Beam 5 (DB12)	45°	70.3	166.6	0.16	31.1	0.026953886	4.591961
Beam 11 (DB12)	45°	53.4	170.9	0.08	39.7	0.01174821	4.432846
Beam 12 (DB12)	45°	70.7	170.9	0.13	39.7	0.019090842	3.980995
Beam 13 (DB12)	45°	85.6	170.9	0.19	39.7	0.027901999	4.730362
Beam 20 (DB12)	45°	42.7	170.9	0.08	39.7	0.01174821	5.098736
Beam 21 (DB12)	45°	64	170.9	0.13	39.7	0.019090842	2.590324
Beam 25 (DB12)	45°	33.9	174.3	0.08	18.6	0.019863026	3.380975
Beam 26 (DB12)	45°	48	174.3	0.13	18.6	0.032277417	3.295687
Beam 29 (DB12)	45°	26	174.3	0.08	18.6	0.019863026	3.401528
Beam 30 (DB12)	45°	31.6	174.3	0.13	18.6	0.032277417	2.79241
Beam 35 (DB12)	45°	81.7	174.3	0.08	59.4	0.009159317	5.490607
Beam 37 (DB12)	45°	85.8	174.3	0.08	59.4	0.009159317	7.096103
Beam 38 (DB12)	45°	80.9	174.3	0.08	59.4	0.009159317	6.274983
Beam 41 (DB12)	45°	74.9	174.3	0.08	59.4	0.009159317	8.693934
Beam 48 (DB09)	45°	53.4	170.9	0.08	39.7	0.01174821	3.256938
Beam 49 (DB09)	45°	70.7	170.9	0.13	39.7	0.019090842	3.132595
Beam 50 (DB09)	45°	85.6	170.9	0.19	39.7	0.027901999	4.735618
Beam 55 (JSCA12)	45°	53.94	235	0.071	36.4	0.015191196	2.997608
Beam 57 (JSCA12)	45°	63.82	235	0.071	36.4	0.015191196	5.962352
Beam 63 (DB08)	45°	41.4	166.6	0.1	31.1	0.016846179	3.161377
Beam 64 (DB08)	45°	40.2	166.6	0.16	31.1	0.026953886	0.956728
Beam 71 (DB11)	45°	53.4	170.9	0.08	39.7	0.01174821	3.255395
Beam 72 (DB11)	45°	70.74	170.9	0.13	39.7	0.019090842	3.13371
Beam 73 (DB11)	45°	85.62	170.9	0.19	39.7	0.027901999	4.735618
Beam 79 (DB11)	45°	42.66	170.9	0.08	39.7	0.01174821	3.995731
Beam 80 (DB11)	45°	64.02	170.9	0.13	39.7	0.019090842	2.593202
Beam 84 (DB10)	45°	33.9	174.3	0.08	18.6	0.019863026	3.453405
Beam 85 (DB10)	45°	48	174.3	0.13	18.6	0.032277417	2.143063
Beam 89 (DB10)	45°	26.04	174.3	0.08	18.6	0.019863026	2.796822
Beam 90 (DB10)	45°	31.56	174.3	0.13	18.6	0.032277417	0.517604
Beam 105 (RR10)	45°	138	124	0.474	43.8	0.047302485	2.902015

Table B1: Continued

Sample No.	θ_f	V_f^{exp} (KN)	E_f (GPa)	ρ_f %	f_{cm} (MPa)	$(E_f * \rho_f) / (f_c^{2/3})$	ε^{exp} %
Beam 107 (RS12)	45°	29.43	45	0.457	34.88	0.019260172	2.859972
Beam 109 (RS12)	45°	58.86	45	0.485	34.88	0.02043881	2.961355
Beam 111 (RS12)	45°	41.69	45	0.388	34.88	0.016351048	5.581167
Beam 113 (RS12)	45°	56.4	45	0.485	34.88	0.02043881	4.941362
Beam 115 (RS12)	45°	68.67	45	0.646	34.88	0.027251746	5.347908
Beam 119 (DN01)	45°	75.2	104.8	0.74	31	0.078539382	0.999401
Beam 120 (DN01)	45°	87.63	104.8	1.035	31	0.109955135	2.555688
Beam 125 (RD07)	45°	32.1	145.7	0.487	29.3	0.074640551	0.691405
Beam 126 (RD07)	45°	22.9	145.7	0.974	29.3	0.149281102	0.461726
Beam 128 (RD07)	45°	26.8	121.5	0.31	29.3	0.039630196	0.36651
Beam 130 (DB)	45°	28.8	150	0.022	49.2	0.002457747	1.615709
Beam 132 (DB)	45°	72.9	150	0.044	49.2	0.004915494	16.3257
Beam 134 (DB)	45°	23.2	150	0.088	56.2	0.008996696	20.66221
Beam 136 (DB)	45°	36.4	150	0.176	56.2	0.017993392	7.081446

Table B2: The Calculations of Figure **13B**

Sample No.	θ_f	V_f^{exp} (KN)	E_f (GPa)	ρ_f %	f_{cm} (MPa)	$(E_f * \rho_f) / (f_c^{2/3})$	ε^{exp} %
Beam 6 (DB12)	60°	35.4	166.6	0.06	31.1	0.010107707	4.143146
Beam 7 (DB12)	60°	61.3	166.6	0.09	31.1	0.016846179	4.093027
Beam 8 (DB12)	60°	69.7	166.6	0.13	31.1	0.026953886	4.591961
Beam 14 (DB12)	60°	49.6	170.9	0.07	39.7	0.01174821	4.432846
Beam 15 (DB12)	60°	54.4	170.9	0.11	39.7	0.019090842	3.980995
Beam 16 (DB12)	60°	65.3	170.9	0.16	39.7	0.027901999	4.730362
Beam 22 (DB12)	60°	43.5	170.9	0.07	39.7	0.019090842	3.996307
Beam 23 (DB12)	60°	51.7	170.9	0.11	39.7	0.01174821	5.098736
Beam 27 (DB12)	60°	33.1	174.3	0.07	18.6	0.032277417	4.55922
Beam 28 (DB12)	60°	42.7	174.3	0.11	18.6	0.019863026	3.380975
Beam 31 (DB12)	60°	25.1	174.3	0.07	18.6	0.027311661	2.565581
Beam 32 (DB12)	60°	35.1	174.3	0.11	18.6	0.019863026	3.401528
Beam 39 (DB12)	60°	84.6	174.3	0.07	59.4	0.01488389	6.160516
Beam 40 (DB12)	60°	127.9	174.3	0.11	59.4	0.009159317	7.096103
Beam 43 (DB12)	60°	73.4	174.3	0.07	59.4	0.012594061	7.026618
Beam 44 (DB12)	60°	72.6	174.3	0.07	59.4	0.009159317	8.693934
Beam 51 (DB09)	60°	49.6	170.9	0.07	39.7	0.01174821	3.256938
Beam 52 (DB09)	60°	54.4	170.9	0.11	39.7	0.019090842	3.132595
Beam 53 (DB09)	60°	65.3	170.9	0.16	39.7	0.027901999	4.735618
Beam 65 (DB08)	60°	35.4	166.6	0.06	31.1	0.010107707	2.622772
Beam 66 (DB08)	60°	46.2	166.6	0.09	31.1	0.016846179	3.161377
Beam 67 (DB08)	60°	54.6	166.6	0.13	31.1	0.026953886	0.956728
Beam 74 (DB11)	60°	49.56	170.9	0.07	39.7	0.01174821	3.255395
Beam 75 (DB11)	60°	54.36	170.9	0.11	39.7	0.019090842	3.13371
Beam 76 (DB11)	60°	65.34	170.9	0.16	39.7	0.027901999	4.735618
Beam 81 (DB11)	60°	43.44	170.9	0.07	39.7	0.019090842	2.999444
Beam 82 (DB11)	60°	51.72	170.9	0.11	39.7	0.01174821	3.995731
Beam 86 (DB10)	60°	33.06	174.3	0.07	18.6	0.032277417	4.557991
Beam 87 (DB10)	60°	42.72	174.3	0.11	18.6	0.019863026	3.453405
Beam 91 (DB10)	60°	25.08	174.3	0.07	18.6	0.032277417	3.401192
Beam 92 (DB10)	60°	35.1	174.3	0.11	18.6	0.019863026	2.796822

Table B3: The Calculations of Figure **13C**

Sample No.	θ_f	V_f^{exp} (KN)	E_f (GPa)	ρ_f %	f_{cm} (MPa)	$(E_f * \rho_f) / (f_c^{2/3})$	ε^{exp} %
Beam 1 (DB12)	90°	40.3	166.6	0.1	31.1	0.016846179	4.143146
Beam 2 (DB12)	90°	63.7	166.6	0.16	31.1	0.026953886	4.093027
Beam 9 (DB12)	90°	57.5	166.6	0.13	39.7	0.019090842	4.432846
Beam 10 (DB12)	90°	71.5	170.9	0.18	39.7	0.026433473	3.980995
Beam 17 (DB12)	90°	31.9	170.9	0.08	39.7	0.01174821	3.996307
Beam 18 (DB12)	90°	40.7	170.9	0.08	39.7	0.01174821	5.098736
Beam 19 (DB12)	90°	33.6	170.9	0.13	39.7	0.019090842	2.590324
Beam 33 (DB12)	90°	44.7	174.3	0.08	59.4	0.009159317	5.490607
Beam 34 (DB12)	90°	81.5	174.3	0.13	59.4	0.01488389	6.160516
Beam 45 (DB09)	90°	20.2	170.9	0.08	39.7	0.01174821	2.533389
Beam 46 (DB09)	90°	42.2	170.9	0.13	39.7	0.019090842	3.256938
Beam 47 (DB09)	90°	56.2	170.9	0.18	39.7	0.026433473	3.132595
Beam 54 (JSCA12)	90°	33.41	235	0.075	36.4	0.016047038	4.944191
Beam 56 (JSCA12)	90°	39.88	235	0.075	36.4	0.016047038	5.901656
Beam 58 (JSCA12)	90°	29.4	235	0.075	36.4	0.016047038	4.35077
Beam 60 (DB08)	90°	25.2	166.6	0.1	31.1	0.016846179	2.622772
Beam 61 (DB08)	90°	48.6	166.6	0.16	31.1	0.026953886	3.161377
Beam 68 (DB11)	90°	20.4	170.9	0.08	39.7	0.01174821	2.558472
Beam 69 (DB11)	90°	42.18	170.9	0.13	39.7	0.019090842	3.255395
Beam 70 (DB11)	90°	56.22	170.9	0.18	39.7	0.026433473	3.13371
Beam 77 (DB11)	90°	31.86	170.9	0.08	39.7	0.01174821	3.995731
Beam 78 (DB11)	90°	33.6	170.9	0.13	39.7	0.019090842	2.593202
Beam 83 (DB10)	90°	28.32	174.3	0.13	18.6	0.032277417	2.143063
Beam 93 (T10)	90°	72.92	124	0.177	25.1	0.025557107	5.778254
Beam 94 (T10)	90°	82.13	124	0.236	25	0.034166952	4.881048
Beam 99 (T10)	90°	97.38	124	0.529	24.9	0.076951059	2.576518
Beam 100 (I08)	90°	151.4	124	0.34	49.75	0.031167733	6.026401
Beam 101 (I08)	90°	81.5	124	0.168	49.75	0.015400527	6.565372
Beam 103 (RR10)	90°	70	124	0.335	43.5	0.033594636	2.902015
Beam 104 (RR10)	90°	103	124	0.335	44.2	0.033238999	4.270108
Beam 106 (RS12)	90	36.78	45	0.323	34.88	0.013619023	7.401865
Beam 108 (RS12)	90°	49.05	45	0.343	34.88	0.014452447	9.301929
Beam 110 (RS12)	90°	66.21	45	0.274	34.88	0.011561958	15.69523
Beam 112 (RS12)	90°	61.51	45	0.343	34.88	0.014452447	11.66487
Beam 114 (RS12)	90°	39.24	45	0.457	34.88	0.01926993	5.581157
Beam 116 (DN01)	90°	25	104.8	0.523	31	0.055535832	0.935269
Beam 117 (DN01)	90°	37.4	104.8	0.732	31	0.077750164	0.999401

Table B3: Continued

Sample No.	θ_f	V_f^{exp} (KN)	E_f (GPa)	ρ_f %	f_{cm} (MPa)	$(E_f * \rho_f) / (f_c^{2/3})$	ε^{exp} %
Beam 118 (DN01)	90°	95.64	104.8	0.732	31	0.077750164	2.555688
Beam 121 (DN01)	90°	53.4	104.8	0.523	31	0.055535832	1.997734
Beam 122 (RD07)	90°	44.4	145.7	0.689	29.3	0.105557873	1.421222
Beam 123 (RD07)	90°	21.6	145.7	0.689	29.3	0.105557873	0.691405
Beam 124 (RD07)	90°	23.4	145.7	1.117	29.3	0.171238328	0.461726
Beam 127 (RD07)	90°	41.3	121.5	0.44	29.3	0.056249311	2.480861
Beam 129 (DB)	90°	29.1	150	0.047	49.2	0.005213403	10.99773
Beam 131 (DB)	90°	59.3	150	0.093	49.2	0.010426806	11.20559
Beam 133 (DB)	90°	28.6	150	0.187	56.2	0.019083901	5.820106
Beam 135 (DB)	90°	31.8	150	0.373	56.2	0.038167802	3.235653

APPENDIX (C): THE CALCULATIONS OF CALIBRATION OF DIAS AND BARROSS' MODEL

Table C1: The Calculations of Figure **14A**

Sample No.	V_f^{exp} (KN)	E_f (GPa)	ρ_f %	ρ_{sw} %	f_{cm} (MPa)	$(\rho_f * E_f + E_{sw} * \rho_{sw}) / f_{cm}^{2/3}$	ε^{exp} %
Beam 1 (DB12)	40.3	166.6	0.1	0.1	31.1	0.037069683	4.607557
Beam 2 (DB12)	63.7	166.6	0.16	0.1	31.1	0.04717739	4.551821
Beam 9 (DB12)	57.5	166.6	0.13	0.1	39.7	0.035796295	4.806487
Beam 10 (DB12)	71.5	170.9	0.18	0.1	39.7	0.043619269	4.194219
Beam 17 (DB12)	31.9	170.9	0.08	0.17	39.7	0.040964064	4.21035
Beam 18 (DB12)	40.7	170.9	0.08	0.17	39.7	0.040964064	5.371826
Beam 19 (DB12)	33.6	170.9	0.13	0.17	39.7	0.048306695	2.80866
Beam 24 (DB12)	43.6	174.3	0.13	0.1	18.6	0.060767128	3.573478
Beam 33 (DB12)	44.7	174.3	0.08	0.1	59.4	0.022296604	5.784685
Beam 34 (DB12)	81.5	174.3	0.13	0.1	59.4	0.028021177	6.67978
Beam 45 (DB09)	20.2	170.9	0.08	0.1	39.7	0.028934007	2.666115
Beam 46 (DB09)	42.2	170.9	0.13	0.1	39.7	0.036276638	3.527543
Beam 47 (DB09)	56.2	170.9	0.18	0.1	39.7	0.043619269	3.296715
Beam 54 (JSCA12)	33.4	235	0.075	0.095	36.4	0.033345972	3.791206
Beam 56 (JSCA12)	39.9	235	0.075	0.095	36.4	0.033345972	4.52539
Beam 58 (JSCA12)	29.4	235	0.075	0.095	36.4	0.033345972	3.33617
Beam 60 (DB08)	25.2	166.6	0.1	0.1	31.1	0.037069683	2.881152
Beam 61 (DB08)	48.6	166.6	0.16	0.1	31.1	0.04717739	3.472818
Beam 68 (DB11)	20.4	170.9	0.08	0.1	39.7	0.028934007	2.692512
Beam 69 (DB11)	42.2	170.9	0.13	0.1	39.7	0.036276638	3.525871
Beam 70 (DB11)	56.2	170.9	0.18	0.1	39.7	0.043619269	3.297888
Beam 77 (DB11)	31.9	170.9	0.08	0.17	39.7	0.040964064	4.205071
Beam 78 (DB11)	33.6	170.9	0.13	0.17	39.7	0.048306695	2.80866
Beam 83 (DB10)	28.3	174.3	0.13	0.1	18.6	0.060767128	2.321121
Beam 93 (T10)	72.9	124	0.1767	0.39	25.1	0.116543991	4.753837
Beam 94 (T10)	82.1	124	0.2356	0.39	25	0.125396306	4.015695
Beam 99 (T10)	97.4	124	0.5292	0.39	24.9	0.168424504	4.761334
Beam 100 (I08)	151	124	0.34	0.204	49.75	0.061330055	4.666275
Beam 101 (I08)	81.5	124	0.168	0.204	49.75	0.045562849	5.037017
Beam 102 (I08)	112.9	124	0.27	0.204	49.72	0.054913169	4.361037
Beam 103 (RR10)	70	124	0.3351	0.1886	43.5	0.064090821	2.8077
Beam 104 (RR10)	103	124	0.3351	0.1886	44.2	0.063412347	4.13133
Beam 106 (RS12)	36.78	45	0.323	0	34.88	0.013619023	5.786431
Beam 108 (RS12)	49.1	45	0.3429	0	34.88	0.014452447	7.266667
Beam 110 (RS12)	66.2	45	0.2743	0	34.88	0.011561958	12.26111

Table C1: Continued

Sample No.	V_f^{exp} (KN)	E_f (GPa)	ρ_f %	ρ_{sw} %	f_{cm} (MPa)	$(\rho_f * E_f + E_{sw} * \rho_{sw}) / f_{cm}^{2/3}$	ε^{exp} %
Beam 112 (RS12)	61.5	45	0.3429	0	34.88	0.014452447	9.112593
Beam 114 (RS12)	39.2	45	0.4571	0	34.88	0.01926993	4.36
Beam 116 (DN01)	25	104.8	0.5229	0	31	0.055535832	0.980973
Beam 117 (DN01)	37.4	104.8	0.7321	0	31	0.077750164	1.048239
Beam 118 (DN01)	95.6	104.8	0.7321	0	31	0.077750164	2.680578
Beam 121 (DN01)	53.4	104.8	0.5229	0.26	31	0.108229959	2.095358
Beam 122 (RD07)	44.4	145.7	0.6886	0.17	29.3	0.142804892	1.054049
Beam 123 (RD07)	21.6	145.7	0.6886	0.17	29.3	0.142804892	0.512781
Beam 124 (RD07)	23.4	145.7	1.117	0.17	29.3	0.208485346	0.342439
Beam 127 (RD07)	41.3	121.5	0.44	0.17	29.3	0.09349633	1.846279
Beam 129 (DB)	29.1	150	0.0467	0	49.2	0.005213403	4.619048
Beam 131 (DB)	59.3	150	0.0933	0	49.2	0.010426806	4.706349
Beam 133 (DB)	28.6	150	0.1867	0	56.2	0.019083901	4.539683
Beam 135 (DB)	31.8	150	0.3733	0	56.2	0.038167802	2.52381

Notice that: E_{sw}= 200Gpa

Table C2: The Calculations of Figure **14B**

Sample No.	V_f^{exp} (KN)	E_f (GPa)	ρ_f %	ρ_{sw} %	f_{cm} (MPa)	$(\rho_f * E_f + E_{sw} * \rho_{sw}) / f_{cm}^{2/3}$	ε^{exp} %
Beam 6 (DB12)	35.4	166.6	0.06	0.1	31.1	0.030331211	6.0183
Beam 7 (DB12)	61.3	166.6	0.09	0.1	31.1	0.035385065	6.25291
Beam 8 (DB12)	69.7	166.6	0.13	0.1	31.1	0.042123536	5.06798
Beam 14 (DB12)	49.6	170.9	0.07	0.1	39.7	0.02746548	6.4697
Beam 15 (DB12)	54.4	170.9	0.11	0.1	39.7	0.033339585	4.73053
Beam 16 (DB12)	65.3	170.9	0.16	0.1	39.7	0.040682217	3.78559
Beam 22 (DB12)	43.5	170.9	0.07	0.17	39.7	0.039495538	5.67403
Beam 23 (DB12)	51.7	170.9	0.11	0.17	39.7	0.045369643	4.40805
Beam 27 (DB12)	33.1	174.3	0.07	0.1	18.6	0.045869858	4.23326
Beam 28 (DB12)	42.7	174.3	0.11	0.1	18.6	0.055801371	3.64069
Beam 31 (DB12)	25.1	174.3	0.07	0.17	18.6	0.065812655	3.21012
Beam 32 (DB12)	35.1	174.3	0.11	0.17	18.6	0.075744168	2.9927
Beam 39 (DB12)	84.6	174.3	0.07	0.1	59.4	0.021151689	10.8198
Beam 40 (DB12)	127.9	174.3	0.11	0.1	59.4	0.025731348	10.905
Beam 43 (DB12)	73.4	174.3	0.07	0.16	59.4	0.029034062	9.38736
Beam 44 (DB12)	72.6	174.3	0.07	0.16	59.4	0.029034062	9.28504
Beam 51 (DB09)	49.6	170.9	0.07	0.1	39.7	0.02746548	6.4697
Beam 52 (DB09)	54.4	170.9	0.11	0.1	39.7	0.033339585	4.73053
Beam 53 (DB09)	65.3	170.9	0.16	0.1	39.7	0.040682217	3.78559
Beam 65 (DB08)	35.4	166.6	0.06	0.1	31.1	0.030331211	6.0183
Beam 66 (DB08)	46.2	166.6	0.09	0.1	31.1	0.035385065	4.71263
Beam 67 (DB08)	54.6	166.6	0.13	0.1	31.1	0.042123536	3.97004
Beam 74 (DB11)	49.56	170.9	0.07	0.1	39.7	0.02746548	6.46448
Beam 75 (DB11)	54.36	170.9	0.11	0.1	39.7	0.033339585	4.72706
Beam 76 (DB11)	65.34	170.9	0.16	0.1	39.7	0.040682217	3.78791
Beam 81 (DB11)	43.44	170.9	0.07	0.17	39.7	0.039495538	5.66621
Beam 82 (DB11)	51.72	170.9	0.11	0.17	39.7	0.045369643	4.49749
Beam 86 (DB10)	33.06	174.3	0.07	0.1	18.6	0.045869858	4.22815
Beam 87 (DB10)	42.72	174.3	0.11	0.1	18.6	0.055801371	3.6424
Beam 91 (DB10)	25.08	174.3	0.07	0.17	18.6	0.065812655	3.20756
Beam 92 (DB10)	35.1	174.3	0.11	0.17	18.6	0.075744168	2.9927

Notice that: E_{sw}= 200Gpa

Table C3: The Calculations of Figure **14C**

Sample No.	V_f^{exp} (KN)	E_f (GPa)	ρ_f %	ρ_{sw} %	f_{cm} (MPa)	$(\rho_f * E_f + E_{sw} * \rho_{sw}) / f_{cm}^{2/3}$	ε^{exp} %
Beam 3 (DB12)	37.9	166.6	0.06	0.1	31.1	0.030331211	7.02807
Beam 4 (DB12)	56.5	166.6	0.1	0.1	31.1	0.037069683	6.28061
Beam 5 (DB12)	70.3	166.6	0.16	0.1	31.1	0.04717739	4.90191
Beam 11 (DB12)	53.4	170.9	0.08	0.1	39.7	0.028934007	7.61402
Beam 12 (DB12)	70.7	170.9	0.13	0.1	39.7	0.036276638	5.75518
Beam 13 (DB12)	85.6	170.9	0.19	0.1	39.7	0.045087796	4.8821
Beam 20 (DB12)	42.7	170.9	0.08	0.17	39.7	0.040964064	6.08836
Beam 21 (DB12)	64	170.9	0.13	0.17	39.7	0.048306695	5.20978
Beam 25 (DB12)	33.9	174.3	0.08	0.1	18.6	0.048352736	4.73933
Beam 26 (DB12)	48	174.3	0.13	0.1	18.6	0.060767128	3.83112
Beam 29 (DB12)	26	174.3	0.08	0.17	18.6	0.068295533	3.63489
Beam 30 (DB12)	31.6	174.3	0.13	0.17	18.6	0.080709925	2.52215
Beam 35 (DB12)	81.7	174.3	0.08	0.1	59.4	0.022296604	11.4219
Beam 37 (DB12)	85.8	174.3	0.08	0.1	59.4	0.022296604	11.9951
Beam 38 (DB12)	80.9	174.3	0.08	0.1	59.4	0.022296604	11.3101
Beam 41 (DB12)	74.9	174.3	0.08	0.16	59.4	0.030178976	10.4713
Beam 48 (DB09)	53.4	170.9	0.08	0.1	39.7	0.028934007	7.61402
Beam 49 (DB09)	70.7	170.9	0.13	0.1	39.7	0.036276638	5.75518
Beam 50 (DB09)	85.6	170.9	0.19	0.1	39.7	0.045087796	4.8821
Beam 55 (JSCA12)	53.94	235	0.071	0.095	36.4	0.03249013	6.49214
Beam 57 (JSCA12)	63.82	235	0.071	0.095	36.4	0.03249013	7.68129
Beam 63 (DB08)	41.4	166.6	0.1	0.1	31.1	0.037069683	4.60208
Beam 64 (DB08)	40.2	166.6	0.16	0.1	31.1	0.04717739	2.80308
Beam 71 (DB11)	53.4	170.9	0.08	0.1	39.7	0.028934007	7.61402
Beam 72 (DB11)	70.74	170.9	0.13	0.1	39.7	0.036276638	5.75844
Beam 73 (DB11)	85.62	170.9	0.19	0.1	39.7	0.045087796	4.88324
Beam 79 (DB11)	42.66	170.9	0.08	0.17	39.7	0.040964064	6.08266
Beam 80 (DB11)	64.02	170.9	0.13	0.17	39.7	0.048306695	5.21141
Beam 84 (DB10)	33.9	174.3	0.08	0.1	18.6	0.048352736	4.73933
Beam 85 (DB10)	48	174.3	0.13	0.1	18.6	0.060767128	3.83112
Beam 89 (DB10)	26.04	174.3	0.08	0.17	18.6	0.068295533	3.64048
Beam 90 (DB10)	31.56	174.3	0.13	0.17	18.6	0.080709925	2.51896
Beam 105 (RR10)	138	124	0.474	0.1886	43.8	0.077659258	3.91396
Beam 107 (RS12)	29.43	45	0.45691	0	34.88	0.019260172	3.27397
Beam 109 (RS12)	58.86	45	0.48487	0	34.88	0.02043881	6.16597
Beam 111 (RS12)	41.69	45	0.3879	0	34.88	0.016351048	5.45913
Beam 113 (RS12)	56.4	45	0.48487	0	34.88	0.02043881	5.90827
Beam 115 (RS12)	68.67	45	0.6465	0	34.88	0.027251746	5.39522

Table C3: Continued

Sample No.	V_f^{exp} (KN)	E_f (GPa)	ρ_f %	ρ_{sw} %	f_{cm} (MPa)	$(\rho_f * E_f + E_{sw} * \rho_{sw}) / f_{cm}^{2/3}$	ε^{exp} %
Beam 119 (DN01)	75.2	104.8	0.73955	0	31	0.078539382	2.08651
Beam 120 (DN01)	87.63	104.8	1.03537	0	31	0.109955135	1.73671
Beam 125 (RD07)	32.1	145.7	0.48689	0.177	29.3	0.111887569	1.0777
Beam 126 (RD07)	22.9	145.7	0.97377	0.177	29.3	0.18652812	0.38441
Beam 128 (RD07)	26.8	121.5	0.31	0.177	29.3	0.076877215	1.69433
Beam 130 (DB)	28.8	150	0.022	0	49.2	0.002457747	4.84873
Beam 132 (DB)	72.9	150	0.044	0	49.2	0.004915494	6.13668
Beam 134 (DB)	23.2	150	0.088	0	56.2	0.008996696	3.90592
Beam 136 (DB)	36.4	150	0.176	0	56.2	0.017993392	3.06413

Notice that: E_{sw}= 200 Gpa

Members of the Editorial Board

Editor in chief

Dr. Mohammad Othman Nassar, Faculty of Computer Science and Informatics, Amman Arab University for Graduate Studies,
Jordan, moanassar@aau.edu.jo , 00962788780593

Editorial Board

GSSRR
Global Society of Scientific Research and Researchers

IJSBAR
International Journal of Sciences: Basic and Applied Research

IJSBAR
International Journal of Sciences: Basic and Applied Research